

Multivariate soft rank via entropic optimal transport: sample efficiency and generative modeling

Shoaib Bin Masud^{*}, Matthew Werenski[†], James M. Murphy[‡], Shuchin Aeron^{**}

May 31, 2022

Abstract

The framework of optimal transport has been leveraged to extend the notion of rank to the multivariate setting while preserving desirable properties of the resulting goodness of-fit (GoF) statistics. In particular, the rank energy (RE) and rank maximum mean discrepancy (RMMD) are distribution-free under the null, exhibit high power in statistical testing, and are robust to outliers. In this paper, we point to and alleviate some of the practical shortcomings of these proposed GoF statistics, namely their high computational cost, high statistical sample complexity, and lack of differentiability with respect to the data. We show that all these practically important issues are addressed by considering entropy-regularized optimal transport maps in place of the rank map, which we refer to as the *soft rank*. We consequently propose two new statistics, the *soft rank energy (sRE)* and *soft rank maximum mean discrepancy (sRMMD)*, which exhibit several desirable properties. Given n sample data points, we provide non-asymptotic convergence rates for the sample estimate of the entropic transport map to its population version that are essentially of the order $n^{-1/2}$. This compares favorably to non-regularized estimates, which typically suffer from the curse-of-dimensionality and converge at rate that is exponential in the data dimension. We leverage this fast convergence rate to demonstrate the sample estimate of the proposed statistics converge rapidly to their population versions, enabling efficient rank-based GoF statistical computation, even in high dimensions. Our statistics are differentiable and amenable to popular machine learning frameworks that rely on gradient methods. We leverage these properties towards showcasing the utility of the proposed statistics for generative modeling on two important problems: image generation and generating valid knockoffs for controlled feature selection.

1 Introduction

It is well-known that in one dimension, the notions of rank and quantile with respect to the distribution of the data are naturally defined via the cumulative distribution function (cdf) and its generalized inverse, respectively. This is because \mathbb{R} has a canonical ordering, which is naturally captured by the cdf. Based on these notions, a number of goodness-of-fit (GoF) statistics and tests have been proposed in the literature, such as the Kolmogorov-Smirnov test [1], Wilcoxon rank test [2], and more recently rank-quantile tests [3]. These rank- and quantile-based statistics are computationally feasible, non-parametric, and are distribution-free under the null, making them desirable in a number of applications, e.g. unsupervised change point detection [4], tests of independence [5, 6], and hierarchical clustering [7].

Recently, meaningful multivariate extensions of the notion of rank and quantile maps were proposed in the pioneering works [8, 9, 10], and more recently in [11] based on the theory of optimal transportation [12, 13]. For a detailed discussion, we refer the reader to a recent survey on the topic [14] and references therein. Essentially, these ideas leverage the convex geometry of the optimal transport (OT) problem with the squared Euclidean metric as the ground cost, where under some mild conditions the optimal maps are gradients of strictly convex functions [15, 16]. These extensions and the corresponding high-dimensional analogues of the rank-based GoF statistics based on these extensions retain some of the useful properties of their one dimensional counterparts, namely they are computationally feasible for small sample sizes and are distribution-free under the null.

In this paper we focus on the multivariate rank-based GoF statistic proposed in [11], namely the rank energy and rank maximum mean discrepancy (MMD), based on a particular choice of the reference measure when

^{*}Emails and Affiliations:

^{*} Department of ECE, Tufts University. Emails: shoaib_bin.masud@tufts.edu, shuchin@ece.tufts.edu

[†] Department of Computer Science, Tufts University. Email: matthew.werenski@tufts.edu

[‡] Department of Mathematics, Tufts University. Email: jm.murphy@tufts.edu

defining the multivariate ranks via optimal transport maps. These statistics are shown to be distribution-free in finite samples (under the null), consistent against alternatives, exhibit high power in statistical testing for heavy-tailed distributions, and are robust to outliers.

However, as we discuss in detail in Section 2.2.2, practical use of the rank energy and rank MMD suffer from the well-known curse of dimensionality associated with the estimation of OT maps as well as high computational costs for large sample sizes. Furthermore, rank energy and rank MMD suffer from lack of differentiability in data, limiting a direct use of iterative gradient-based optimization methods. This inhibits their use for learning a generative model by using these GoF statistics as a loss function, as has been successfully done with MMD and Wasserstein distances [17, 18].

In this context, our paper makes the following main contributions.

- (C1) We introduce the notion of *entropic rank map* that exploits the recent developments in computational optimal transport, namely entropic relaxation [19]. We then propose the *soft rank energy (sRE)*, a new multivariate GoF statistic, and the related *soft rank maximum mean discrepancy (sRMMD)*. In Proposition 1 and Proposition 2, we establish the properties of soft rank energy and its convergence to rank energy, which together suggest its use for measuring GoF in two-sample testing.
- (C2) We provide a new result (Theorem 2) on the convergence rate of a sample-driven estimate for general entropic maps which enjoys a fast convergence rate of $n^{-1/2}$ to the population entropic map, even in high dimensions. This result is then used in Theorem 3 and Theorem 4 to establish the statistical convergence of sample sRE and sample sRMMD, respectively, to their population versions with rate $n^{-1/2}$. Our analysis also clarifies the impact of key design parameters in our proposed statistics.
- (C3) We show the practical advantages of our proposed methods on several real generative modeling problems. First, we use sRE and sRMMD as the loss functions in a simple generative model architecture to produce MNIST-digits. Under an appropriate choice of the entropic regularization parameter, we show that using sRE and sRMMD as the loss functions can generate all of the digits successfully, and does not suffer from mode collapse. We then utilize the sRMMD in a deep generative model in order to produce valid knockoffs [20]. We showcase improved tradeoffs between detection power versus false discovery rate (FDR) compared to other benchmarks of knockoff generation techniques on different Gaussian and non-Gaussian distributional settings. We also test our approach for provable biomarker selection in metabolomics.¹

Paper outline: The paper is organized as follows. In Section 2, we provide the required background on optimal transport theory and its entropy-regularized variant as well as discuss the multivariate rank energy. In Section 3 we introduce the soft rank energy (sRE) and the soft rank maximum mean discrepancy (sRMMD), and sample versions thereof. In Section 4 we state our main theorems which establish the favorable properties of the soft rank energy. We also prove finite sample convergence rates for the sample sRE and sRMMD to their population versions. In Section 5, we provide extensive simulations to establish soft rank energy as a GoF measure and include two applications where we use it as the loss function of a generative model.

Notation: Throughout the paper we consider the space of measures $\mathcal{P}(\Omega)$ on a bounded set $\Omega \subset \mathbb{R}^d$. We will let X, Y denote random vectors in \mathbb{R}^d and we will use superscripts to denote their entries $X = (X^1, \dots, X^d)$. A bold \mathbf{X} will denote a matrix. $\|\cdot\|$ will denote the Euclidean norm in \mathbb{R}^d . $\stackrel{d}{=}$ will denote equality in distribution. We write $a \lesssim b$ if there exists a constant C such that $a \leq Cb$. The rest of the notations is standard and clear from the context. We also include in Table 1 a list of notations introduced later for easy reference.

2 Background on Optimal Transport and Rank Energy

Throughout this work we consider measures contained in $\mathcal{P}_{ac}(\Omega)$, the space of absolutely continuous measure on $\Omega \subset \mathbb{R}^d$ i.e. those characterized by a density function with respect to the Lebesgue measure. We will assume throughout that Ω is bounded and contained in the ball $B_2^d(0, r)$.

¹Codes to reproduce the results are available at <https://github.com/ShoaibBinMasud/soft-rank-energy-and-applications>

Symbol	Meaning
$B_2^d(0, r)$	Euclidean ball of radius r in \mathbb{R}^d
$P_\lambda = \lambda P_X + (1 - \lambda)P_Y$	Mixture distribution, $\lambda \in (0, 1)$.
T	Optimal transport map
T_ε	Entropic map
$T_\varepsilon^{n,n}$	Two-sample entropic map
R_λ	Rank map. T from P_λ to $\text{Unif}([0, 1]^d)$
$R_{\lambda,\varepsilon}$	Entropic rank map. T_ε from P_λ to $\text{Unif}([0, 1]^d)$
$R_{\lambda,\varepsilon}^{m+n}$	Sample entropic rank map
RE_λ	Rank energy
$sRE_{\lambda,\varepsilon}$	Soft rank energy
$sRE_{\lambda,\varepsilon}^{m,n}$	Sample soft rank energy
$sRMMD_{\lambda,\varepsilon,k}$	Soft rank MMD
$sRMMD_{\lambda,\varepsilon,k}^{m,n}$	Sample soft rank MMD

Table 1: Frequently used notation throughout the paper.

2.1 Optimal Transport

Given two distributions $P, Q \in \mathcal{P}(\Omega)$, where $\mathcal{P}(\Omega)$ denotes the space of Borel probability measures on Ω , the *Monge problem* [21] seeks a measurable map $T : \Omega \rightarrow \Omega$ that pushes P to Q with a minimal cost. Precisely, it solves

$$\inf_T \int \frac{1}{2} \|x - T(x)\|^2 dP(x), \quad \text{subject to } T_\# P = Q, \quad (1)$$

where $T_\# P$ denotes the *push-forward measure*, which satisfies $(T_\# P)[A] = P[T^{-1}(A)]$ for all measurable sets A .

Throughout we will make heavy use of the optimal map T which minimizes (1). It is therefore important to establish the existence, uniqueness, and important properties of T , which are established by the following celebrated theorem.

Theorem 1 (Brenier-McCann [15, 16]). *Let $P \in \mathcal{P}_{ac}(\Omega)$ and $Q \in \mathcal{P}(\Omega)$. Then there exists a convex function $\phi : \Omega \rightarrow \mathbb{R}$ whose gradient $\nabla \phi : \Omega \rightarrow \Omega$ pushes P forward to Q . Moreover, if P and Q have finite second moments, then $\nabla \phi$ is the unique (up to sets of measure 0) solution to the Monge problem (1).*

2.1.1 Entropic Optimal Transport

Towards developing the notion of soft rank energy we first state a relaxation of the *Monge problem*, where instead of a map, one seeks an optimal “coupling” π between a source distribution P and a target distribution Q . The *Kantorovich relaxation* [22] solves

$$\min_{\pi \in \Pi(P, Q)} \int \frac{1}{2} \|x - y\|^2 d\pi(x, y), \quad (2)$$

where $\Pi(P, Q)$ is the set of joint probability measure on $\mathcal{P}(\Omega \otimes \Omega)$ with marginals P and Q . When a solution to the Monge problem 1 exists, then the solution to Kantorovich relaxation coincides with it in the sense that the optimal plan is concentrated on $\{(x, T(x)) : x \in \text{supp}(P)\}$ [22].

The statistic we propose relies on an *entropy-regularized* version of (2). For $\varepsilon > 0$, the primal formulation of the entropy-regularized optimal transport primal is given by

$$\min_{\pi \in \Pi(P, Q)} \int \frac{1}{2} \|x - y\|^2 d\pi(x, y) + \varepsilon \text{KL}(\pi \parallel P \otimes Q), \quad (3)$$

where

$$\text{KL}(\pi \parallel P \otimes Q) \triangleq \int \ln \left(\frac{d\pi(x, y)}{dP(x)dQ(y)} \right) d\pi(x, y).$$

This problem has been extensively studied both for its theoretical properties, as well as for the efficient algorithms that are used to solve it (See [23, 19, 24] and references therein). Importantly, (3) admits the

following dual formulation that follows from the Fenchel-Rockafellar duality theorem [25], a derivation of which may be found in [26, 19]

$$\max_{f,g} \int f(x)dP(x) + \int g(y)dQ(y) - \varepsilon \int \int \exp \left[\frac{1}{\varepsilon} (f(x) + g(y) - (1/2)\|x - y\|^2) \right] dP(x)dQ(y) + \varepsilon, \quad (4)$$

where the maximization is over the pairs $f \in L^1(P), g \in L^1(Q)$ of functions over Ω . The optimal entropic potentials for ε are the pair of functions $(f_\varepsilon, g_\varepsilon)$ which achieve the maximum in (4). Furthermore, there is an optimality relation between (3) and (4) given by

$$d\pi_\varepsilon(x, y) = \exp \left[\frac{1}{\varepsilon} \left(f_\varepsilon(x) + g_\varepsilon(y) - \frac{1}{2}\|x - y\|^2 \right) \right] dP(x)dQ(y), \quad (5)$$

where π_ε denotes the solution to (3). We emphasize the fact that π_ε is not a map, but a diffused coupling, and that the degree of diffusion depends on the entropic regularization parameter ε [19]. In the finite sample setting, entropic optimal transport significantly reduces computational complexity [23] and also yields a differentiable loss function [27].

2.2 Rank and Quantile Maps

Let $P \in \mathcal{P}(\Omega)$ for $\Omega \subset \mathbb{R}^d$ and consider a random variable $X \sim P$. When $d = 1$, the rank map, or cumulative distribution function, is $F_X(t) = \mathbb{P}\{X \leq t\}$, and the quantile map is its generalized inverse, $F_X^{-1}(p) = \inf\{x \in \mathbb{R} : p \leq F_X(x)\}$. The rank and quantile maps are always monotonic increasing and are continuous when P has a density. When F_X is continuous one can show that the random variable $F_X(X)$ is distributed according to $\text{Unif}([0, 1])$. Similarly, when the quantile map is continuous $F_X^{-1}(U)$ is distributed according to X where $U \sim \text{Unif}([0, 1])$.

The key insight in using the theory of optimal transport to define multivariate rank and quantile maps comes from noticing that in one dimension, the optimal map between two measures, P and Q , is given by $T = F_Q^{-1} \circ F_P$, where F_P is the rank map of P and F_Q^{-1} is the quantile map of Q [10]. When $Q = \text{Unif}([0, 1])$, one has $F_Q^{-1} = \text{Id}$ and therefore $F_Q^{-1} \circ F_P = \text{Id} \circ F_P = F_P$. By the push-forward constraint we know that $F_P \# P = \text{Unif}([0, 1])$ which is just one way of observing that $F_P(X) \sim \text{Unif}([0, 1])$. The main intuition is that the rank map is exactly the optimal map from P to $\text{Unif}([0, 1])$. Analogously, with Theorem 1 ensuring the existence of a unique optimal T that is monotone (being a gradient of a convex function), [11] generalizes the notion of rank and quantile maps to dimensions $d \geq 2$ as optimal transport maps to and from $\text{Unif}([0, 1]^d)$.

Definition 1 (Definition 2.1 [11]). Let $P \in \mathcal{P}_{ac}(\Omega)$ and let $Q = \text{Unif}([0, 1]^d)$. The multivariate rank and quantile maps for P are defined as $\mathbf{R} = \nabla\phi$ and $\mathbf{Q} = \nabla\phi^*$, respectively, where ϕ is the *strictly* convex function as in Theorem 1 such that $\nabla\phi$ optimally transports P to Q . Here ϕ^* denotes the standard convex conjugate² of the convex function ϕ .

With the high-dimensional analogue of the rank defined, we can now state the candidate GoF statistics proposed in [11].

Definition 2 (Definition 3.2 [11]). Let $P_X, P_Y \sim \mathcal{P}_{ac}(\Omega)$ and let $X, X' \sim P_X$ and $Y, Y' \sim P_Y$ be independent. Let $P_\lambda = \lambda P_X + (1 - \lambda)P_Y$ denote the mixture distribution for any $\lambda \in (0, 1)$ and let \mathbf{R}_λ be the multivariate rank map of P_λ as in Definition 1. The (*population*) *rank energy* is defined

$$\begin{aligned} \text{RE}_\lambda(P_X, P_Y)^2 &\triangleq C_d \int_{\mathcal{S}^{d-1}} \int_{\mathbb{R}} (\mathbb{P}(a^\top \mathbf{R}_\lambda(X) \leq t) - \mathbb{P}(a^\top \mathbf{R}_\lambda(Y) \leq t))^2 dt d\kappa(a) \\ &= 2\mathbb{E}\|\mathbf{R}_\lambda(X) - \mathbf{R}_\lambda(Y)\| - \mathbb{E}\|\mathbf{R}_\lambda(X) - \mathbf{R}_\lambda(X')\| - \mathbb{E}\|\mathbf{R}_\lambda(Y) - \mathbf{R}_\lambda(Y')\|, \end{aligned} \quad (6)$$

where $\mathcal{S}^{d-1} \triangleq \{x \in \mathbb{R}^d : \|x\| = 1\}$ is the unit sphere in \mathbb{R}^d , $\kappa(\cdot)$ is the uniform measure on \mathcal{S}^{d-1} , and $C_d = (2\Gamma(d/2))^{-1} \sqrt{\pi}(d-1)\Gamma((d-1)/2)$ is an appropriate normalizing constant.

Note that RE_λ^2 closely resembles the definition of energy distance [28],

$$\text{En}(P_X, P_Y)^2 \triangleq C_d \int_{\mathcal{S}^{d-1}} \int_{\mathbb{R}} (\mathbb{P}(a^\top X \leq t) - \mathbb{P}(a^\top Y \leq t))^2 dt d\kappa(a)$$

a widely used GoF statistic in two-sample testing. This definition is motivated by the continuity and uniqueness of characteristic functions. Namely, $P_X = P_Y$ if and only if $a^\top X \stackrel{d}{=} a^\top Y$ (that is, equality in

²for any proper function $f : \Omega \rightarrow \mathbb{R}$, the convex conjugate $f^* : \Omega \rightarrow \mathbb{R}$ is defined as: $f^*(y) \triangleq \sup_x \langle x, y \rangle - f(x)$ for all $y \in \Omega$.

distribution) for κ -almost everywhere a ; indeed, the integration over the sphere aggregates the discrepancy in characteristic functions in every direction. For a discussion showing the equivalence of the formulation in (6) using integrals over \mathcal{S}^{d-1} and the formulation in terms of expectations of \mathbf{R}_λ , see [29]. One advantage of RE_λ^2 over the energy distance is that RE_λ^2 is distribution-free under the null for all sample sizes [11].

One can generalize the rank energy by replacing the pairwise distance with a kernel function [30]. Given $k : \mathbb{R}^d \times \mathbb{R}^d \rightarrow \mathbb{R}$ a characteristic kernel ³, we can interpret this distance as *rank maximum mean discrepancy*,

$$\text{RMMD}_\lambda(P_X, P_Y)^2 \triangleq \mathbb{E}[k(\mathbf{R}_\lambda(X), \mathbf{R}_\lambda(X'))] + \mathbb{E}[k(\mathbf{R}_\lambda(Y), \mathbf{R}_\lambda(Y'))] - 2\mathbb{E}[k(\mathbf{R}_\lambda(X), \mathbf{R}_\lambda(Y))]. \quad (7)$$

Note that $\text{RMMD}_\lambda(P_X, P_Y)^2$ closely follows the definition of maximum mean discrepancy [31] which is a widely used statistic in the framework of two-sample testing: $\text{MMD}(P_X, P_Y)^2 \triangleq \mathbb{E}[k(X, X')] + \mathbb{E}[k(Y, Y')] - 2\mathbb{E}[k(X, Y)]$.

One can simply view RE_λ^2 and RMMD_λ^2 as the ‘‘rank-transformed’’ energy distance and maximum mean discrepancy, respectively.

In practice one can rarely evaluate the RE_λ^2 and RMMD_λ^2 directly since the exact multivariate rank \mathbf{R}_λ often unavailable. Instead the statistic must be estimated from samples, a procedure outlined in the next subsection.

2.2.1 Sample Rank Map and Rank Energy

Given i.i.d. samples $X_1, \dots, X_m \sim P$, the empirical measure is defined as $P^m = \frac{1}{m} \sum_{i=1}^m \delta_{X_i}$ where δ_{X_i} is a Dirac distribution placed at X_i . Given two empirical measures $P^m = \frac{1}{m} \sum_{i=1}^m \delta_{X_i}$, $Q^m = \frac{1}{m} \sum_{j=1}^m \delta_{Y_j}$, where $Y_1, \dots, Y_m \sim Q$, the plug-in estimate of the transport map T^m between P and Q is obtained by solving (1) between P^m, Q^m

$$T^m \triangleq \arg \min_{T: T_\# P^m = Q^m} \int \frac{1}{2} \|x - T(x)\|^2 dP^m(x) = \arg \min_{T: T_\# P^m = Q^m} \frac{1}{m} \sum_{i=1}^m \frac{1}{2} \|X_i - T(X_i)\|^2. \quad (8)$$

This problem can be converted to a standard linear program and solved either by tailored methods or general linear program solvers [19]. To obtain the sample rank map for a measure P , one performs the procedure above with $Q = \text{Unif}([0, 1]^d)$ and takes \mathbf{R}^m to be the estimate T^m . In practice, one may generate the samples from $\text{Unif}([0, 1]^d)$ using a pseudo-random sequence of points. In [11], Halton sequences [32] are used and we do the same in our experiments. Nevertheless, any sequence which weakly converges to $\text{Unif}([0, 1]^d)$ can be used.

With the sample rank map defined, one can immediately extend the definition of the rank energy. Given two sets of samples $X_1, \dots, X_m \sim P_X$ and $Y_1, \dots, Y_n \sim P_Y$, define P^{m+n} as

$$P^{m+n} = \frac{1}{m+n} \left(\sum_{i=1}^m \delta_{X_i} + \sum_{j=1}^n \delta_{Y_j} \right),$$

the empirical mixture of the two sets of samples. Next, let $Q^{n+m} = \frac{1}{m+n} \sum_{i=1}^{n+m} \delta_{U_i}$ where $U_i \sim \text{Unif}([0, 1]^d)$. Using these measures, one obtains \mathbf{R}^{m+n} and then computes the sample rank energy as

$$\begin{aligned} \text{RE}_{m,n}(P_X, P_Y)^2 \triangleq & \frac{2}{mn} \sum_{i=1}^m \sum_{j=1}^n \|\mathbf{R}^{m+n}(X_i) - \mathbf{R}^{m+n}(Y_j)\| - \frac{1}{m^2} \sum_{i,j=1}^m \|\mathbf{R}^{m+n}(X_i) - \mathbf{R}^{m+n}(X_j)\| \\ & - \frac{1}{n^2} \sum_{i,j=1}^n \|\mathbf{R}^{m+n}(Y_i) - \mathbf{R}^{m+n}(Y_j)\|. \end{aligned} \quad (9)$$

The authors in [11] also define the sample version of rank maximum mean discrepancy as

$$\begin{aligned} \text{RMMD}_{m,n}(P_X, P_Y)^2 \triangleq & \frac{1}{m^2} \sum_{i,j=1}^m k(\mathbf{R}^{m+n}(X_i), \mathbf{R}^{m+n}(X_j)) + \frac{1}{n^2} \sum_{i,j=1}^n k(\mathbf{R}^{m+n}(Y_i), \mathbf{R}^{m+n}(Y_j)) \\ & - \frac{2}{mn} \sum_{i=1}^m \sum_{j=1}^n k(\mathbf{R}^{m+n}(X_i), \mathbf{R}^{m+n}(Y_j)), \end{aligned} \quad (10)$$

for some characteristic kernel k . Both $\text{RE}_{m,n}^2$ and $\text{RMMD}_{m,n}^2$ are distribution-free under the null for any fixed sample size [11].

³a kernel k is said to be characteristic if the map $P \rightarrow \int_{\mathcal{X}} k(\cdot, x) dP(x)$ is injective, where P is a measure defined on the topological space \mathcal{X} .

2.2.2 Practical Issues with Rank Energy

While the rank energy enjoys certain desirable properties, it also suffers from important drawbacks. We focus on two below.

Complexity, sample and computational: In practice, to compute the test statistic proposed in [11], one needs to solve the discrete version of the Monge problem. Given n samples, solving this problem exactly using typical methods requires $O(n^3 \log n)$ computations [19], and the standard procedure is not amenable to parallelization. To make matters worse, when the samples are in \mathbb{R}^d , (8) has a large sample complexity in the sense that when $\lambda = m/(m+n)$ and in the absence of further assumptions, one only has

$$\frac{1}{m+n} \mathbb{E} \left[\sum_{i=1}^m \|\mathbf{R}^{m+n}(X_i) - \mathbf{R}_\lambda(X_i)\| + \sum_{j=1}^n \|\mathbf{R}^{m+n}(Y_j) - \mathbf{R}_\lambda(Y_j)\| \right] \lesssim (m+n)^{-1/d}.$$

Unfortunately, this rate which depends exponentially on d can be tight [33], implying the need for extremely large sample sizes when working in high dimension to get a faithful estimate of the map \mathbf{R}_λ which is required to estimate $\mathbf{RE}_\lambda(P_X, P_Y)^2$. Together, these observations mean the approach of [11] exhibits a statistical-computational bottleneck that precludes its use in high dimensions: one needs n large to get a good estimate, but computing the estimate for large n is computationally infeasible.

Gradient issues: Another reason that one may be interested in obtaining the rank statistic is to use it as a loss function for generative modelling. For example, if X_1, \dots, X_m are real samples and Y_1, \dots, Y_n are from a standard model (e.g., $Y_i \sim N(0, I_d)$) one may seek to solve⁴

$$\min_{\theta} \mathbf{RE}_{m,n}(\{X_i\}_{i=1}^m, \{T_\theta(Y_j)\}_{j=1}^n)^2 \quad (11)$$

where $\mathbf{RE}_{m,n}^2$ is the (squared) sample rank energy (defined in (9)) and $T_\theta : \Omega \rightarrow \Omega$ is a learnable transformation parameterized by θ . In this setting, a small statistic indicates that T_θ is successfully transforming the samples $\{Y_i\}_{i=1}^n$ in such a way that they are difficult to distinguish from the $\{X_i\}_{i=1}^m$. To obtain θ^* , a (near) minimizer of (11), many standard procedures start at a random θ_0 and then use a gradient based procedure which requires access to $\nabla_{\theta} \mathbf{RE}_{m,n}(\{X_i\}_{i=1}^m, \{T_\theta(Y_i)\}_{i=1}^n)^2$ to obtain a sequence of improving θ_i (for example, $\theta_{i+1} = \theta_i - \eta \nabla_{\theta_i} \mathbf{RE}_{m,n}(\{X_i\}_{i=1}^m, \{T_\theta(Y_j)\}_{j=1}^n)^2$ for some learning rate $\eta > 0$) [34, 35].

This gradient descent approach will not work for the rank energy in typical settings for two reasons. First, one needs to rely on special methods to back-propagate through the construction of the rank map which is the argmin of a convex optimization problem (one is forced to rely on so-called convex optimization layers [36], for example). Second, when $n = m$, even if the gradient is computed, it will typically be exactly zero. This is because the rank energy is invariant to sufficiently small perturbations of the samples (see Section 7 for a precise description). In the absence of a non-zero gradient, the methods above will not be able to incrementally improve the setting of θ , or even choose a direction in the parameter space to search along. In practice the first-order methods above are by far the most popular and are often the only feasible methods when θ is extremely high-dimensional (i.e. represents the weights of a deep neural network). The absence of a proper gradient severely restricts the utility of the rank energy in broader contexts.

These two drawbacks are not isolated to the rank energy, but are present whenever an empirical rank map is involved. This also limits the utility of the rank maximum mean discrepancy. In contrast, many other GoF measures in statistics (e.g., maximum mean discrepancy (MMD) [37], energy distance [38]), can be used as a loss function in a generative model to learn a new distribution as close as possible to a target distribution. Motivated by the use of a rank-based GoF statistic towards generative modeling, we propose *soft rank energy* and *soft rank maximum mean discrepancy*, which largely alleviate the defects of their rank counterparts.

3 Entropic Rank and Soft Rank Energy

Based on the primal-dual relationship in equations (3),(4), we note the following definition of the entropic map.

⁴Technically this should be written $\mathbf{RE}_{m,n}(P_X, (T_\theta)_\# P_Y)$, but for clarity we avoid this notation here.

Definition 3 (Entropic map [39]). Given an optimal entropic plan π_ε or the optimal entropic potentials $(f_\varepsilon, g_\varepsilon)$ between $P \in \mathcal{P}_{ac}(\Omega)$ and $Q \in \mathcal{P}_{ac}(\Omega)$, the *entropic map* is defined by

$$T_\varepsilon(x) \triangleq \int \pi_\varepsilon(y|x) = \mathbb{E}_{\pi_\varepsilon}[Y|X=x] = \frac{\int y \exp\left(\frac{1}{\varepsilon}\left(g_\varepsilon(y) - \frac{1}{2}\|x-y\|^2\right)\right) dQ(y)}{\int \exp\left(\frac{1}{\varepsilon}\left(g_\varepsilon(y) - \frac{1}{2}\|x-y\|^2\right)\right) dQ(y)} \quad (12)$$

where $\pi_\varepsilon(y|x)$ denotes the conditional distribution of π_ε .

In [39], the latter form is used to define a sample version of the entropic map. Given samples $X_1, \dots, X_n \sim P$ and $Y_1, \dots, Y_n \sim Q$ and optimal entropic potentials $(f_\varepsilon^n, g_\varepsilon^n)$ solving (4) between P^n, Q^n , the sample entropic map is defined as

$$T_\varepsilon^{n,n}(x) \triangleq \frac{\sum_{i=1}^n Y_i \exp\left(\frac{1}{\varepsilon}\left(g_\varepsilon^n(Y_i) - \frac{1}{2}\|x - Y_i\|^2\right)\right)}{\sum_{i=1}^n \exp\left(\frac{1}{\varepsilon}\left(g_\varepsilon^n(Y_i) - \frac{1}{2}\|x - Y_i\|^2\right)\right)}. \quad (13)$$

We adopt these definitions in constructing the entropic rank maps.

Definition 4 (Entropic Rank). The *entropic rank* map \mathbf{R}_ε for a measure P is the entropic map from P to $Q = \text{Unif}([0, 1]^d)$ as in (12). The sample entropic rank map \mathbf{R}_ε^n is defined as the sample entropic map from P^n to Q^n as in (13).

With these alternatives to the original rank map, the definition of the soft rank energy is as follows.

Definition 5 (Soft Rank Energy). Let $P_X, P_Y \in \mathcal{P}_{ac}(\Omega)$ and let $X, X' \stackrel{i.i.d.}{\sim} P_X, Y, Y' \stackrel{i.i.d.}{\sim} P_Y$. Let $P_\lambda = \lambda P_X + (1 - \lambda) P_Y$ for $\lambda \in (0, 1)$ and let $\mathbf{R}_{\lambda, \varepsilon}$ be the entropic rank map of P_λ .

(a) *soft rank energy* (sRE) is defined as:

$$\begin{aligned} \text{sRE}_{\lambda, \varepsilon}(P_X, P_Y)^2 &\triangleq C_d \int_{\mathcal{S}^{d-1}} \int_{\mathbb{R}} (\mathbb{P}(a^\top \mathbf{R}_{\lambda, \varepsilon}(X) \leq t) - \mathbb{P}(a^\top \mathbf{R}_{\lambda, \varepsilon}(Y) \leq t))^2 dt d\kappa(a) \\ &= 2\mathbb{E}\|\mathbf{R}_{\lambda, \varepsilon}(X) - \mathbf{R}_{\lambda, \varepsilon}(Y)\| - \mathbb{E}\|\mathbf{R}_{\lambda, \varepsilon}(X) - \mathbf{R}_{\lambda, \varepsilon}(X')\| - \mathbb{E}\|\mathbf{R}_{\lambda, \varepsilon}(Y) - \mathbf{R}_{\lambda, \varepsilon}(Y')\|, \end{aligned} \quad (14)$$

where C_d and κ are the same as in Definition 2.

(b) Let $X_1, \dots, X_m \stackrel{i.i.d.}{\sim} P_X, Y_1, \dots, Y_n \stackrel{i.i.d.}{\sim} P_Y$ and let $\mathbf{R}_{\lambda, \varepsilon}^{m+n}$ be an independently estimated entropic rank map using $m+n$ samples from P_λ . The *sample soft rank energy* is defined as

$$\begin{aligned} \text{sRE}_{\lambda, \varepsilon}^{m,n}(P_X, P_Y)^2 &\triangleq \frac{2}{mn} \sum_{i=1}^m \sum_{j=1}^n \|\mathbf{R}_{\lambda, \varepsilon}^{m+n}(X_i) - \mathbf{R}_{\lambda, \varepsilon}^{m+n}(Y_j)\| - \frac{1}{m^2} \sum_{i,j=1}^m \|\mathbf{R}_{\lambda, \varepsilon}^{m+n}(X_i) - \mathbf{R}_{\lambda, \varepsilon}^{m+n}(X_j)\| \\ &\quad - \frac{1}{n^2} \sum_{i,j=1}^n \|\mathbf{R}_{\lambda, \varepsilon}^{m+n}(Y_i) - \mathbf{R}_{\lambda, \varepsilon}^{m+n}(Y_j)\|. \end{aligned} \quad (15)$$

The equivalence of the formulation in terms of integrals over \mathcal{S}^{d-1} and the formulation in terms of expectations of $\mathbf{R}_{\lambda, \varepsilon}$ is shown in Proposition 1. Comparing the definition of the rank energy (Definition 2) to the soft rank energy, the only change is the use of the entropic rank map instead of the rank map. In the subsequent sections we establish several properties of the entropic rank map and soft rank energy which motivate this choice both practically and theoretically.

The reason for using separate batches of samples is a technical artifact and is required only because our analysis requires independence between the samples used to compute the estimate of the soft rank energy and those used to estimate the map. Imposing this condition only requires a doubling of the number of samples, and in fact the choice to use $m+n$ samples to estimate the map is somewhat arbitrary, and we use this convention to make the notation and statement of the results more compact. In practice, one may even choose not to use separate batches of samples for map estimation and calculating the statistic at all, and we adopt this strategy in our experiments in Section 5.

Using a similar approach to the one taken in (7), one can also generalize soft rank energy by using a kernel function $k: \mathbb{R}^d \times \mathbb{R}^d \rightarrow \mathbb{R}$ instead of pairwise Euclidean distances.

Definition 6. Let $k : \mathbb{R}^d \times \mathbb{R}^d \rightarrow \mathbb{R}$ be a characteristic kernel. Let P_X and P_Y be two probability measures and let $X, X' \stackrel{i.i.d.}{\sim} P_X, Y, Y' \stackrel{i.i.d.}{\sim} P_Y$. Let $\mathbf{R}_{\lambda, \varepsilon}$ denote the entropic rank map of P_λ for $\lambda \in (0, 1)$.

(a) The *soft rank maximum mean discrepancy* (sRMMD) is defined as

$$\text{sRMMD}_{\lambda, \varepsilon, k}(P_X, P_Y)^2 \triangleq \mathbb{E}[k(\mathbf{R}_{\lambda, \varepsilon}(X), \mathbf{R}_{\lambda, \varepsilon}(X'))] + \mathbb{E}[k(\mathbf{R}_{\lambda, \varepsilon}(Y), \mathbf{R}_{\lambda, \varepsilon}(Y'))] \\ - 2\mathbb{E}[k(\mathbf{R}_{\lambda, \varepsilon}(X), \mathbf{R}_{\lambda, \varepsilon}(Y))].$$

(b) Let $X_1, \dots, X_m \stackrel{i.i.d.}{\sim} P_X, Y_1, \dots, Y_n \stackrel{i.i.d.}{\sim} P_Y$ and let $\mathbf{R}_{\lambda, \varepsilon}^{m+n}$ be an independently estimated rank map using $m+n$ samples from P_λ . The *sample soft rank maximum mean discrepancy* is defined as

$$\text{sRMMD}_{\lambda, \varepsilon, k}^{m, n}(P_X, P_Y)^2 \triangleq \frac{1}{m^2} \sum_{i, j=1}^m k(\mathbf{R}_{\lambda, \varepsilon}^{m+n}(X_i), \mathbf{R}_{\lambda, \varepsilon}^{m+n}(X_j)) + \frac{1}{n^2} \sum_{i, j=1}^n k(\mathbf{R}_{\lambda, \varepsilon}^{m+n}(Y_i), \mathbf{R}_{\lambda, \varepsilon}^{m+n}(Y_j)) \\ - \frac{2}{mn} \sum_{i=1}^m \sum_{j=1}^n k(\mathbf{R}_{\lambda, \varepsilon}^{m+n}(X_i), \mathbf{R}_{\lambda, \varepsilon}^{m+n}(Y_j)).$$

4 Properties of the Soft Rank Energy

4.1 Estimation of the Entropic Map

As a first step for many of our results we give a convergence rate of the sample entropic map to the population entropic map.

Theorem 2. For $P, Q \in \mathcal{P}(B_2^d(0, r))$, let T_ε be the entropic map from P to Q and let $T_\varepsilon^{n, n}$ be the estimated entropic map from P^n to Q^n . Then

$$\mathbb{E} \|T_\varepsilon^{n, n} - T_\varepsilon\|_{L^2(P)}^2 \leq C_{r, d}(\varepsilon^{-1} + \varepsilon^{1-d'/2}) \log(n)n^{-1/2} + C\sqrt{d} \exp(4r^2/\varepsilon)n^{-1/2},$$

where $d' = 2\lceil d/2 \rceil$, $C_{r, d}$ is a constant which depends only on r and d , and C is a universal constant. In particular, with everything held constant besides n we have

$$\mathbb{E} \|T_\varepsilon^{n, n} - T_\varepsilon\|_{L^2(P)}^2 \lesssim \log(n)n^{-1/2}.$$

For convenience later on, we define a shorthand for the upper bound in the Theorem 2,

$$g(n, r, d, \varepsilon) \triangleq C_{r, d}(\varepsilon^{-1} + \varepsilon^{1-d'/2}) \log(n)n^{-1/2} + C\sqrt{d} \exp(4r^2/\varepsilon)n^{-1/2}.$$

The proof of Theorem 2 is deferred to Section 8 in the supplement. The argument builds on tools developed in [40] and techniques from empirical process theory. This result stands out against results for the non-regularized transport map in that the rate is (up to log factors) $n^{-1/2}$ and only requires the support be bounded. In contrast in [41] the authors showed that under some technical conditions that the minimax optimal rate (up to log factors) is $n^{-\frac{2\alpha}{2\alpha-2+d}}$ where α is an assumed smoothness parameter of the optimal map. These rates can be incredibly slow when the dimension d dominates the smoothness α . This suggests that entropic regularization helps break the curse of dimensionality for OT map estimation.

The fact that the dimension does not play a substantial role in the sample complexity makes the entropic map an incredibly attractive tool for working with high-dimensional data. In particular, every term except for the \sqrt{d} can be controlled by choosing ε sufficiently large relative to the dimension and radius r . On the other hand, the \sqrt{d} is a relatively weak dependence since one only needs (up to log factors) to obtain enough samples to bound $\sqrt{d/n}$ instead of the typical $n^{-1/d}$. This theorem plays a key role in the subsequent results we consider and in particular it allows one to control the convergence rate of the sample soft-rank energy to the rank energy.

4.2 Fast Convergence of $\text{sRE}_{\lambda, \varepsilon}^{m, n}(P_X, P_Y)^2$

We first establish a few preliminary facts about $\text{sRE}_{\lambda, \varepsilon}(P_X, P_Y)^2$ which will be useful when combined with Theorem 2 and also demonstrate some of the important properties of the soft rank energy as a GoF statistic.

Proposition 1. *The soft rank energy satisfies the following properties:*

(a) Let $X, X' \stackrel{i.i.d.}{\sim} P_X$ and $Y, Y' \stackrel{i.i.d.}{\sim} P_Y$. Then the soft rank energy $\mathbf{sRE}_{\lambda, \varepsilon}^2$ can also be expressed as

$$\begin{aligned} \mathbf{sRE}_{\lambda, \varepsilon}(P_X, P_Y)^2 &= 2\mathbb{E}\|\mathbf{R}_{\lambda, \varepsilon}(X) - \mathbf{R}_{\lambda, \varepsilon}(Y)\| - \mathbb{E}\|\mathbf{R}_{\lambda, \varepsilon}(X) - \mathbf{R}_{\lambda, \varepsilon}(X')\| \\ &\quad - \mathbb{E}\|\mathbf{R}_{\lambda, \varepsilon}(Y) - \mathbf{R}_{\lambda, \varepsilon}(Y')\|. \end{aligned}$$

(b) $\mathbf{sRE}_{\lambda, \varepsilon}(P_X, P_Y)^2 = \mathbf{sRE}_{\lambda, \varepsilon}(P_Y, P_X)^2$.

(c) $\mathbf{sRE}_{\lambda, \varepsilon}(P_X, P_Y)^2 = 0$ if $P_X = P_Y$.

The proof is deferred to Section 9 of the supplement. Property (a) is particularly useful because it allows one to use an easily computed formula instead of estimating the integrals and probabilities in (14). Properties (b) and (c) make $\mathbf{sRE}_{\lambda, \varepsilon}(P_X, P_Y)^2$ a good candidate for measuring the GoF between distributions.

One can also show that under some regularity conditions that the original rank energy is recovered by sending ε to 0, which further motivates the notion of the soft rank energy.

Proposition 2. Let $P_X, P_Y \in \mathcal{P}_{ac}([0, 1]^d)$ and $\lambda \in (0, 1)$ be such that for $\mathbf{R}_\lambda = \nabla\phi$ we have $aI \preceq \nabla\phi \preceq bI$ for some $0 < a, b$, and $\mathbf{R}_\lambda^{-1} \in \mathcal{C}^\alpha$ for some $\alpha \geq 2$. Then

$$\lim_{\varepsilon \rightarrow 0^+} \mathbf{sRE}_{\lambda, \varepsilon}(P_X, P_Y)^2 = \mathbf{RE}_\lambda(P_X, P_Y)^2.$$

The proof appears in the supplement. Implicit in the proof of Proposition 2 is a result that also characterizes the degree of approximation of soft rank energy with rank energy as a function of the entropy regularization ε .

An important consequence of Theorem 2 is a matching convergence rate for the sample soft rank energy:

Theorem 3. Let $\lambda \in (0, 1)$ and $P_X, P_Y \in \mathcal{P}(B_2^d(0, r))$ for $r \geq \sqrt{d}$. Then

$$\|\mathbf{sRE}_{\lambda, \varepsilon}^{m, n}(P_X, P_Y)^2 - \mathbf{sRE}_{\lambda, \varepsilon}(P_X, P_Y)^2\|_{L^2}^2 \leq \frac{72}{\min(\lambda, 1 - \lambda)} g(m + n, r, d, \varepsilon) + \frac{9d(m + n)}{mn}$$

The proof, which is deferred to Section 11 in the supplement, relies on four ingredients: Theorem 2, Proposition 1 (a), several applications of the triangle and reverse triangle inequalities, as well as the Efron-Stein inequality ([42] Theorem 3.1). The first term in the bound can be thought of as the amount of error incurred from estimating $\mathbf{R}_{\lambda, \varepsilon}$ using $m + n$ samples, while the second term bounds the error incurred from estimating an expectation by sampling.

The factor of $\frac{1}{\min(\lambda, 1 - \lambda)}$ comes from the fact that in $\mathbf{sRE}_{\lambda, \varepsilon}^{m, n}(P_X, P_Y)^2$ there is an equal weight given to both $\{X_1, \dots, X_m\}$ and $\{Y_1, \dots, Y_n\}$, even if $m \ll n$ or vice versa. In contrast, the estimate of $\mathbf{R}_{\lambda, \varepsilon}^{m+n}$ weights P_X and P_Y proportionally to λ and $(1 - \lambda)$ respectively. The intuition here is that if one pays little attention to constructing a good map on the support of P_X then one should expect a large amount of error for $\mathbf{R}_\lambda(X_i)$ which the weighting scheme only amplifies when computing the statistic.

In a similar flavor, one can show that sample version of sRMMD converges quickly in expectation to the population version. Again this is a consequence of Theorem 2.

Theorem 4. Let k be a characteristic kernel such that for all x , the function $k(x, \cdot)$ is l -Lipschitz with respect to the Euclidean norm. Then sample version of the soft rank maximum mean discrepancy satisfies

$$\|\mathbf{sRMMD}_{\lambda, \varepsilon, k}^{m, n}(P_X, P_Y)^2 - \mathbf{sRMMD}_{\lambda, \varepsilon, k}(P_X, P_Y)^2\|_{L^2}^2 \leq \frac{72l^2}{\min(\lambda, 1 - \lambda)} g(m + n, r, d, \varepsilon) + \frac{9dl^2(m + n)}{mn}.$$

The proof follows essentially the same arguments as the one used to prove Theorem 3, but uses the Lipschitz assumption in place of the reverse-triangle inequality. A discussion of this trick is given in Section 12. We remark that many of the most popular kernels do satisfy a Lipschitz continuity condition, and practically all do when restricted to bounded domains, so this restriction is not stringent.

4.3 Utility as a Loss Function

There are many examples in practice where one will try to train a generative model to create high-dimensional data (for example images, video or, audio signals), which requires a measure of how closely an artificially generated dataset matches a real dataset. In high dimensions there is a need for test statistics that converge

rapidly since otherwise one won't be able to distinguish model performance from statistical fluctuations. This is one of the main reasons (along with computational ease) that MMD and energy distances have become prominent in generative modelling. These statistics both have $n^{-1/2}$ convergence rates to their population variants, which is also achieved (up to logarithmic factors) by both of our proposed sRE and sRMMD. We believe this makes sRE and SRMMD strong contenders for high-dimensional generative modelling.

Another important note is that the computation of a high fidelity estimate of the soft rank energy is easily done through the use of Sinkhorn's algorithm [23] which is based on fixed point iterations. One can perform a fixed number of iterations and then employ automatic differentiation [43] to obtain a gradient through this method. This approach is not novel to this work and so-called "Sinkhorn layers" have become popular in the neural network literature [44, 45, 46]. With these in hand, the computation of the soft rank energy and soft rank MMD becomes straightforward: simply attach a series of Sinkhorn layers to the end of a generative model to obtain the entropic rank map, use that rank map to transform the data, and then compute the soft rank energy or MMD on the transformed data.

5 Applications

5.1 sRE and sRMMD as the Loss Function in a Generative Model

Generative modeling is used to implicitly approximate a complex, high-dimensional distribution from a finite number of samples. When trained successfully, it allows one to draw new samples from the underlying distribution. A seminal framework to learn the generative model is the *generative adversarial network (GAN)* [47] that optimizes a difficult minimax program. A simpler approach known as a *generative moment matching network (GMMN)* [37] instead minimizes the differentiable MMD [31]. In this section, we train a generative model to minimize the proposed sRE and sRMMD and illustrate their effectiveness compared to GMMN on the benchmark MNIST digits data set [48]. A brief description of the model architecture and the training procedure is given below.

Architecture: We use the same architecture used in [37] which consists of (a) a generative network and (b) an auto-encoder [49]. The generative network consists of 3 intermediate ReLU nonlinear layers and one logistic sigmoid output layer. The auto-encoder has 4 layers, 2 for the encoder and 2 for the decoder with sigmoid nonlinearities. The auto-encoder is used to learn an almost lossless low-dimensional latent space for the high-dimensional, complex data. The generative network is used to generate samples in this low-dimensional space. The trained decoder then turns these samples into meaningful high-dimensional data. For further details, we refer the reader to [37].

Training: We train the auto-encoder and generator network separately. First an auto-encoder is learned to produce a low-dimensional representation for the MNIST digits with latent dimension of 8. Then we train the generative network to learn to generate samples in this low-dimensional representation space via minimizing either sRE or sRMMD. Both sRE and sRMMD are computed with entropic regularizer $\varepsilon = 1$, where the soft rank maps are obtained via Sinkhorn's algorithm [19] with a maximum of 5000 iterations. To compute sRMMD, we employ a Gaussian mixture kernel $k(x, x') = \frac{1}{6} \sum_{q=1}^6 \exp(-\frac{\|x-x'\|^2}{2\sigma_q^2})$ with the bandwidth parameter $\sigma = (1, 2, 4, 8, 16, 32)$.

Both the auto-encoder and the generator are trained on a minibatch size of 256 using the Adam optimizer [50] with a learning rate of 0.001 over 100 epochs.

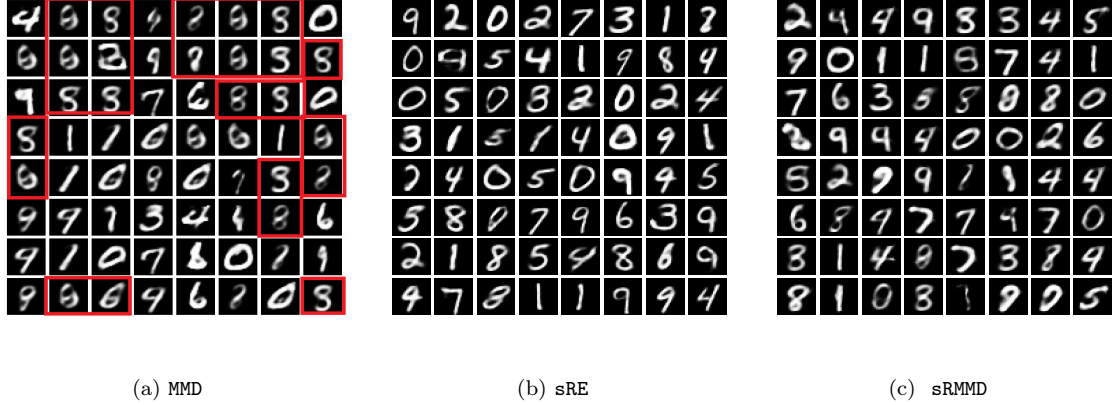


Figure 1: Comparison of the MNIST digits generated via minimizing MMD, sRE, and sRMMD. The model architecture and training procedure are kept same for all methods. Red boxes in (a) indicate the abundance of the same digit e.g., 8 when using MMD.

Result: It is apparent that the generator minimizing MMD lacks in diversity (mostly producing 8’s). Besides, most of the digits are barely recognizable which indicates that the generator performs poorly if it is trained to minimize MMD. In contrast, the generator minimizing either sRE or sRMMD produces a diverse set of digits and almost all of them are unambiguous. Thus, both sRE and sRMMD appear to be better choices to minimize than MMD. Though in the current setup, the generator minimizing sRMMD works well, we empirically observe that the performance (e.g., diversity, unambiguity) heavily depends on the choice of the bandwidth parameter σ and the entropic regularizer ε . In our case, we find it beneficial to use smaller σ when using a larger ε . Plots showing the dependency of the sRMMD generator on ε and σ can be found in Section 14.1 in the supplement.

5.2 Generating Valid Knockoffs using sRMMD

In applications where the goal is to discover relevant features that can explain certain outcomes (e.g., metabolites or genes related to Crohn’s disease [51, 52]), it is important that the set of selected features contains as few false discoveries as possible. One way to do that is to control the false discovery rate (FDR) at a prespecified level $q \in (0, 1)$. The classical setup to control FDR depends on assumptions on how the features and the outcomes are related [53, 54]. A novel FDR control framework, namely Model-X knockoffs [55], provides an alternative to the traditional methods by assuming no knowledge about the association between the features and the outcomes. Given the set of explanatory random variables $X = (X^1, \dots, X^d) \in \mathbb{R}^d$ and the outcome variable $Y \in \mathbb{R}$, the Model-X knockoff framework works in four steps to select relevant variables while controlling the FDR.

- (a) Generate a synthetic set of features called knockoffs $\tilde{X} = (\tilde{X}^1, \dots, \tilde{X}^d)$ which are independent of Y conditionally on X , and satisfy what is referred to as the *pairwise exchangeability condition*.

$$(X, \tilde{X})_{\text{swap}(B)} \stackrel{d}{=} (X, \tilde{X}), \forall B \subset \{1, \dots, d\}, \quad (16)$$

where $\text{swap}(B)$ exchanges the positions of any variable $X_j, j \in B$, with its knockoff \tilde{X}_j .

- (b) Produce a knockoff statistic $W_j = w_j([X, \tilde{X}], y)$ for $j \in \{1, \dots, d\}$ to assess the importance of each feature. Here, $w_j(\cdot)$ is any function with the flip sign property⁵.
- (c) Find a data dependent threshold τ via,

$$\tau = \min_{t > 0} \left\{ t : \frac{1 + |\{j : W_j \leq -t\}|}{|\{j : W_j \geq t\}|} \leq q \right\}. \quad (17)$$

- (d) Select the set of variables: $\hat{S} = \{j : W_j \geq \tau\}$.

⁵a function f is said to have flip-sign property if $f(u, v) = -f(v, u)$.

Performance of the Model-X framework depends on the quality of the knockoffs, that is, to what extent they satisfy pairwise exchangeability. One way to achieve this is to approximate only the first two moments (mean and covariance) assuming that the joint distribution of X is a multivariate Gaussian. This is often called a second-order method [55]. Other methods proposed in [56, 57, 58, 59] take a generative modeling approach to satisfy (18) and sample the knockoffs. A brief descriptions of these methods is provided in Section 13 in the supplement.

In this paper, we take a generative modeling approach where we propose to use sRMMD as the loss to satisfy the pairwise exchangeability condition (16).

5.2.1 An sRMMD-Based Knockoff Generator

We use a generative model similar to the one used in [58]. The generative model has a deep neural network f_θ that takes $X \sim P_X \in \mathbb{R}^d$ and a noise vector $V \sim \mathcal{N}(0, I_d) \in \mathbb{R}^d$ as inputs and returns an approximate copy of knockoff $\tilde{X} = f_\theta(X, V) \in \mathbb{R}^d$. Here θ denotes the set of the parameters which is learned from the data. The network is fed with $\{X_i\}_{i=1}^n \in \mathbb{R}^d$ independent observations and generates $\tilde{X}_i = f_\theta(X_i, V_i)$ for $1 \leq i \leq n$. Let $\mathbf{X}, \tilde{\mathbf{X}} \in \mathbb{R}^{n \times d}$ be the matrices having these observations and their knockoffs as row vectors, respectively. To ensure that the knockoffs are of good quality (i.e., the joint distribution of (X_i, \tilde{X}_i) satisfies (16) and X_i and \tilde{X}_i are as different as possible, for $1 \leq i \leq n$), we minimize the following loss,

$$\ell(\mathbf{X}, \tilde{\mathbf{X}}) = \underbrace{\text{sRMMD}\left[(\mathbf{X}', \tilde{\mathbf{X}}'), (\tilde{\mathbf{X}}'', \mathbf{X}'')\right]}_{\text{full-swap}} + \underbrace{\text{sRMMD}\left[(\mathbf{X}', \tilde{\mathbf{X}}'), (\mathbf{X}'', \tilde{\mathbf{X}}'')\right]}_{\text{partial-swap}} + \gamma \ell_{Decor}(\mathbf{X}, \tilde{\mathbf{X}}), \quad (18)$$

where $\mathbf{X}', \mathbf{X}'' \in \mathbb{R}^{n/2 \times d}$, and $\tilde{\mathbf{X}}', \tilde{\mathbf{X}}'' \in \mathbb{R}^{n/2 \times d}$ are obtained by randomly splitting \mathbf{X} and $\tilde{\mathbf{X}}$ in half and B is a chosen random subset of $\{1, \dots, d\}$, such that $j \in B$ with probability $1/2$. We adapt the idea of splitting and swapping from [58]. The first two terms in (18) help to achieve pairwise exchangeability. The last term in (18) trades off power versus FDR by decorrelating the variables with the knockoffs. We adapt this loss term from [58] with hyperparameter $\gamma > 0$, which is defined as

$$\ell_{Decor}(\mathbf{X}, \tilde{\mathbf{X}}) = \|\text{diag}(\Sigma_{X\tilde{X}}) - 1 + s_{\text{SDP}}^*(\Sigma_{XX})\|_2^2.$$

Σ_{XX} and $\Sigma_{X\tilde{X}}$ are the empirical covariance matrix of X and the empirical cross covariance matrix between X and \tilde{X} , respectively, and $s_{\text{SDP}}^*(\Sigma_{XX}) = \arg \min_{s \in [0, 1]^d} \sum_{j=1}^d |1 - s_j|$ such that $2\Sigma_{XX} \succeq \text{diag}(s) \succeq 0$. The loss (18) is differentiable and therefore any gradient descent method can be adopted to train the generative model. Generally training is done in minibatches size of $m \ll n$. At each epoch of training, for each batch of size m , only one B is picked randomly to compute (18), which may prevent one to achieve pairwise exchangeability (16) to a great extent. That is why, we recommend generating multiple batches by reshuffling the training set of size n several times at each epoch so that multiple sets of random B are picked. To train efficiently and effectively, we also suggest using $\varepsilon \propto d$ to compute sRMMD. This suggestion is backed by the empirical evidence shown in Section 14.2 in the supplement. In addition, we provide empirical justification for using sRMMD over sRE in (18) in Section 14.3 in the supplement.

The details of the generative model and the training procedure for any fixed ε and γ are summarized in Sections 13.1 and 13.2 in the supplement, respectively.

5.2.2 Knockoff Experiments on Synthetic Benchmarks

We compare the performance of sRMMD knockoffs with other benchmarks, namely second-order knockoffs [55], knockoffGAN [60], deep knockoff [58], and deep direct likelihood knockoff (DDLK) [59] on several synthetic (four Gaussian and non-Gaussian distributional settings adapted from [58]) and a real-world dataset. To be on an equal footing with deep knockoff, we remove the second-order term from the loss used in [58] and denote it as the MMD knockoff. For all comparisons, we use publicly available implementations of the code and used their recommended configurations and hyperparameters (if available).

For each distributional setting, we train the knockoff generator on a set of $n = 2000$ samples each of dimension $d = 100$. We compute sRMMD using a Gaussian mixture kernel $k(x, x') = \frac{1}{8} \sum_{k=1}^8 \exp(-\|x - x'\| / (2\sigma_k^2))_2^2$ with $\sigma = (1, 2, 4, 8, 16, 32, 64, 128)$, where the entropic ranks are obtained via Sinkhorn's algorithm (with a maximum of 5000 iterations). We update the network (18) using stochastic gradient descent with momentum [34]. The minibatch size, learning rate and the number of epochs are set to 500, 0.01, and 100, respectively. The training procedure is detailed in Algorithm 13.2 in the supplement.

Below, we briefly describe each distributional setting and other optimal hyperparameters e.g., ε, γ for training.

- (a) **Multivariate Gaussian AR1:** An autoregressive model of order one in which $X \sim \mathcal{N}(0, \Sigma)$, $\Sigma_{ij} = \rho^{|i-j|}$, $\rho = 0.5$. We set the decorrelation penalty $\gamma = 1$, entropic regularizer $\varepsilon = 100$.
- (b) **Gaussian Mixture Model (GMM):** $X \sim \sum_{k=1}^4 \tau_k \mathcal{N}(0, \Sigma_k)$, where the covariance matrix is $(\Sigma_k)_{ij} = \rho_k^{|i-j|}$ for $k = 1, \dots, 4$. $(\rho_1, \rho_2, \rho_3, \rho_4) = (0.6, 0.4, 0.2, 0.1)$, $(\tau_1, \tau_2, \tau_3, \tau_4) = (0.27, 0.23, 0.23, 0.27)$. We set $\gamma = 1$, and $\varepsilon = 100$.
- (c) **Multivariate Student's t -Distribution:** A heavy-tailed distribution with zero mean and $\nu = 3$ degrees of freedom, such that $X = \sqrt{\frac{\nu-2}{\nu}} \frac{Z}{\sqrt{\Gamma}}$, where $Z \sim \mathcal{N}(0, \Sigma)$ with Σ as in (a) and Γ is independently drawn from a Gamma distribution with shape and rate parameters both equal to $\nu/2$. We set $\gamma = 1$ and $\varepsilon = 100$.
- (d) **Sparse Gaussian:** Given $W \sim \mathcal{N}(0, 1)$ and a random subset $A \in \{1, \dots, p\}$ of size $|A| = L$, we set
$$X_j = \sqrt{\frac{\binom{L}{p}}{\binom{L-1}{p-1}}} \begin{cases} W, & \text{if } j \in A, \\ 0, & \text{otherwise.} \end{cases} \quad \text{We set } L = 30, \gamma = 0.1 \text{ and } \varepsilon = 100.$$

After training, we draw $m_t = 200$ new i.i.d. samples as the test set and simulate the outcome as $\mathbf{y} = \mathbf{X}_t \beta + \mathbf{z}$, where $\mathbf{X}_t \in \mathbb{R}^{m_t \times d}$, $d = 100$, $\mathbf{y} \in \mathbb{R}^{m_t}$, $\mathbf{z} \sim \mathcal{N}(0, I)$, and $\beta \in \mathbb{R}^d$ is the coefficient vector. The vector β is all zeros except randomly chosen 20 entries, each having an amplitude equal to $v/\sqrt{m_t}$, where v is the amplitude parameter. Then we generate the knockoff matrix $\tilde{\mathbf{X}}_t$ and perform LASSO regression [61] on $[\mathbf{X}_t, \tilde{\mathbf{X}}_t]$ via solving,

$$\begin{bmatrix} \hat{\beta} \\ \hat{\tilde{\beta}} \end{bmatrix} = \arg \min_{(\beta, \tilde{\beta})} \frac{1}{m_t} \left\| \mathbf{y} - [\mathbf{X}_t \tilde{\mathbf{X}}_t] \begin{bmatrix} \beta \\ \tilde{\beta} \end{bmatrix} \right\|_2^2 + \alpha_L \left\| \begin{bmatrix} \beta \\ \tilde{\beta} \end{bmatrix} \right\|_1, \quad (19)$$

where the $\hat{\beta} \in \mathbb{R}^d$ and $\hat{\tilde{\beta}} \in \mathbb{R}^d$ are the coefficient vectors corresponding to the original variables, and knockoff variables, respectively and α_L is the LASSO penalty. We consider LASSO regression since it works best when the true model is close to linear. We estimate the coefficient vectors using $\alpha_L = 0.01$ and take the absolute difference $W_j = |\hat{\beta}_j| - |\hat{\tilde{\beta}}_j|$ as the knockoff statistic for $1 \leq j \leq d$. We repeat the experiments 500 times for different values of v , and compare the power versus FDR tradeoff with the benchmarks.

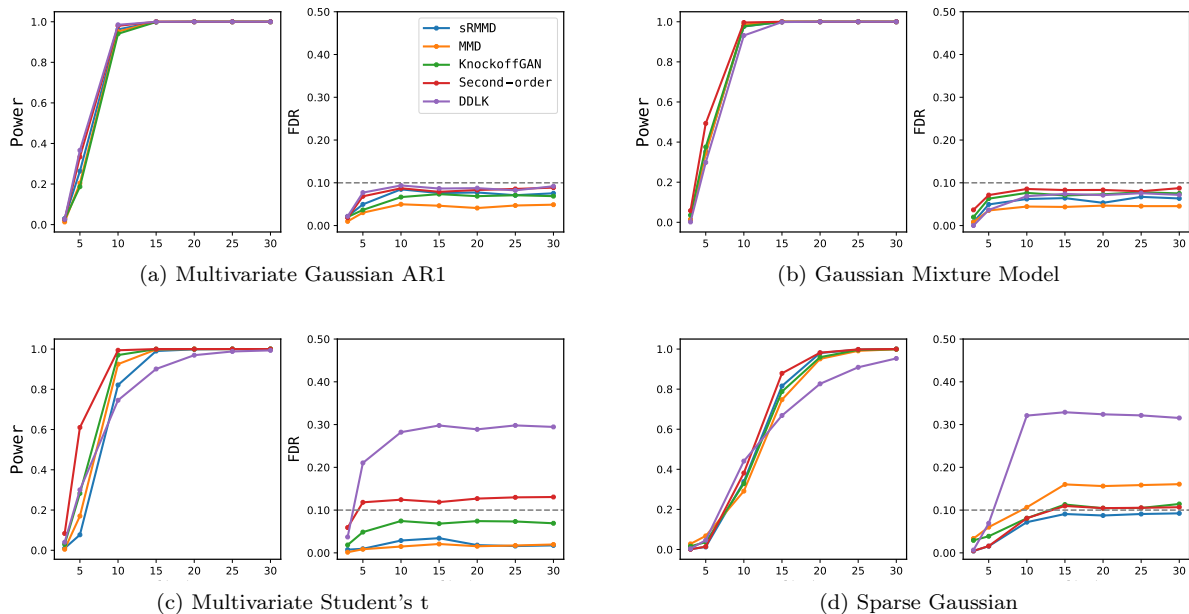


Figure 2: Average FDR and power computed over 500 independent experiments are shown on the y -axis for each synthetic benchmark. The FDR level is set to 0.1. The x -axis represents the amplitude parameter v .

Result: Figure 2 shows the FDR versus power tradeoff with respect to the amplitude parameter v . In case of Gaussian AR1 setting, all methods showcase similar detection power and FDR control at level $q = 0.1$ over the entire amplitude region. In the GMM setting, we observe that each method achieves similar power and controls the FDR at $q = 0.1$ like the multivariate Gaussian setting. This can be explained by the fact

that here the GMM and Gaussian settings belong to the same exact family of distributions since the sum of independent Gaussians is a Gaussian. For the heavy-tailed multivariate Student’s t -distribution, sRMMD, MMD and knockoffGAN can control the FDR at $q = 0.1$, however, the second-order method fails to control the FDR, likely because it assumes that the underlying distribution is multivariate Gaussian. DDLK also fails to control the FDR in this case. For the sparse Gaussian setting, sRMMD knockoffs showcase the best FDR versus power tradeoff among all methods over the entire amplitude region. Second-order, and knockoffGAN methods also achieve similar power and control the FDR at $q = 0.1$. In contrast, MMD and DDLK knockoffs fail to control the FDR at $q = 0.1$.

We do acknowledge the fact that in all settings knockoffGAN also achieves high power and controls the FDR at $q = 0.1$. KnockoffGAN is a complex generative adversarial architecture that requires training of four interconnected neural networks. Instead of minimizing a GoF statistic (e.g., MMD or sRMMD), knockoffGAN minimizes the binary cross-entropy loss in order to satisfy the pairwise exchangeability condition. In addition, knockoffGAN uses the mutual information loss to make the variables and their knockoffs as independent as possible which is a much stronger notion than decorrelation. In contrast to knockoffGAN, our method is simple and easy to implement, yet achieves comparable FDR versus power tradeoff.

5.2.3 Application to a Real Metabolomics Dataset

We apply the proposed knockoff filter to a publicly available metabolomics dataset in order to discover important biomarkers with FDR guarantees. We use a study titled *Longitudinal Metabolomics of the Human Microbiome in Inflammatory Bowel Disease* [51] which is available at the Metabolomics Workbench through the National Metabolomics Data Repository (NMDR) website <https://www.metabolomicsworkbench.org/> under the project DOI: 10.21228/M82T15 and sponsored by the Common Fund of the NIH. The study is related inflammatory bowel disease (IBD) and conditions including ulcerative colitis (UC) and Crohn’s disease (CD), and seeks to identify important metabolites (biological products produced as intermediates during metabolism) associated with these diseases. We use the *C18 Reverse-Phase Negative Mode* dataset which was collected under this study. The dataset contains 546 samples, each having an average of 91 metabolites. Each sample belongs to one of the three classes (UC, CD, and non-IBD) and assign the response y to one of $\{0, 1, 2\}$ to reflect this. We preprocess the dataset in three steps: (i) removing the metabolites that have more than 20% missing values which retains only 80 metabolites out of 91, (ii) applying k-nearest neighbor (KNN) missing value imputation technique to fill out the existing missing values, and (ii) standardizing the features by removing the mean and scaling to unit variance. For this dataset, we use the same generative architecture described in Section 5.2.1. We choose entropic regularizer $\varepsilon = 50$ and kernel bandwidth $\sigma = (1, 2, 4, 8, 16, 32, 64, 128)$ to compute sRMMD. We pick $\gamma = 1$. We train the generator on a minibatch of 250 samples according to Algorithm 13.2.

After training, we generate the knockoffs, apply the random forest (RF) classifier [62] to produce knockoff statistics. The two RF parameters—the number of features that are randomly selected at each node and the number of trees—are set to 9 (the closest integer to the recommended $\sqrt{80}$) and 500, respectively. We take the difference between the feature importance scores [62] corresponding to the original variables and the knockoffs as the knockoff statistics. Since the generated knockoffs are random, we repeat the whole procedure 100 times and select those metabolites that appear at least 70 times out of 100 instances, setting the FDR level at $q = 0.05$. In absence of the ground truth, to qualitatively analyze the performance we cross-reference the selected metabolites with published literature. We list the selected metabolites along the references in Table 2.

Method (N)	sRMMD (21)	Second Order (16)	MMD (27)	KnockoffGAN (20)	Reference
Metabolites					
1.2.3.4-tetrahydro-beta-carboline-1.3-dicarboxylate	✓	✓	✓	✓	[63]
urobilin	✓	✓	✓	✓	[64]
adrenate	✓	✓	✓	✓	[51]
12.13-diHOME	✓	✓	✓	✓	[65]
salicylate	✓	✓	✓	✓	[66]
saccharin	✓	✓	✓	✓	[64]
caproate	✓	✓	✓	✓	[67]
olmesartan	✓	✓	✓	✓	[68]
phenyllactate	✓	x	✓	✓	[69]
tauroolithocholate	✓	x	✓	x	[70]
docosapentaenoate	✓	✓	✓	✓	[71]
docosahexaenoate	✓	x	✓	✓	[71]
dodecanedioate	✓	x	✓	x	[67]
hydrocinnamate	✓	✓	✓	✓	[67]
eicosatrienoate	✓	x	✓	✓	[72]
9.10-diHOME	✓	✓	✓	✓	[51]
arachidonate	x	x	✓	✓	[51]
myristate	x	x	x	x	[73]
Total = 18	16	11	17	15	
Detection power (%)	76	69	63	75	

Table 2: N is the total number of selected metabolites. DDLK finds almost every metabolites as significant, therefore loses its purpose as a FDR control technique. That is why we refrain from adding it here.

Out of 80, we have found 18 metabolites to have an impact on IBD in the published literature. Though MMD knockoffs detect most of the significant metabolites, the detection percentage is very low. Second-order method performs better compared to MMD in terms of power though it misses several significant metabolites. On the other hand, sRMMD and KnockoffGAN have almost the same detection power, and outperform second-order and MMD methods.

6 Conclusion and Future Directions

In this paper, we identified some major limitations in use of the recently proposed multivariate rank-based GoF statistics based on the theory of optimal transportation, namely high sample and computational complexity in high dimensions and lack of differentiability, which limits their use in gradient-based machine learning methods. We show that using entropic maps derived from entropic regularization of the optimal transportation problem alleviates these issues and leads to efficient statistics for GoF testing. Furthermore, we show that this relaxation allows the use of these GoF statistics for generative modeling in high dimensions.

One future research direction is to evaluate the effect of different distributions as the target distribution in place of $\text{Unif}([0, 1]^d)$ such as spherical uniform distribution [9]. It may be important to characterize the effect of this choice for the soft rank and soft rank-based statistics proposed in this paper.

A related problem concerns the dependence on ε in the entropic regularization. In particular, the *convergence rate* of the sRE and sRMMD to the RE and RMMD as $\varepsilon \rightarrow 0^+$ is the subject of ongoing work. While Proposition 2 provides a coarse convergence result, we conjecture that a more precise bound may hold and that the extra smoothness assumptions on the measures may not be required for this result to be true, and that compactness and together with weaker smoothness assumptions may suffice. Beyond analyzing the convergence rate in ε , it is important to understand the advantages of taking $\varepsilon \gg 0$, beyond the improvements in statistical and computational complexity. For example, one may wish to understand the impact ε has on the robustness, or stability, of sRE in response to small perturbations in the distributions.

Acknowledgements

This research was sponsored by the U.S. Army DEVCOM Soldier Center, and was accomplished under Cooperative Agreement Number W911QY-19-2-0003. The views and conclusions contained in this document are those of the authors and should not be interpreted as representing the official policies, either expressed or implied, of the U.S. Army DEVCOM Soldier Center, or the U.S. Government. The U. S. Government is authorized to reproduce and distribute reprints for Government purposes notwithstanding any copyright notation hereon.

SM was totally supported by W911QY-19-2-0003. MW is supported by NSF CCF-1553075. JMM acknowledges support from the NSF through grants DMS-1912737, DMS-1924513. SA acknowledges support by NSF CCF-1553075, NSF DRL 1931978, NSF EEC 1937057, and AFOSR FA9550-18-1-0465. All authors acknowledge support through the Tufts TRIPODS Institute, supported by the NSF under grant CCF-1934553.

References

- [1] Nikolai V. Smirnov. On the estimation of the discrepancy between empirical curves of distribution for two independent samples. *Bull. Math. Univ. Moscou*, 2(2):3–14, 1939.
- [2] Frank Wilcoxon. Probability tables for individual comparisons by ranking methods. *Biometrics*, 3(3):119–122, 1947.
- [3] Aaditya Ramdas, Nicolás García Trillos, and Marco Cuturi. On wasserstein two-sample testing and related families of nonparametric tests. *Entropy*, 19(2):47, 2017.
- [4] Kevin C. Cheng, Eric L. Miller, Michael C. Hughes, and Shuchin Aeron. On matched filtering for statistical change point detection. *IEEE Open Journal of Signal Processing*, 1:159–176, 2020.
- [5] Arthur Gretton, Kenji Fukumizu, Choon Teo, Le Song, Bernhard Schölkopf, and Alex Smola. A kernel statistical test of independence. *Advances in neural information processing systems*, 20, 2007.
- [6] Ruth Heller, Yair Heller, and Malka Gorfine. A consistent multivariate test of association based on ranks of distances. *Biometrika*, 100(2):503–510, 2013.
- [7] Gabor J Szekely, Maria L Rizzo, et al. Hierarchical clustering via joint between-within distances: Extending ward’s minimum variance method. *Journal of classification*, 22(2):151–184, 2005.
- [8] Marc Hallin. On distribution and quantile functions, ranks and signs in \mathbb{R}^d . *ECARES Working Papers*, 2017.
- [9] Marc Hallin, Eustasio del Barrio, Juan Cuesta-Albertos, and Carlos Matrán. Distribution and quantile functions, ranks and signs in dimension d : A measure transportation approach. *The Annals of Statistics*, 49(2):1139–1165, 2021.
- [10] Victor Chernozhukov, Alfred Galichon, Marc Hallin, and Marc Henry. Monge–Kantorovich depth, quantiles, ranks and signs. *Annals of Statistics*, 45(1):223–256, 2017.
- [11] Nabarun Deb and Bodhisattva Sen. Multivariate rank-based distribution-free nonparametric testing using measure transportation. *Journal of the American Statistical Association*, pages 1–16, 2021.
- [12] Cédric Villani. *Optimal Transport: Old and New*, volume 338. Springer, 2009.
- [13] Filippo Santambrogio. Optimal transport for applied mathematicians. *Birkhäuser, NY*, 55(58-63):94, 2015.
- [14] Marc Hallin. Measure transportation and statistical decision theory. *Annual Review of Statistics and its Application*, 9, 2021.
- [15] Robert J. McCann. Existence and uniqueness of monotone measure-preserving maps. *Duke Mathematical Journal*, 80(2):309–324, 1995.
- [16] Yann Brenier. Polar factorization and monotone rearrangement of vector-valued functions. *Communications on Pure and Applied Mathematics*, 44(4):375–417, 1991.
- [17] Chun-Liang Li, Wei-Cheng Chang, Yu Cheng, Yiming Yang, and Barnabás Póczos. MMD GAN: Towards deeper understanding of moment matching network. *Advances in neural information processing systems*, 30, 2017.
- [18] Martin Arjovsky, Soumith Chintala, and Léon Bottou. Wasserstein generative adversarial networks. In *International conference on machine learning*, pages 214–223. PMLR, 2017.
- [19] Gabriel Peyré, Marco Cuturi, et al. Computational optimal transport: With applications to data science. *Foundations and Trends® in Machine Learning*, 11(5-6):355–607, 2019.
- [20] Rina Foygel Barber and Emmanuel J. Candès. Controlling the false discovery rate via knockoffs. *Annals of Statistics*, 43(5):2055–2085, 2015.
- [21] Gaspard Monge. *Mémoire sur la théorie des déblais et des remblais*. De l’Imprimerie Royale, 1781.
- [22] Filippo Santambrogio. Optimal transport for applied mathematicians. *Birkhäuser, NY*, 55(58-63):94, 2015.

- [23] Marco Cuturi. Sinkhorn distances: Lightspeed computation of optimal transport. *Advances in neural information processing systems*, 26:2292–2300, 2013.
- [24] Aude Genevay, Marco Cuturi, Gabriel Peyré, and Francis Bach. Stochastic optimization for large-scale optimal transport. *Advances in neural information processing systems*, 29, 2016.
- [25] Christian Clason, Dirk A Lorenz, Hinrich Mahler, and Benedikt Wirth. Entropic regularization of continuous optimal transport problems. *Journal of Mathematical Analysis and Applications*, 494(1):124432, 2021.
- [26] Aude Genevay. *Entropy-regularized optimal transport for machine learning*. PhD thesis, Paris Sciences et Lettres (ComUE), 2019.
- [27] Morgan A Schmitz, Matthieu Heitz, Nicolas Bonneel, Fred Ngole, David Coeurjolly, Marco Cuturi, Gabriel Peyré, and Jean-Luc Starck. Wasserstein dictionary learning: Optimal transport-based unsupervised nonlinear dictionary learning. *SIAM Journal on Imaging Sciences*, 11(1):643–678, 2018.
- [28] Gábor J Székely and Maria L Rizzo. Energy statistics: A class of statistics based on distances. *Journal of Statistical Planning and Inference*, 143(8):1249–1272, 2013.
- [29] Ludwig Baringhaus and Carsten Franz. On a new multivariate two-sample test. *Journal of Multivariate Analysis*, 88(1):190–206, 2004.
- [30] Jeff M Phillips and Suresh Venkatasubramanian. A gentle introduction to the kernel distance. *arXiv preprint arXiv:1103.1625*, 2011.
- [31] Arthur Gretton, Karsten M Borgwardt, Malte J. Rasch, Bernhard Schölkopf, and Alexander Smola. A kernel two-sample test. *The Journal of Machine Learning Research*, 13(1):723–773, 2012.
- [32] Roswitha Hofer. On the distribution properties of Niederreiter–Halton sequences. *Journal of Number Theory*, 129(2):451–463, 2009.
- [33] R. M. Dudley. The Speed of Mean Glivenko-Cantelli Convergence. *The Annals of Mathematical Statistics*, 40(1):40 – 50, 1969.
- [34] Léon Bottou. Stochastic gradient descent tricks. In *Neural networks: Tricks of the trade*, pages 421–436. Springer, 2012.
- [35] Stephen Boyd, Stephen P. Boyd, and Lieven Vandenbergh. *Convex optimization*. Cambridge university press, 2004.
- [36] Akshay Agrawal, Brandon Amos, Shane Barratt, Stephen Boyd, Steven Diamond, and J. Zico Kolter. Differentiable convex optimization layers. *Advances in neural information processing systems*, 32, 2019.
- [37] Yujia Li, Kevin Swersky, and Rich Zemel. Generative moment matching networks. In *International Conference on Machine Learning*, pages 1718–1727. PMLR, 2015.
- [38] Marc G. Bellemare, Ivo Danihelka, Will Dabney, Shakir Mohamed, Balaji Lakshminarayanan, Stephan Hoyer, and Rémi Munos. The Cramer distance as a solution to biased Wasserstein gradients. *arXiv*, 2017.
- [39] Jonathan Niles-Weed and Philippe Rigollet. Estimation of Wasserstein distances in the spiked transport model. *arXiv preprint arXiv:1909.07513*, 2019.
- [40] Aram-Alexandre Pooladian and Jonathan Niles-Weed. Entropic estimation of optimal transport maps. *arXiv preprint arXiv:2109.12004*, 2021.
- [41] Jan-Christian Hütter and Philippe Rigollet. Minimax estimation of smooth optimal transport maps. *The Annals of Statistics*, 49(2):1166 – 1194, 2021.
- [42] Stéphane Boucheron, Gábor Lugosi, and Pascal Massart. *Concentration inequalities: A nonasymptotic theory of independence*. Oxford university press, 2013.
- [43] Adam Paszke, Sam Gross, Soumith Chintala, Gregory Chanan, Edward Yang, Zachary DeVito, Zeming Lin, Alban Desmaison, Luca Antiga, and Adam Lerer. Automatic differentiation in pytorch, 2017.
- [44] Ryan Prescott Adams and Richard S. Zemel. Ranking via Sinkhorn propagation, 2011.

- [45] Patrick Emami and Sanjay Ranka. Learning permutations with Sinkhorn policy gradient. *arXiv preprint arXiv:1805.07010*, 2018.
- [46] Jean Feydy, Thibault Séjourné, François-Xavier Vialard, Shun-ichi Amari, Alain Trounev, and Gabriel Peyré. Interpolating between optimal transport and MMD using Sinkhorn divergences. In *The 22nd International Conference on Artificial Intelligence and Statistics*, pages 2681–2690. PMLR, 2019.
- [47] Ian J. Goodfellow, Jean Pouget-Abadie, Mehdi Mirza, Bing Xu, David Warde-Farley, Sherjil Ozair, Aaron Courville, and Yoshua Bengio. Generative adversarial networks. *arXiv preprint arXiv:1406.2661*, 2014.
- [48] Yann LeCun, Léon Bottou, Yoshua Bengio, and Patrick Haffner. Gradient-based learning applied to document recognition. *Proceedings of the IEEE*, 86(11):2278–2324, 1998.
- [49] Diederik P. Kingma and Max Welling. Auto-encoding variational Bayes. *arXiv preprint arXiv:1312.6114*, 2013.
- [50] Diederik P. Kingma and Max Welling. An introduction to variational autoencoders. *arXiv preprint arXiv:1906.02691*, 2019.
- [51] Jason Lloyd-Price, Cesar Arze, Ashwin N Ananthakrishnan, Melanie Schirmer, Julian Avila-Pacheco, Tiffany W Poon, Elizabeth Andrews, Nadim J Ajami, Kevin S Bonham, Colin J Brislawn, et al. Multi-omics of the gut microbial ecosystem in inflammatory bowel diseases. *Nature*, 569(7758):655–662, 2019.
- [52] Andre Franke, Dermot PB McGovern, Jeffrey C Barrett, Kai Wang, Graham L Radford-Smith, Tariq Ahmad, Charlie W Lees, Tobias Balschun, James Lee, Rebecca Roberts, et al. Genome-wide meta-analysis increases to 71 the number of confirmed crohn’s disease susceptibility loci. *Nature genetics*, 42(12):1118–1125, 2010.
- [53] Yoav Benjamini and Yosef Hochberg. Controlling the false discovery rate: a practical and powerful approach to multiple testing. *Journal of the Royal Statistical Society: Series B (Methodological)*, 57(1):289–300, 1995.
- [54] Yulia Gavrilov, Yoav Benjamini, and Sanat K Sarkar. An adaptive step-down procedure with proven fdr control under independence. *The Annals of Statistics*, 37(2):619–629, 2009.
- [55] Emmanuel Candes, Yingying Fan, Lucas Janson, and Jinchi Lv. Panning for gold: Model-X knockoffs for high-dimensional controlled variable selection. *arXiv preprint arXiv:1610.02351*, 2016.
- [56] Tim Salimans, Ian Goodfellow, Wojciech Zaremba, Vicki Cheung, Alec Radford, and Xi Chen. Improved techniques for training GANs. *arXiv preprint arXiv:1606.03498*, 2016.
- [57] Ying Liu and Cheng Zheng. Auto-encoding knockoff generator for fdr controlled variable selection. *arXiv preprint arXiv:1809.10765*, 2018.
- [58] Yaniv Romano, Matteo Sesia, and Emmanuel Candès. Deep knockoffs. *Journal of the American Statistical Association*, 115(532):1861–1872, 2020.
- [59] Mukund Sudarshan, Wesley Tansey, and Rajesh Ranganath. Deep direct likelihood knockoffs. *arXiv preprint arXiv:2007.15835*, 2020.
- [60] James Jordon, Jinsung Yoon, and Mihaela van der Schaar. Knockoffgan: Generating knockoffs for feature selection using generative adversarial networks. In *International Conference on Learning Representations*, 2018.
- [61] Jerome Friedman, Trevor Hastie, and Rob Tibshirani. Regularization paths for generalized linear models via coordinate descent. *Journal of Statistical Software*, 33(1):1, 2010.
- [62] Patrick J. Trainor, Andrew P. DeFilippis, and Shesh N. Rai. Evaluation of classifier performance for multiclass phenotype discrimination in untargeted metabolomics. *Metabolites*, 7(2):30, 2017.
- [63] Angelina Volkova and Kelly V. Ruggles. Predictive metagenomic analysis of autoimmune disease identifies robust autoimmunity and disease specific microbial signatures. *Frontiers in Microbiology*, 12:418, 2021.
- [64] Xiaofa Qin. Etiology of inflammatory bowel disease: a unified hypothesis. *World Journal of Gastroenterology*, 18(15):1708, 2012.

- [65] Sophia R. Levan, Kelsey A. Starnes, Din L. Lin, Ariane R. Panzer, Elle Fukui, Kathryn McCauley, Kei E. Fujimura, Michelle McKean, Dennis R. Ownby, Edward M. Zoratti, et al. Elevated faecal 12, 13-dihomo concentration in neonates at high risk for asthma is produced by gut bacteria and impedes immune tolerance. *Nature Microbiology*, 4(11):1851–1861, 2019.
- [66] Renzo Caprilli, Monica Cesarini, Erika Angelucci, and Giuseppe Frieri. The long journey of salicylates in ulcerative colitis: The past and the future. *Journal of Crohn’s and Colitis*, 3(3):149–156, 2009.
- [67] Thomas Lee, Thomas Clavel, Kirill Smirnov, Annemarie Schmidt, Ilias Lagkouvardos, Alesia Walker, Marianna Lucio, Bernhard Michalke, Philippe Schmitt-Kopplin, Richard Fedorak, et al. Oral versus intravenous iron replacement therapy distinctly alters the gut microbiota and metabolome in patients with ibd. *Gut*, 66(5):863–871, 2017.
- [68] Sameh Saber, Rania M Khalil, Walied S Abdo, Doaa Nassif, and Eman El-Ahwany. Olmesartan ameliorates chemically-induced ulcerative colitis in rats via modulating NF κ b and Nrf-2/HO-1 signaling crosstalk. *Toxicology and Applied Pharmacology*, 364:120–132, 2019.
- [69] Aonghus Lavelle and Harry Sokol. Gut microbiota-derived metabolites as key actors in inflammatory bowel disease. *Nature Reviews Gastroenterology & Hepatology*, 17(4):223–237, 2020.
- [70] Cristina Bauset, Laura Gisbert-Ferrándiz, and Jesús Cosín-Roger. Metabolomics as a promising resource identifying potential biomarkers for inflammatory bowel disease. *Journal of Clinical Medicine*, 10(4):622, 2021.
- [71] Tiina Solakivi, Katri Kaukinen, Tarja Kunnas, Terho Lehtimäki, Markku Mäki, and Seppo Tapio Nikkari. Serum fatty acid profile in subjects with irritable bowel syndrome. *Scandinavian Journal of Gastroenterology*, 46(3):299–303, 2011.
- [72] Fumitoshi Kuroki, Mitsuo Iida, Takayuki Matsumoto, Kunihiro Aoyagi, Kohki Kanamoto, and Masatoshi Fujishima. Serum n3 polyunsaturated fatty acids are depleted in Crohn’s disease. *Digestive Diseases and Sciences*, 42(6):1137–1141, 1997.
- [73] D.J. Fretland, D.L. Widomski, S. Levin, and T.S. Gaginella. Colonic inflammation in the rabbit induced by phorbol-12-myristate-13-acetate. *Inflammation*, 14(2):143–150, 1990.
- [74] Aude Genevay, Lénaïc Chizat, Francis Bach, Marco Cuturi, and Gabriel Peyré. Sample complexity of Sinkhorn divergences. In *The 22nd International Conference on Artificial Intelligence and Statistics*, pages 1574–1583. PMLR, 2019.
- [75] Roman Vershynin. *High-dimensional probability: An introduction with applications in data science*, volume 47. Cambridge university press, 2018.
- [76] Aram-Alexandre Pooladian, Marco Cuturi, and Jonathan Niles-Weed. Debiasser beware: Pitfalls of centering regularized transport maps. *arXiv preprint arXiv:2202.08919*, 2022.
- [77] Lénaïc Chizat, Pierre Roussillon, Flavien Léger, François-Xavier Vialard, and Gabriel Peyré. Faster Wasserstein distance estimation with the Sinkhorn divergence. *Advances in Neural Information Processing Systems*, 33:2257–2269, 2020.
- [78] Bing Xu, Naiyan Wang, Tianqi Chen, and Mu Li. Empirical evaluation of rectified activations in convolutional network. *arXiv preprint arXiv:1505.00853*, 2015.

Supplement

7 Lack of Gradient for the Rank Energy

The issue is to estimate the gradient of $\ell(\theta) = \text{RE}_{m,n}(\{X_i\}_{i=1}^m, \{T_\theta(Y_j)\}_{j=1}^n)^2$ with respect to θ . In our notation this expression should actually be written $\text{RE}_{m,n}(P_X, (T_\theta)_\#P_Y)^2$. Recalling the definition of $\text{RE}_{m,n}(P_X, (T_\theta)_\#P_Y)^2$, we have

$$\begin{aligned} & \text{RE}_{m,n}(\{X_i\}_{i=1}^m, \{T_\theta(Y_j)\}_{j=1}^n)^2 \\ &= \text{RE}_{m,n}(X_m, T_\theta(Y_n))^2 \\ &= \frac{2}{mn} \sum_{i=1}^m \sum_{j=1}^n \|\mathbb{R}^{m+n}(X_i) - \mathbb{R}^{m+n}(T_\theta(Y_j))\| - \frac{1}{m^2} \sum_{i,j=1}^m \|\mathbb{R}^{m+n}(X_i) - \mathbb{R}^{m+n}(X_j)\| \\ &\quad - \frac{1}{n^2} \sum_{i,j}^n \|\mathbb{R}^{m+n}(T_\theta(Y_i)) - \mathbb{R}^{m+n}(T_\theta(Y_j))\| \\ &= \frac{2}{mn} \sum_{i=1}^m \sum_{j=1}^n \|U_{\sigma_\theta(X_i)} - U_{\sigma_\theta(T_\theta(Y_j))}\| - \frac{1}{m^2} \sum_{i,j=1}^m \|U_{\sigma_\theta(X_i)} - U_{\sigma_\theta(X_j)}\| - \frac{1}{n^2} \sum_{i,j}^n \|U_{\sigma_\theta(T_\theta(Y_i))} - U_{\sigma_\theta(T_\theta(Y_j))}\|, \end{aligned}$$

where σ_θ is the optimal permutation for transporting $\{X_1, \dots, X_m\} \cup \{T_\theta(Y_1), \dots, T_\theta(Y_n)\}$ to $\{U_1, \dots, U_{m+n}\}$ where $U_i \sim \text{Unif}([0, 1]^d)$. From the last expression it is clear that the expression only changes value when the permutation σ_θ changes. This poses problems for the derivative of the loss functions with respect to θ . If $T_\theta(y)$ varies smoothly with y then any small enough change in θ can either leave the value of $\text{RE}^{m,n}(X_m, T_\theta(Y_n))^2$ unchanged since the permutation is unchanged, or it causes a jump in the objective when the permutation changes. In the first case the derivative is zero, and in the second it is not well-defined.

8 Proof of Theorem 2

The proof of this result is quite involved. We first review some background and notation and then build up to the result using a series of lemmas and propositions. To help with the exposition, the proofs of these steps are given at the end of the section. We also will adopt the convention that all constants $C, C_i, C_{j,r,d}$ do not change values from line to line. At the end of the section we include a table of the constants, including their relations to each other or the source from which they are taken.

We first introduce the notation for the entropy-regularized optimal transport distance between P, Q :

$$S_\varepsilon(P, Q) = \inf_{\pi \in \Pi(P, Q)} \int \int \frac{1}{2} \|x - y\|^2 d\pi(x, y) + \varepsilon D_{KL}(\pi \| P \otimes Q) \quad (20)$$

$$\begin{aligned} &= \sup_{f \in L^1(P), g \in L^1(Q)} \int f dP + \int g dQ \\ &\quad - \varepsilon \int \int \exp\left(\frac{1}{\varepsilon} \left[f(x) + g(y) - \frac{1}{2} \|x - y\|^2 \right]\right) dP(x) dQ(y) + \varepsilon. \end{aligned} \quad (21)$$

The optimal coupling of (P, Q) in (20) will be denoted π_ε , and for (P, Q^n) it will be denoted π_ε^n . These are both guaranteed to exist if P, Q have finite second moment which is always the case for bounded distributions. The optimal dual potentials of (P, Q) in (21) will be denoted $(f_\varepsilon, g_\varepsilon)$. For (P, Q^n) the optimal dual potentials will be denoted $(f_\varepsilon^n, g_\varepsilon^n)$. As a consequence of (5), we can always choose $f_\varepsilon, g_\varepsilon$ to satisfy

$$\int \exp\left(\frac{1}{\varepsilon} \left[f_\varepsilon(x) + g_\varepsilon(y) - \frac{1}{2} \|x - y\|^2 \right]\right) dP(x) = 1 \text{ for all } y \in \mathbb{R}^d \quad (22)$$

$$\int \exp\left(\frac{1}{\varepsilon} \left[f_\varepsilon(x) + g_\varepsilon(y) - \frac{1}{2} \|x - y\|^2 \right]\right) dQ(y) = 1 \text{ for all } x \in \mathbb{R}^d \quad (23)$$

and we will make use of this property many times. This is because $\exp\left(\frac{1}{\varepsilon} \left[f_\varepsilon(x) + g_\varepsilon(y) - \frac{1}{2} \|x - y\|^2 \right]\right) dP(x)$ is the conditional density of π_ε given y while $\exp\left(\frac{1}{\varepsilon} \left[f_\varepsilon(x) + g_\varepsilon(y) - \frac{1}{2} \|x - y\|^2 \right]\right) dQ(y)$ is the conditional density of π_ε given x .

For brevity we introduce the notations

$$c(x, y) \triangleq \frac{1}{2} \|x - y\|^2 \quad \text{and} \quad \gamma(x, y) \triangleq \exp\left(\frac{1}{\varepsilon} [f_\varepsilon(x) + g_\varepsilon(y) - c(x, y)]\right).$$

To start we borrow a result which shows that one can take the supremum in (21) over an even larger space of functions.

Proposition 3 ([40] Proposition 1). *Letting π_ε denote the optimal coupling in (20) between P and Q . Then*

$$S_\varepsilon(P, Q) = \sup_{\eta \in L^1(\pi_\varepsilon)} \int \eta(x, y) d\pi_\varepsilon(x, y) - \varepsilon \left(\int \int \exp\left(\frac{1}{\varepsilon} \left[\eta(x, y) - \frac{1}{2} \|x - y\|^2 \right]\right) dQ(y) dP(x) - 1 \right).$$

This is a very useful formula when combined with a clever restriction of the class of test functions. The following result does this by considering functions η of the form

$$\eta(x, y) = \varepsilon \chi(x, y) + f_\varepsilon(x) + g_\varepsilon(y),$$

where $\chi \in L^1(\pi_\varepsilon^n)$.

Proposition 4. *Let π_ε^n be the optimal coupling in (20) between P and Q^n and let $(f_\varepsilon, g_\varepsilon)$ be the optimal dual potentials for (P, Q) . Then*

$$\begin{aligned} & \sup_{\chi \in L^1(\pi_\varepsilon^n)} \int \chi(x, y) d\pi_\varepsilon^n(x, y) - \left(\int \int \exp(\chi(x, y)) \gamma(x, y) dQ^n(y) dP(x) - 1 \right) \\ & \leq \frac{1}{\varepsilon} \left(S_\varepsilon(P, Q^n) - S_\varepsilon(P, Q) + \int g_\varepsilon(y) d(Q^n - Q)(y) \right). \end{aligned}$$

For convenience we define $G \triangleq S_\varepsilon(P, Q^n) - S_\varepsilon(P, Q) + \int g_\varepsilon(y) d(Q^n - Q)(y)$. Importantly, G is a *random* scalar variable, determined by the random batch of samples observed.

Proposition 4 is useful for two reasons. The first reason is that both terms on the right hand side have been studied before and can be shown to have good convergence properties as n grows. Indeed, the first term has been analyzed in [40] and the second term is easily controlled using standard ideas in Monte Carlo integration since g_ε is known to have good regularity properties [74]. Therefore, the right hand side is generally easy to control. The second reason is that there is still sufficient flexibility for choosing a test functions on the left hand side. In particular we will further restrict the supremum to χ of the form

$$\chi(x, y) = h(x)^T (y - T_\varepsilon^n(x)) - a \|h(x)\|^2$$

for $a > 0$ and $h : \mathbb{R}^d \rightarrow \mathbb{R}^d$. The motivation for this choice is that we don't know the exact form of $T_\varepsilon^n(x) - T_\varepsilon(x)$, since T_ε^n is itself random, and instead we aim for uniform control over a function class which surely contains it, regardless of the random samples drawn. The extra variable a allows us to establish a few useful inequalities later.

Proposition 5. *Let π_ε^n be the optimal coupling in (20) between P and Q^n and let $(f_\varepsilon, g_\varepsilon)$ be the optimal dual potentials for (P, Q) . Then for any $a > 0$,*

$$\begin{aligned} & \sup_h \int (h(x)^T (y - T_\varepsilon^n(x)) - a \|h(x)\|^2) d\pi_\varepsilon^n(x, y) \\ & - \left(\int \int \exp(h(x)^T (y - T_\varepsilon^n(x)) - a \|h(x)\|^2) \gamma(x, y) dQ^n(y) dP(x) - 1 \right) \\ & \leq \frac{1}{\varepsilon} G \end{aligned}$$

where the supremum is over all $h : \mathbb{R}^d \rightarrow \mathbb{R}^d$ such that $h(x)^T (y - T_\varepsilon^n(x)) - a \|h(x)\|^2 \in L^1(\pi_\varepsilon^n)$.

Essentially the proof is just restricting the supremum in Proposition 4 to the class of test functions of the form $h(x)^T (y - T_\varepsilon^n(x)) - a \|h(x)\|^2 \in L^1(\pi_\varepsilon^n)$ for some h . In principle one could go directly from Proposition 4 to Proposition 5 by considering functions of the form $\eta = \varepsilon (h(x)^T (y - T_\varepsilon^n(x)) - a \|h(x)\|^2) + f_\varepsilon(x) + g_\varepsilon(y)$, however the proof using this approach is incredibly cumbersome.

Importantly, we have managed to insert T_ε^n into the left hand side above. The next result marks a large amount of progress and boils down to a choice of h and a large number of simplifications.

Lemma 1. Define $h_0 : \mathbb{R}^d \rightarrow \mathbb{R}^d$ by $h_0(x) = \frac{1}{2a} (T_\varepsilon^n(x) - T_\varepsilon(x))$. Then in the setting of Proposition 5 we have

$$\frac{1}{4a} \|T_\varepsilon^n - T_\varepsilon\|_{L^2(P)}^2 \leq \frac{1}{\varepsilon} G + \left(\int \int \exp(h_0(x)^T(y - T_\varepsilon(x)) - a\|h_0(x)\|^2) \gamma(x, y) dQ^n(y) dP(x) - 1 \right).$$

The next step is to swap the trailing “−1” in the bound above for a term which will make the convergence more explicit. This is done in the following lemma.

Lemma 2. For $a \geq C_0 r^2$ and h_0 defined as above it holds that

$$\int \int \exp(h_0(x)^T(y - T_\varepsilon(x)) - a\|h_0(x)\|^2) \gamma(x, y) dQ(y) dP(x) \leq 1$$

where C_0 is an absolute constant.

Combining Corollary 2 and Lemma 1 we obtain the following.

Proposition 6. For $a \geq C_0 r^2$ and h_0 defined as above we immediately obtain the following.

$$\frac{1}{4a} \|T_\varepsilon^n - T_\varepsilon\|_{L^2(P)}^2 \leq \frac{1}{\varepsilon} G + \int \int \exp(h_0(x)^T(y - T_\varepsilon(x)) - a\|h_0(x)\|^2) \gamma(x, y) [dQ^n - dQ](y) dP(x).$$

If for a moment one ignores the randomness in h_0 , the right hand side would be expected to converge to 0 at rate $n^{-1/2}$, since it would be the error in Monte Carlo integration of a single variable function. However, since the function h_0 is random one needs to work a bit harder and introduce tools from empirical process theory.

Lemma 3. Let $C_1 = \max(C_0, 2)$. Then with h_0 defined as in Lemma 1 for $a \geq C_1 r^2$ we have

$$\mathbb{E} \int \int \exp(h_0(x)^T(y - T_\varepsilon(x)) - a\|h_0(x)\|^2) \gamma(x, y) [dQ^n - dQ](y) dP(x) \leq \frac{C_2 \sqrt{d} \exp(4r^2/\varepsilon)}{\sqrt{n}}$$

where C_2 is an absolute constant.

Having controlled the right most term in Proposition 6, we now turn our attention to controlling G . This has already been done in the literature and we state these results for completeness. The first term is controlled by the following result.

Proposition 7 ([40] Corollary 3 (adapted)). Using the notation and assumptions above, one has

$$\mathbb{E} S_\varepsilon(P, Q^n) - S_\varepsilon(P, Q) \leq C_{0,r,d} (1 + \varepsilon^{1-d'/2}) \log(n) n^{-1/2}$$

where $d' = 2\lceil d/2 \rceil$ and $C_{0,r,d}$ is a constant which may depend only on r and d .

For the other term we have simply that

$$\mathbb{E} \int g_\varepsilon(y) d(Q^n - Q)(y) = 0.$$

We can now state the “one-sample theorem” for the convergence of the entropic map.

Theorem 5. With the notation above we have

$$\mathbb{E} \|T_\varepsilon^n - T_\varepsilon\|_{L^2(P)}^2 \leq \frac{r^2}{n^{1/2}} \left(C_{1,r,d} (\varepsilon^{-1} + \varepsilon^{-d'/2}) \log(n) + C_3 \sqrt{d} \exp(4r^2/\varepsilon) \right)$$

where C_3 is an absolute constant and $C_{1,r,d}$ is a constant which may only depend on r and d .

To obtain the “two-sample theorem” we recall one last result controlling the deviations between the one-sample entropic map and the two-sample entropic map.

Theorem 6 ([40] Theorem 5 (adapted)). Let $T_\varepsilon^{n,n}$ be the entropic map from P^n to Q^n , and let T_ε^n be the entropic map from P to Q^n . Then $T_\varepsilon^{n,n}$ satisfies

$$\mathbb{E} \|T_\varepsilon^{n,n} - T_\varepsilon^n\|_{L^2(P)}^2 \leq C_{2,r,d} \left((\varepsilon^{-1} + \varepsilon^{1-d'/2}) \log(n) n^{-1/2} \right)$$

where $d' = 2\lceil d/2 \rceil$ and $C_{2,r,d}$ is a constant which may depend on r and d .

Combining Theorems 5 and 6 we have our result.

Proof. (Theorem 2)

$$\begin{aligned}
\mathbb{E}\|T_\varepsilon^{n,n} - T_\varepsilon\|_{L^2(P)}^2 &= \mathbb{E}\|(T_\varepsilon^{n,n} - T_\varepsilon^n) + (T_\varepsilon^n - T_\varepsilon)\|_{L^2(P)}^2 \\
&\leq \mathbb{E}\left(\|(T_\varepsilon^{n,n} - T_\varepsilon^n)\|_{L^2(P)} + \|(T_\varepsilon^n - T_\varepsilon)\|_{L^2(P)}\right)^2 \\
&\leq 2\mathbb{E}\|(T_\varepsilon^{n,n} - T_\varepsilon^n)\|_{L^2(P)}^2 + 2\mathbb{E}\|(T_\varepsilon^n - T_\varepsilon)\|_{L^2(P)}^2 \\
&\leq \frac{2r^2}{n^{1/2}} \left(C_{1,r,d}(\varepsilon^{-1} + \varepsilon^{-d'/2}) \log(n) + C_3\sqrt{d} \exp(4r^2/\varepsilon) \right) \\
&\quad + 2C_{2,r,d} \left((\varepsilon^{-1} + \varepsilon^{1-d'/2}) \log(n)n^{-1/2} \right) \\
&= C_{r,d}(\varepsilon^{-1} + \varepsilon^{1-d'/2}) \log(n)n^{-1/2} + C\sqrt{d} \exp(4r^2/\varepsilon)n^{-1/2}
\end{aligned}$$

where $C_{r,d} = 2r^2C_{1,r,d} + 2C_{2,r,d}$ and $C = 2C_3$ □

8.1 Proof of Proposition 4

Proof. Let $\chi \in L^1(\pi_\varepsilon^n)$ and define η by

$$\eta(x, y) = \varepsilon\chi(x, y) + f_\varepsilon(x) + g_\varepsilon(y).$$

Note that $\eta \in L^1(\pi_\varepsilon^n)$ since $\chi, (f_\varepsilon + g_\varepsilon) \in L^1(\pi_\varepsilon^n)$. By Proposition 1 and the fact that P, Q^n are the marginals of π_ε^n it follows

$$\begin{aligned}
S_\varepsilon(P, Q^n) &\geq \int \eta(x, y) d\pi_\varepsilon^n(x, y) - \varepsilon \left(\int \int \exp\left(\frac{1}{\varepsilon} \left[\eta(x, y) - \frac{1}{2} \|x - y\|^2 \right]\right) dQ^n(y) dP(x) - 1 \right) \\
&= \int [\varepsilon\chi(x, y) + f_\varepsilon(x) + g_\varepsilon(y)] d\pi_\varepsilon^n(x, y) \\
&\quad - \varepsilon \left(\int \int \exp\left(\frac{1}{\varepsilon} \left[\varepsilon\chi(x, y) + f_\varepsilon(x) + g_\varepsilon(y) - \frac{1}{2} \|x - y\|^2 \right]\right) dQ^n(y) dP(x) - 1 \right) \\
&= \varepsilon \int \chi(x, y) d\pi_\varepsilon^n(x, y) + \int f_\varepsilon(x) dP(x) + \int g_\varepsilon(y) dQ^n(y) \\
&\quad - \varepsilon \left(\int \int \exp\left(\chi(x, y) + \frac{1}{\varepsilon} \left[f_\varepsilon(x) + g_\varepsilon(y) - \frac{1}{2} \|x - y\|^2 \right]\right) dQ^n(y) dP(x) - 1 \right) \\
&= \varepsilon \int \chi(x, y) d\pi_\varepsilon^n(x, y) + \int f_\varepsilon(x) dP(x) + \int g_\varepsilon(y) dQ^n(y) \\
&\quad - \varepsilon \left(\int \int \exp(\chi(x, y)) \gamma(x, y) dQ^n(y) dP(x) - 1 \right).
\end{aligned}$$

Rearranging we have

$$\begin{aligned}
&\int \chi(x, y) d\pi_\varepsilon^n(x, y) - \left(\int \int \exp(\chi(x, y)) \gamma(x, y) dQ^n(y) dP(x) - 1 \right) \\
&\leq \frac{1}{\varepsilon} S_\varepsilon(P, Q^n) - \frac{1}{\varepsilon} \left(\int f_\varepsilon(x) dP(x) + \int g_\varepsilon(y) dQ^n(y) \right). \tag{24}
\end{aligned}$$

Dropping for a moment the $\frac{1}{\varepsilon}$ we have

$$\begin{aligned}
&S_\varepsilon(P, Q^n) - \left(\int f_\varepsilon(x) dP(x) + \int g_\varepsilon(y) dQ^n(y) \right) \\
&= (S_\varepsilon(P, Q^n) - S_\varepsilon(P, Q)) + \left(S_\varepsilon(P, Q) - \int f_\varepsilon(x) dP(x) + \int g_\varepsilon(y) dQ(y) \right) + \int g_\varepsilon(y) d(Q^n - Q)(y) \\
&= S_\varepsilon(P, Q^n) - S_\varepsilon(P, Q) + \int g_\varepsilon(y) d(Q^n - Q)(y). \tag{25}
\end{aligned}$$

In the last line we have used that by (22)

$$-\varepsilon \int \int \exp\left(\frac{1}{\varepsilon} \left[f_\varepsilon(x) + g_\varepsilon(y) - \frac{1}{2} \|x - y\|^2 \right]\right) dQ(y) dP(x) + \varepsilon = -\varepsilon \int 1 dQ(y) + \varepsilon = 0$$

and therefore

$$\begin{aligned} S_\varepsilon(P, Q) &= \int f_\varepsilon dP + \int g_\varepsilon dQ - \varepsilon \int \int \exp\left(\frac{1}{\varepsilon} \left[f_\varepsilon(x) + g_\varepsilon(y) - \frac{1}{2} \|x - y\|^2 \right]\right) dQ(y) dP(x) + \varepsilon \\ &= \int f_\varepsilon dP + \int g_\varepsilon dQ \end{aligned}$$

which implies

$$S_\varepsilon(P, Q) - \int f_\varepsilon dP + \int g_\varepsilon dQ = 0.$$

Plugging (25) into (24) we obtain

$$\begin{aligned} & \int \chi(x, y) d\pi_\varepsilon^n(x, y) - \left(\int \int \exp(\chi(x, y)) \gamma(x, y) dQ^n(y) dP(x) - 1 \right) \\ & \leq \frac{1}{\varepsilon} \left[S_\varepsilon(P, Q^n) - S_\varepsilon(P, Q) + \int g_\varepsilon(y) d(Q^n - Q)(y) \right]. \end{aligned}$$

Since χ was chosen arbitrarily in $L^1(\pi_\varepsilon^n)$, this bound holds uniformly over the class. Therefore we have

$$\begin{aligned} & \sup_{\chi \in L^1(\pi_\varepsilon^n)} \int \chi(x, y) d\pi_\varepsilon^n(x, y) - \left(\int \int \exp(\chi(x, y)) \gamma(x, y) dQ^n(y) dP(x) - 1 \right) \\ & \leq \frac{1}{\varepsilon} (S_\varepsilon(P, Q^n) - S_\varepsilon(P, Q)) + \frac{1}{\varepsilon} \int g_\varepsilon(y) d(Q^n - Q)(y) \end{aligned}$$

as desired. \square

8.2 Proof of Proposition 5

Proof. Define the set

$$\mathcal{H} = \left\{ H(x, y) = h(x)^T (y - T_\varepsilon^n(x)) - a \|h(x)\|^2 : h : \mathbb{R}^d \rightarrow \mathbb{R}^d; \int |h(x)^T (y - T_\varepsilon^n(x)) - a \|h(x)\|^2| d\pi_\varepsilon^n < \infty \right\}.$$

Then $\mathcal{H} \subset L^1(\pi_\varepsilon^n)$ and by Proposition 4 we have

$$\begin{aligned} & \sup_h \int h(x)^T (y - T_\varepsilon^n(x)) - a \|h(x)\|^2 d\pi_\varepsilon^n(x, y) \\ & - \left(\int \int \exp(h(x)^T (y - T_\varepsilon^n(x)) - a \|h(x)\|^2) \gamma(x, y) dQ^n(y) dP(x) - 1 \right) \\ & = \sup_{H \in \mathcal{H}} \int H(x, y) d\pi_\varepsilon^n(x, y) - \left(\int \int \exp(H(x, y)) \gamma(x, y) dQ^n(y) dP(x) - 1 \right) \\ & \leq \sup_{\chi \in L^1(\pi_\varepsilon^n)} \int \chi(x, y) d\pi_\varepsilon^n(x, y) - \left(\int \int \exp(\chi(x, y)) \gamma(x, y) dQ^n(y) dP(x) - 1 \right) \\ & \leq \frac{1}{\varepsilon} (S_\varepsilon(P, Q^n) - S_\varepsilon(P, Q)) + \frac{1}{\varepsilon} \int g_\varepsilon(y) d(Q^n - Q)(y) = \frac{1}{\varepsilon} G. \end{aligned}$$

\square

8.3 Proof of Lemma 1

Proof. Using that the first marginal of π_ε^n is P we have

$$\int (h_0(x)^T (y - T_\varepsilon(x)) - a \|h_0(x)\|^2) d\pi_\varepsilon^n(x, y) = \int h_0(x)^T (y - T_\varepsilon(x)) d\pi_\varepsilon^n(x, y) - \int a \|h_0(x)\|^2 dP(x). \quad (26)$$

Now let us consider the two integrals separately. For the first we have the following chain.

$$\begin{aligned}
& \int h_0(x)^T (y - T_\varepsilon(x)) d\pi_\varepsilon^n(x, y) \\
&= \int \left(\frac{1}{2a} (T_\varepsilon^n(x) - T_\varepsilon(x)) \right)^T (y - T_\varepsilon(x)) d\pi_\varepsilon^n(x, y) \\
&= \frac{1}{2a} \int (T_\varepsilon^n(x) - T_\varepsilon(x))^T y d\pi_\varepsilon^n(x, y) - \frac{1}{2a} \int (T_\varepsilon^n(x) - T_\varepsilon(x))^T T_\varepsilon(x) d\pi_\varepsilon^n(x, y) \\
&= \frac{1}{2a} \int (T_\varepsilon^n(x) - T_\varepsilon(x))^T y d\pi_\varepsilon^n(x, y) - \frac{1}{2a} \int (T_\varepsilon^n(x) - T_\varepsilon(x))^T T_\varepsilon(x) dP(x) \\
&= \frac{1}{2a} \int (T_\varepsilon^n(x) - T_\varepsilon(x))^T T_\varepsilon^n(x) dP(x) - \frac{1}{2a} \int (T_\varepsilon^n(x) - T_\varepsilon(x))^T T_\varepsilon(x) dP(x) \tag{27}
\end{aligned}$$

$$\begin{aligned}
&= \frac{1}{2a} \int (T_\varepsilon^n(x) - T_\varepsilon(x))^T (T_\varepsilon^n(x) - T_\varepsilon(x)) dP(x) \\
&= \frac{1}{2a} \int \|T_\varepsilon^n(x) - T_\varepsilon(x)\|^2 dP(x) = \frac{1}{2a} \|T_\varepsilon^n - T_\varepsilon\|_{L^2(P)}^2. \tag{28}
\end{aligned}$$

The third equality uses that P is the marginal of π_ε^n . To see (27), note

$$\begin{aligned}
\int (T_\varepsilon^n(x) - T_\varepsilon(x))^T y d\pi_\varepsilon^n(x, y) &= \int \left[\int (T_\varepsilon^n(x) - T_\varepsilon(x))^T y d\pi_\varepsilon^n(y|x) \right] dP(x) \\
&= \int (T_\varepsilon^n(x) - T_\varepsilon(x))^T \left[\int y d\pi_\varepsilon^n(y|x) \right] dP(x) \quad (\text{Linearity}) \\
&= \int (T_\varepsilon^n(x) - T_\varepsilon(x))^T T_\varepsilon^n(x) dP(x). \quad (\text{Eq12})
\end{aligned}$$

For the second integral we have

$$\begin{aligned}
\int a \|h_0(x)\|^2 dP(x) &= \int a \left\| \frac{1}{2a} [T_\varepsilon^n(x) - T_\varepsilon(x)] \right\|^2 dP(x) \\
&= \frac{1}{4a} \|T_\varepsilon^n - T_\varepsilon\|_{L^2(P)}^2 \tag{29}
\end{aligned}$$

Plugging (28),(29) into (26) we have

$$\int h_0(x)^T (y - T_\varepsilon(x)) - a \|h(x)\|^2 d\pi_\varepsilon^n(x, y) = \frac{1}{2a} \|T_\varepsilon^n - T_\varepsilon\|_{L^2(P)}^2 - \frac{1}{4a} \|T_\varepsilon^n - T_\varepsilon\|_{L^2(P)}^2 = \frac{1}{4a} \|T_\varepsilon^n - T_\varepsilon\|_{L^2(P)}^2.$$

Now by Proposition 5 we have

$$\begin{aligned}
\frac{1}{\varepsilon} G &\geq \sup_h \int h(x)^T (y - T_\varepsilon(x)) - a \|h(x)\|^2 d\pi_\varepsilon^n(x, y) \\
&\quad - \left(\int \int \exp(h(x)^T (y - T_\varepsilon(x)) - a \|h(x)\|^2) \gamma(x, y) dQ^n(y) dP(x) - 1 \right) \\
&\geq \int h_0(x)^T (y - T_\varepsilon(x)) - a \|h_0(x)\|^2 d\pi_\varepsilon^n(x, y) \\
&\quad - \left(\int \int \exp(h_0(x)^T (y - T_\varepsilon(x)) - a \|h_0(x)\|^2) \gamma(x, y) dQ^n(y) dP(x) - 1 \right) \\
&= \frac{1}{4a} \|T_\varepsilon^n - T_\varepsilon\|_{L^2(P)}^2 - \left(\int \int \exp(h_0(x)^T (y - T_\varepsilon(x)) - a \|h_0(x)\|^2) \gamma(x, y) dQ^n(y) dP(x) - 1 \right).
\end{aligned}$$

If we re-arrange the first and last inequality we have

$$\frac{1}{4a} \|T_\varepsilon^n - T_\varepsilon\|_{L^2(P)}^2 \leq \frac{1}{\varepsilon} G + \left(\int \int \exp(h_0(x)^T (y - T_\varepsilon(x)) - a \|h_0(x)\|^2) \gamma(x, y) dQ^n(y) dP(x) - 1 \right)$$

which proves the result. \square

8.4 Proof of Lemma 2

In order to prove this result we first collect two further facts. The first is proved by a direct calculation.

Lemma 4. *In the setting of Proposition 5, for any h*

$$\int h(x)^T (y - T_\varepsilon(x)) \gamma(x, y) dQ(y) = 0.$$

Proof. By linearity we have

$$\int h(x)^T (y - T_\varepsilon(x)) \gamma(x, y) dQ(y) = h(x)^T \left[\int (y - T_\varepsilon(x)) \gamma(x, y) dQ(y) \right]$$

and the integral on the inside can be expressed as

$$\begin{aligned} & \int (y - T_\varepsilon(x)) \gamma(x, y) dQ(y) \\ &= \int y \gamma(x, y) - \gamma(x, y) \left[\frac{\int y_0 \exp\left(\frac{1}{\varepsilon} [g_\varepsilon(y_0) - c(x, y_0)]\right) dQ(y_0)}{\int \exp\left(\frac{1}{\varepsilon} [g_\varepsilon(y_1) - c(x, y_1)]\right) dQ(y_1)} \right] dQ(y) && \text{(Def of } T_\varepsilon) \\ &= \int y \gamma(x, y) - \gamma(x, y) \left[\frac{\int y_0 \exp\left(\frac{1}{\varepsilon} [g_\varepsilon(y_0) + f_\varepsilon(x) - c(x, y_0)]\right) dQ(y_0)}{\int \exp\left(\frac{1}{\varepsilon} [g_\varepsilon(y_1) + f_\varepsilon(x) - c(x, y_1)]\right) dQ(y_1)} \right] dQ(y) \\ &= \int y \gamma(x, y) - \gamma(x, y) \left[\int y_0 \exp\left(\frac{1}{\varepsilon} [g_\varepsilon(y_0) + f_\varepsilon(x) - c(x, y_0)]\right) dQ(y_0) \right] dQ(y) && \text{(Eq. 23)} \\ &= \int y \gamma(x, y) dQ(y) - \int \gamma(x, y) \left[\int y_0 \gamma(x, y_0) dQ(y_0) \right] dQ(y) \\ &= \int y \gamma(x, y) dQ(y) - \left[\int y_0 \gamma(x, y_0) dQ(y_0) \right] \int \gamma(x, y) dQ(y) \\ &= \int y \gamma(x, y) dQ(y) - \int y_0 \gamma(x, y_0) dQ(y_0) = 0. && \text{(Eq 22)} \end{aligned}$$

□

In particular this result holds when $h = h_0$, and going a step further, it holds *independent* of both the choice of x and the form of the random function h_0 . This is critical for establishing uniform control. The mean-zero condition also enables us to use a key inequality which only holds for mean-zero random variables.

Lemma 5. *There exists an absolute constant C_0 such that for all $a \geq C_0 r^2$ and h_0 defined as in Lemma 1, it holds for all x that*

$$\int \exp(h_0(x))^T (y - T_\varepsilon(x)) \gamma(x, y) dQ(y) \leq \exp(a \|h_0(x)\|^2).$$

Proof. We need a few facts from [75]. First, if X is a bounded random variable such that $\|X\|_\infty < B$ then

$$\|X\|_{\psi_2} \leq C_4 B$$

where $\|X\|_\psi$ denotes the sub-gaussian norm of X and C_4 is an absolute constant (see Example 2.5.8.iii in [75]). Second, if X is mean-zero, then for all $\lambda \in \mathbb{R}$,

$$\mathbb{E} \exp(\lambda X) \leq \exp(C_5 \lambda^2 \|X\|_{\psi_2}^2) \quad (30)$$

where C_5 is another absolute constant (See Proposition 2.5.2 or (2.16) in [75]).

Now for a fixed x , let Y^x be the random variable whose law is the conditional distribution of π_ε with $X = x$. Further define

$$Z^x \triangleq (T_\varepsilon^n(x) - T_\varepsilon(x))^T (Y^x - T_\varepsilon(x)) = h_0(x)^T (Y^x - T_\varepsilon(x)).$$

First note that since $T_\varepsilon(x), T_\varepsilon^n(x), Y^x \in B_2^d(0, r)$ we have

$$\begin{aligned} |Z^x| &= |(T_\varepsilon^n(x) - T_\varepsilon(x))^T (Y^x - T_\varepsilon(x))| \\ &\leq \|T_\varepsilon^n(x) - T_\varepsilon(x)\| \|Y^x - T_\varepsilon(x)\| \\ &\leq (2r) \|T_\varepsilon^n(x) - T_\varepsilon(x)\| \\ \implies \|Z^x\|_{\psi_2} &\leq 2r C_4 \|T_\varepsilon^n(x) - T_\varepsilon(x)\|. \end{aligned} \quad (31)$$

Next, we have by Lemma 4

$$\mathbb{E}[Z^x] = \int (T_\varepsilon^n(x) - T_\varepsilon(x))^T (Y^x - T_\varepsilon(x)) d\pi_\varepsilon^x(y) = \int (T_\varepsilon^n(x) - T_\varepsilon(x))^T (Y^x - T_\varepsilon(x)) \gamma(x, y) dQ(y) = 0.$$

This shows that Z^x satisfies the conditions to use (30). Doing so we obtain

$$\begin{aligned} & \int \exp(h_0(x))^T (y - T_\varepsilon(x)) \gamma(x, y) dQ(y) \\ &= \int \exp\left(\frac{1}{2a} (T_\varepsilon^n(x) - T_\varepsilon(x))^T (Y^x - T_\varepsilon(x))\right) \gamma(x, y) dQ(y) \\ &= \mathbb{E}\left[\exp\left(\frac{1}{2a} Z^x\right)\right] \\ &\leq \exp\left(C_5 \frac{1}{4a^2} 4C_4^2 r^2 \|T_\varepsilon^n(x) - T_\varepsilon(x)\|^2\right) \quad (\text{Eq.(30) and (31)}) \\ &= \exp\left(C_6 \frac{r^2}{a^2} \|T_\varepsilon^n(x) - T_\varepsilon(x)\|^2\right) \end{aligned}$$

where $C_6 = C_4^2 C_5$.

From here it is enough to show that

$$\exp\left(C_6 \frac{r^2}{a^2} \|T_\varepsilon^n(x) - T_\varepsilon(x)\|^2\right) \leq \exp\left(\frac{1}{4a} \|T_\varepsilon^n(x) - T_\varepsilon(x)\|^2\right) = \exp(a \|h_0(x)\|^2).$$

By monotonicity of \exp it is enough to show that

$$C_6 \frac{r^2}{a^2} \|T_\varepsilon^n(x) - T_\varepsilon(x)\|^2 \leq \frac{1}{4a} \|T_\varepsilon^n(x) - T_\varepsilon(x)\|^2$$

and this holds true if $a \geq 4C_6 r^2$. Letting $C_0 = 4C_6$ proves the result. \square

With the preceding lemma in hand, the proof of Lemma 2 becomes straightforward.

Proof. (Lemma 2) For $a \geq C_0 r^2$ we have

$$\begin{aligned} & \int \int \exp(h_0(x))^T (y - T_\varepsilon(x)) - a \|h_0(x)\|^2 \gamma(x, y) dQ(y) dP(x) \\ &= \int \exp(-a \|h_0(x)\|^2) \left[\int \exp(h_0(x))^T (y - T_\varepsilon(x)) \gamma(x, y) dQ(y) \right] dP(x) \\ &\leq \int \exp(-a \|h_0(x)\|^2) [\exp(a \|h_0(x)\|^2)] dP(x) \quad (\text{Lemma 5}) \\ &= 1. \end{aligned}$$

\square

8.5 Proof of Lemma 3

Before proceeding to the proof of the lemma, we first establish a necessary rough upper bound on one of the terms we need to control later, as state a standard tool in empirical process theory.

Lemma 6. *Under the assumptions above, we have for all $x, y \in B_2^d(0, r)$ that*

$$f_\varepsilon(x) + g_\varepsilon(y) \leq 4r^2$$

and therefore for all $x, y \in B_2^d(0, r)$,

$$\gamma(x, y) = \exp\left(\frac{1}{\varepsilon} \left[f_\varepsilon(x) + g_\varepsilon(y) - \frac{1}{2} \|x - y\|^2 \right]\right) \leq \exp\left(\frac{1}{\varepsilon} [f_\varepsilon(x) + g_\varepsilon(y)]\right) \leq \exp(4r^2/\varepsilon). \quad (32)$$

Proof. We first recall an important property of the optimal entropic potentials.

Proposition 8 ([74] Proposition 1 (adapted)). *If the supports of P, Q are compact sets in \mathbb{R}^d and the cost c is C^∞ , then $f_\varepsilon, g_\varepsilon$ are L -Lipschitz where L is the Lipschitz constant of c .*

For our purposes $c(x, y) = \frac{1}{2}\|x - y\|^2$ and the Lipschitz bound can be taken to be

$$L = \sup_{x \neq y \in B_2^d(0, r)} \frac{\frac{1}{2}\|x - y\|^2}{\|x - y\|} = \frac{1}{2} \sup_{x \neq y \in B_2^d(0, r)} \|x - y\| = r.$$

Suppose for contradiction there is a pair (x^*, y^*) such that $f(x^*) + g(y^*) > 4r^2$. Then we would have

$$\begin{aligned} 1 &= \int \exp\left(\frac{1}{\varepsilon} \left[f_\varepsilon(x^*) + g_\varepsilon(y) - \frac{1}{2}\|x^* - y\|^2 \right]\right) dQ(y) \\ &\geq \int \exp\left(\frac{1}{\varepsilon} \left[f_\varepsilon(x^*) + g_\varepsilon(y^*) - r\|y - y^*\| - \frac{1}{2}\|x^* - y\|^2 \right]\right) dQ(y) \\ &\geq \int \exp\left(\frac{1}{\varepsilon} [f_\varepsilon(x^*) + g_\varepsilon(y^*) - 2r^2 - 2r^2]\right) dQ(y) \\ &> \int \exp\left(\frac{1}{\varepsilon} [4r^2 - 4r^2]\right) dQ(y) = 1 \end{aligned}$$

which is a contradiction. Here we have used that since g_ε is r Lipschitz we have the bound, valid for all y, y' in the domain that $g_\varepsilon(y) > g_\varepsilon(y') - L\|y - y'\|$ applied with $y' = y^*$ and used bounded assumptions on x, y in several places. \square

The following result is a standard bound in empirical process theory which will help us to control the randomness of h_0 . To state it we must introduce the notation $\mathcal{N}(T, d_T, \delta)$ which is the covering number of the metric space (T, d_T) by balls of radius at most δ whose centers lie in T .

Theorem 7 ([75] Theorem 8.1.3). *Let $(X_t)_{t \in T}$ be a mean-zero random process on a metric space (T, d_T) with sub-gaussian increments satisfying $\|X_t - X_s\|_{\psi_2} \leq K d_T(t, s)$ for all $t, s \in T$. Then*

$$\mathbb{E} \sup_{t \in T} X_t \leq C_7 K \int_0^\infty \sqrt{\log \mathcal{N}(T, d_T, \delta)} d\delta.$$

The following result is a standard bound for the covering numbers of balls in \mathbb{R}^d , a proof of which can be found in [75].

Lemma 7. *For $\delta \geq r$ we have $\mathcal{N}(B_2^d(0, r), \|\cdot\|, r) = 1$ and for $0 < \delta < r$ we have*

$$\mathcal{N}(B_2^d(0, r), \|\cdot\|, \delta) \leq \left(\frac{3r}{\delta}\right)^d.$$

Having collected the necessary results we now proceed to the proof of Lemma 3.

Proof. First we re-write our integral in a form that is more convenient for us.

$$\begin{aligned} &\int \int \exp(h_0(x)^T (y - T_\varepsilon(x)) - a\|h_0(x)\|^2) \gamma(x, y) [dQ^n - dQ](y) dP(x) \\ &= \int \int \exp\left(\frac{1}{2a} (T_\varepsilon^n(x) - T_\varepsilon(x))^T (y - T_\varepsilon(x)) - \frac{1}{4a} \|T_\varepsilon^n(x) - T_\varepsilon(x)\|^2\right) \gamma(x, y) [dQ^n - dQ](y) dP(x). \end{aligned}$$

Now note that $T_\varepsilon^n(x)$ is a vector contained in $B_2^d(0, r)$ so we always have the following bound (since we can choose $v = T_\varepsilon^n(x)$)

$$\begin{aligned} &\int \int \exp\left(\frac{1}{2a} (T_\varepsilon^n(x) - T_\varepsilon(x))^T (y - T_\varepsilon(x)) - \frac{1}{4a} \|T_\varepsilon^n(x) - T_\varepsilon(x)\|^2\right) \gamma(x, y) [dQ^n - dQ](y) dP(x) \\ &\leq \int \left[\sup_{v \in B_2^d(0, r)} \int \exp\left(\frac{1}{2a} (v - T_\varepsilon(x))^T (y - T_\varepsilon(x)) - \frac{1}{4a} \|v - T_\varepsilon(x)\|^2\right) \gamma(x, y) [dQ^n - dQ](y) \right] dP(x) \end{aligned}$$

Taking the expectation of both sides of this inequality, and subsequently changing the order of integration we have

$$\begin{aligned}
& \mathbb{E}_{Y^n} \int \int \exp(h_0(x)^T(y - T_\varepsilon(x)) - a\|h_0(x)\|^2) \gamma(x, y) [dQ^n - dQ](y) dP(x) \\
& \leq \mathbb{E}_{Y^n} \int \left[\sup_{v \in B_2^d(0, r)} \int \exp\left(\frac{1}{2a}(v - T_\varepsilon(x))^T(y - T_\varepsilon(x)) - \frac{1}{4a}\|v - T_\varepsilon(x)\|^2\right) \gamma(x, y) [dQ^n - dQ](y) \right] dP(x) \\
& = \int \mathbb{E}_{Y^n} \left[\sup_{v \in B_2^d(0, r)} \int \exp\left(\frac{1}{2a}(v - T_\varepsilon(x))^T(y - T_\varepsilon(x)) - \frac{1}{4a}\|v - T_\varepsilon(x)\|^2\right) \gamma(x, y) [dQ^n - dQ](y) \right] dP(x)
\end{aligned}$$

Therefore it is enough to uniformly bound over x the inner expectation, which is what we do now. From here, x is treated as fixed.

Recall that $Q^n = \frac{1}{n} \sum_{i=1}^n \delta_{Y_i}$ where Y_1, \dots, Y_n are i.i.d. according to Q . We now define the empirical process $(Z_v)_{v \in B_2^d(0, r)}$ where Z_v is defined by

$$\begin{aligned}
Z_v & \triangleq \int \exp\left(\frac{1}{2a}(v - T_\varepsilon(x))^T(y - T_\varepsilon(x)) - \frac{1}{4a}\|v - T_\varepsilon(x)\|^2\right) \gamma(x, y) [dQ^n - dQ](y) \\
& = \frac{1}{n} \sum_{i=1}^n \exp\left(\frac{1}{2a}(v - T_\varepsilon(x))^T(Y_i - T_\varepsilon(x)) - \frac{1}{4a}\|v - T_\varepsilon(x)\|^2\right) \gamma(x, Y_i) \\
& \quad - \mathbb{E}_Y \exp\left(\frac{1}{2a}(v - T_\varepsilon(x))^T(Y - T_\varepsilon(x)) - \frac{1}{4a}\|v - T_\varepsilon(x)\|^2\right) \gamma(x, Y) \\
& = \frac{1}{n} \sum_{i=1}^n A_v^i - \mathbb{E}A_v
\end{aligned}$$

where $A_v^i \triangleq \exp\left(\frac{1}{2a}(v - T_\varepsilon(x))^T(Y_i - T_\varepsilon(x)) - \frac{1}{4a}\|v - T_\varepsilon(x)\|^2\right) \gamma(x, Y_i)$.

Our first task is to control the increments of the process Z_v . Namely, we seek a bound of the form

$$\|Z_u - Z_v\|_{\psi_2} \leq K\|u - v\|.$$

By applying Lemma 2.6.8 and then Proposition 2.6.1 from [75] we have

$$\begin{aligned}
\|Z_u - Z_v\|_{\psi_2} & = \left\| \left(\frac{1}{n} \sum_{i=1}^n A_u^i - \mathbb{E}A_u \right) - \left(\frac{1}{n} \sum_{i=1}^n A_v^i - \mathbb{E}A_v \right) \right\|_{\psi_2} \\
& = \left\| \frac{1}{n} \sum_{i=1}^n (A_u^i - A_v^i) - \mathbb{E}(A_u - A_v) \right\|_{\psi_2} \\
& \leq C_8 \left\| \frac{1}{n} \sum_{i=1}^n (A_u^i - A_v^i) \right\|_{\psi_2} \\
& \leq C_8 C_9 \frac{1}{n} \left(\sum_{i=1}^n \|A_u^i - A_v^i\|_{\psi_2}^2 \right)^{1/2} \tag{33}
\end{aligned}$$

where C_8 and C_9 are absolute constants. Let $C_{10} = C_8 C_9$

Now we need to control $\|A_u^i - A_v^i\|_{\psi_2}$. For the moment suppressing the dependence on i , this can be done as

follows

$$\begin{aligned}
|A_u - A_v| &= \left| \exp\left(\frac{1}{2a}(u - T_\varepsilon(x))^T(Y - T_\varepsilon(x)) - \frac{1}{4a}\|u - T_\varepsilon(x)\|^2\right) \gamma(x, Y) \right. \\
&\quad \left. - \exp\left(\frac{1}{2a}(v - T_\varepsilon(x))^T(Y - T_\varepsilon(x)) - \frac{1}{4a}\|v - T_\varepsilon(x)\|^2\right) \gamma(x, Y) \right| \\
&= \gamma(x, Y) \left| \exp\left(\frac{1}{2a}(u - T_\varepsilon(x))^T(Y - T_\varepsilon(x)) - \frac{1}{4a}\|u - T_\varepsilon(x)\|^2\right) \right. \\
&\quad \left. - \exp\left(\frac{1}{2a}(v - T_\varepsilon(x))^T(Y - T_\varepsilon(x)) - \frac{1}{4a}\|v - T_\varepsilon(x)\|^2\right) \right| \\
&\leq \exp(4r^2/\varepsilon) \left| \exp\left(\frac{1}{2a}(u - T_\varepsilon(x))^T(Y - T_\varepsilon(x)) - \frac{1}{4a}\|u - T_\varepsilon(x)\|^2\right) \right. \\
&\quad \left. - \exp\left(\frac{1}{2a}(v - T_\varepsilon(x))^T(Y - T_\varepsilon(x)) - \frac{1}{4a}\|v - T_\varepsilon(x)\|^2\right) \right|
\end{aligned}$$

where we have used Lemma 6 to bound $\gamma(x, Y)$.

Now by the assumption that $a \geq 2r^2$ and the fact that $u, v, Y, T_\varepsilon(x) \in B_2^d(0, r)$ we have both

$$\begin{aligned}
\frac{1}{2a}(u - T_\varepsilon(x))^T(Y - T_\varepsilon(x)) - \frac{1}{4a}\|u - T_\varepsilon(x)\|^2 &\leq \frac{1}{2a}(u - T_\varepsilon(x))^T(Y - T_\varepsilon(x)) \\
&\leq \frac{1}{2a}\|u - T_\varepsilon(x)\|\|Y - T_\varepsilon(x)\| \\
&\leq \frac{4r^2}{2a} \leq \frac{4r^2}{4r^2} = 1
\end{aligned}$$

and by an analogous computation replacing u be v ,

$$\frac{1}{2a}(v - T_\varepsilon(x))^T(Y - T_\varepsilon(x)) - \frac{1}{4a}\|v - T_\varepsilon(x)\|^2 \leq 1.$$

Using this, and the inequality valid for all $a, b \leq 1$ that $|e^a - e^b| \leq e|a - b|$, we have

$$\begin{aligned}
&\left| \exp\left(\frac{1}{2a}(u - T_\varepsilon(x))^T(Y - T_\varepsilon(x)) - \frac{1}{4a}\|u - T_\varepsilon(x)\|^2\right) \right. \\
&\quad \left. - \exp\left(\frac{1}{2a}(v - T_\varepsilon(x))^T(Y - T_\varepsilon(x)) - \frac{1}{4a}\|v - T_\varepsilon(x)\|^2\right) \right| \\
&\leq e \left| \frac{1}{2a}(u - T_\varepsilon(x))^T(Y - T_\varepsilon(x)) - \frac{1}{4a}\|u - T_\varepsilon(x)\|^2 - \frac{1}{2a}(v - T_\varepsilon(x))^T(Y - T_\varepsilon(x)) - \frac{1}{4a}\|v - T_\varepsilon(x)\|^2 \right| \\
&= \frac{e}{2a} \left| (u - v)^T(Y - T_\varepsilon(x)) + \frac{1}{2}\|v - T_\varepsilon(x)\|^2 - \frac{1}{2}\|u - T_\varepsilon(x)\|^2 \right| \\
&= \frac{e}{2a} \left| (u - v)^TY + \frac{1}{2}\|v\|^2 - \frac{1}{2}\|u\|^2 \right| \\
&\leq \frac{e}{2a}\|u - v\|\|Y\| + \frac{e}{4a}(|\|u\| - \|v\||)(\|u\| + \|v\|) \\
&\leq \frac{re}{2a}\|u - v\| + \frac{re}{2a}\|u - v\| \\
&= \frac{re}{a}\|u - v\|.
\end{aligned}$$

Using this and the chain above we can conclude

$$|A_u - A_v| \leq \exp(4r^2/\varepsilon) \frac{re}{a} \|u - v\|$$

which implies (as in the proof of Lemma 5)

$$\|A_u - A_v\|_{\psi_2} \leq C_4 \exp(4r^2/\varepsilon) \frac{re}{a} \|u - v\|. \quad (34)$$

Now plugging (34) into (33) we obtain

$$\begin{aligned}
\|Z_u - Z_v\|_{\psi_2} &\leq C_{10} \frac{1}{n} \left(\sum_{i=1}^n \left(C_4 \exp(4r^2/\varepsilon) \frac{re}{a} \|u - v\| \right)^2 \right)^{1/2} \\
&= \frac{1}{\sqrt{n}} C_{11} \exp(4r^2/\varepsilon) \frac{re}{a} \|u - v\|
\end{aligned}$$

where $C_{11} = C_4 C_{10}$. Now using Theorem 7 above with $K = \frac{1}{\sqrt{n}} C_{11} \exp(4r^2/\varepsilon) \frac{re}{a}$ we have

$$\begin{aligned}
& \mathbb{E}_{Y^n} \left[\sup_{v \in B_2^d(0,r)} \int \exp \left(\frac{1}{2a} (v - T_\varepsilon(x))^T (y - T_\varepsilon(x)) - \frac{1}{4a} \|v - T_\varepsilon(x)\|^2 \right) \gamma(x, y) [dQ^n - dQ](y) \right] \\
&= \mathbb{E} \sup_{v \in B_2^d(0,r)} Z_v \\
&\leq C_6 K \int_0^\infty \sqrt{\log \mathcal{N}(B_2^d(0,r), \|\cdot\|, \delta)} d\delta \\
&= C_7 K \int_0^r \sqrt{\log \mathcal{N}(B_2^d(0,r), \|\cdot\|, \delta)} d\delta \\
&\leq C_7 K \int_0^r \sqrt{\log \left(\frac{3r}{\delta} \right)^d} d\delta \\
&= C_7 K \sqrt{d} \int_0^r \sqrt{\log(3) + \log(r/\delta)} d\delta \\
&\leq C_7 K \sqrt{d} \int_0^r \sqrt{\log(3) + \sqrt{\log(r/\delta)}} d\delta \\
&= C_7 K r \sqrt{d} (\sqrt{\log 3} + \sqrt{\pi}/2) \\
&= C_{12} K r \sqrt{d}
\end{aligned}$$

where we have used that

$$\int_0^r \sqrt{\log(r/\delta)} d\delta = r \int_0^1 \sqrt{\log(1/\delta)} = \frac{r\sqrt{\pi}}{2}.$$

Recombining, we have for an upper bound

$$\begin{aligned}
C_{12} K r \sqrt{d} &= C_{12} C_{11} \frac{1}{\sqrt{n}} \exp(4r^2/\varepsilon) \frac{re}{a} r \sqrt{d} \\
&\leq \frac{C_2 \sqrt{d} \exp(4r^2/\varepsilon)}{\sqrt{n}},
\end{aligned}$$

where we have used that $r^2/a \leq 1/2$ to cancel the r and the a . Integrating this bound with respect to P proves the result with $C_2 = (e/2)C_{11}C_{12}$. \square

8.6 Proof of Theorem 5

Proof. Choosing $a = C_1 r^2$ and combining Proposition 6 with Lemma 3 and Proposition 7 and taking expectations we have

$$\begin{aligned}
\mathbb{E} \frac{1}{4C_1 r^2} \|T_\varepsilon^n - T_\varepsilon\|_{L^2(P)}^2 &\leq \mathbb{E} \left[\frac{1}{\varepsilon} G + \int \int \exp(h_0(x)^T (y - T_\varepsilon(x)) - a \|h_0(x)\|^2) \gamma(x, y) [dQ^n - dQ](y) dP(x) \right] \\
&\leq C_{0,r,d} (1 + \varepsilon^{1-d'/2}) \log(n) n^{-1/2} + C_2 \sqrt{d} \exp(4r^2/\varepsilon) n^{-1/2}.
\end{aligned}$$

Letting $C_3 = 4C_1$ and multiplying both sides by $C_3 r^2$ we have

$$\mathbb{E} \|T_\varepsilon^n - T_\varepsilon\|_{L^2(P)}^2 \leq C_3 r^2 C_{0,r,d} (1 + \varepsilon^{1-d'/2}) \log(n) n^{-1/2} + C_3 r^2 C_2 \sqrt{d} \exp(4r^2/\varepsilon) n^{-1/2}$$

which proves the result with $C_{1,r,d} = C_3 C_{0,r,d}$. \square

9 Proof of Proposition 1

Proof. (a) Given $X, X' \stackrel{i.i.d.}{\sim} \mu_X \in \mathcal{P}(\Omega)$, and $Y, Y' \stackrel{i.i.d.}{\sim} \mu_Y \in \mathcal{P}(\Omega)$, using Lemmas 2.2, 2.3 from [29], we have,

$$2\mathbb{E}\|X - Y\| - \mathbb{E}\|X - X'\| - \mathbb{E}\|Y - Y'\| = C_d \int_{\mathcal{S}^{d-1}} \int_{\mathbb{R}} (\mathbb{P}(a^\top X \leq t) - \mathbb{P}(a^\top Y \leq t))^2 d\kappa(a) dt.$$

Constant	First Introduction	Value or Source
C	Statement of Theorem 2	$2C_3$
$C_{r,d}$	Statement of Theorem 2	$2r^2C_{1,r,d} + 2C_{2,r,d}$
C_0	Statement of Lemma 2	$4C_4^2C_5$
C_1	Statement of Lemma 3	$\max(C_0, 2)$
C_2	Statement of Lemma 3	$(\epsilon/2)C_{11}C_{12}$
$C_{0,r,d}$	Statement of Proposition 6	[40]Corollary 3
C_3	Statement of Theorem 5	$4C_1$
$C_{1,r,d}$	Statement of Theorem 5	$C_3C_{0,r,d}$
$C_{2,r,d}$	Statement of Theorem 6	[40] Theorem 5
C_4	Proof of Lemma 2	(2.3.8.iii) in [75], can be taken as $(\log 2)^{-1/2}$
C_5	Proof of Lemma 2	(2.5.2) in [75]
C_6	Proof of Lemma 2	$C_4^2C_5$
C_7	Proof of Lemma 3	(8.1.3) in [75]
C_8	Proof of Lemma 3	(2.6.8) in [75]
C_9	Proof of Lemma 3	(2.6.1) in [75]
C_{10}	Proof of Lemma 3	C_8C_9
C_{11}	Proof of Lemma 3	C_4C_{10}
C_{12}	Proof of Lemma 3	$C_7(\sqrt{\log 3} + \sqrt{\pi}/2)$

Table 3: Table of constants used in the proofs of the theoretical results.

Following the above expression, for the rank transformed random variables $\mathbf{R}_{\lambda,\epsilon}(X)$, $\mathbf{R}_{\lambda,\epsilon}(X')$, $\mathbf{R}_{\lambda,\epsilon}(Y)$, and $\mathbf{R}_{\lambda,\epsilon}(Y')$ corresponding to X , X' , Y , and Y' , respectively, we can express the soft rank energy as,

$$2\mathbb{E}\|\mathbf{R}_{\lambda,\epsilon}(X) - \mathbf{R}_{\lambda,\epsilon}(Y)\| - \mathbb{E}\|\mathbf{R}_{\lambda,\epsilon}(X) - \mathbf{R}_{\lambda,\epsilon}(X')\| - \mathbb{E}\|\mathbf{R}_{\lambda,\epsilon}(Y) - \mathbf{R}_{\lambda,\epsilon}(Y')\| \\ = C_d \int_{\mathcal{S}^{d-1}} \int_{\mathbb{R}} (\mathbb{P}(a^\top \mathbf{R}_{\lambda,\epsilon}(X) \leq t) - \mathbb{P}(a^\top \mathbf{R}_{\lambda,\epsilon}(Y) \leq t))^2 d\kappa(a) dt.$$

(b) Following the definition of $\mathbf{sRE}_{\lambda,\epsilon}$,

$$\mathbf{sRE}_{\lambda,\epsilon}(P_X, P_Y)^2 = C_d \int_{\mathbb{R}} \int_{\mathcal{S}^{d-1}} (\mathbb{P}(a^\top \mathbf{R}_{\lambda,\epsilon}(X) \leq t) - \mathbb{P}(a^\top \mathbf{R}_{\lambda,\epsilon}(Y) \leq t))^2 d\kappa(a) dt \\ = C_d \int_{\mathbb{R}} \int_{\mathcal{S}^{d-1}} (\mathbb{P}(a^\top \mathbf{R}_{\lambda,\epsilon}(Y) \leq t) - \mathbb{P}(a^\top \mathbf{R}_{\lambda,\epsilon}(X) \leq t))^2 d\kappa(a) dt \\ = \mathbf{sRE}_{\lambda,\epsilon}(P_Y, P_X)^2.$$

(c) Assuming $X \stackrel{d}{=} Y$, we have $\mathbb{P}(a^\top X \leq t) = \mathbb{P}(a^\top Y \leq t)$ for all $a \in \mathcal{S}^{d-1}$ and $t \in \mathbb{R}$ [29]. Since $\mathbf{R}_{\lambda,\epsilon}(X)$, $\mathbf{R}_{\lambda,\epsilon}(Y)$ are also mapped random vectors corresponding to X, Y , respectively, we see that $\mathbb{P}(a^\top \mathbf{R}_{\lambda,\epsilon}(X) \leq t) = \mathbb{P}(a^\top \mathbf{R}_{\lambda,\epsilon}(Y) \leq t)$ and the result follows. \square

10 Proof of Proposition 2

Proof. It is equivalent to show that

$$\lim_{\epsilon \rightarrow 0^+} |\mathbf{sRE}_{\lambda,\epsilon}(P_X, P_Y)^2 - \mathbf{RE}_\lambda(P_X, P_Y)^2| = 0.$$

Using the original definitions, we have

$$\begin{aligned}
& |\mathfrak{sRE}_{\lambda,\varepsilon}(P_X, P_Y)^2 - \mathfrak{RE}_{\lambda}(P_X, P_Y)^2| \\
&= \left| 2\mathbb{E} \left[\left| \|\mathbf{R}_{\lambda,\varepsilon}(X) - \mathbf{R}_{\lambda,\varepsilon}(Y)\| - \|\mathbf{R}_{\lambda}(X) - \mathbf{R}_{\lambda}(Y)\| \right| - \mathbb{E} \left[\left| \|\mathbf{R}_{\lambda,\varepsilon}(X) - \mathbf{R}_{\lambda,\varepsilon}(X')\| - \|\mathbf{R}_{\lambda}(X) - \mathbf{R}_{\lambda}(X')\| \right| \right] \right. \right. \\
&\quad \left. \left. - \mathbb{E} \left[\left| \|\mathbf{R}_{\lambda,\varepsilon}(Y) - \mathbf{R}_{\lambda,\varepsilon}(Y')\| - \|\mathbf{R}_{\lambda}(Y) - \mathbf{R}_{\lambda}(Y')\| \right| \right] \right| \right| \\
&\leq 2\mathbb{E} \left| \|\mathbf{R}_{\lambda,\varepsilon}(X) - \mathbf{R}_{\lambda,\varepsilon}(Y)\| - \|\mathbf{R}_{\lambda}(X) - \mathbf{R}_{\lambda}(Y)\| \right| + \mathbb{E} \left| \|\mathbf{R}_{\lambda,\varepsilon}(X) - \mathbf{R}_{\lambda,\varepsilon}(X')\| - \|\mathbf{R}_{\lambda}(X) - \mathbf{R}_{\lambda}(X')\| \right| \\
&\quad + \mathbb{E} \left| \|\mathbf{R}_{\lambda,\varepsilon}(Y) - \mathbf{R}_{\lambda,\varepsilon}(Y')\| - \|\mathbf{R}_{\lambda}(Y) - \mathbf{R}_{\lambda}(Y')\| \right| \\
&\leq 2\mathbb{E} \left| [\mathbf{R}_{\lambda,\varepsilon}(X) - \mathbf{R}_{\lambda,\varepsilon}(Y)] - [\mathbf{R}_{\lambda}(X) - \mathbf{R}_{\lambda}(Y)] \right| + \mathbb{E} \left| [\mathbf{R}_{\lambda,\varepsilon}(X) - \mathbf{R}_{\lambda,\varepsilon}(X')] - [\mathbf{R}_{\lambda}(X) - \mathbf{R}_{\lambda}(X')] \right| \\
&\quad + \mathbb{E} \left| [\mathbf{R}_{\lambda,\varepsilon}(Y) - \mathbf{R}_{\lambda,\varepsilon}(Y')] - [\mathbf{R}_{\lambda}(Y) - \mathbf{R}_{\lambda}(Y')] \right| \\
&\leq 4\mathbb{E} \|\mathbf{R}_{\lambda}(X) - \mathbf{R}_{\lambda,\varepsilon}(X)\| + 4\mathbb{E} \|\mathbf{R}_{\lambda}(Y) - \mathbf{R}_{\lambda,\varepsilon}(Y)\| \\
&\leq 4\sqrt{\mathbb{E} \|\mathbf{R}_{\lambda}(X) - \mathbf{R}_{\lambda,\varepsilon}(X)\|^2} + 4\sqrt{\mathbb{E} \|\mathbf{R}_{\lambda}(Y) - \mathbf{R}_{\lambda,\varepsilon}(Y)\|^2} \\
&\leq 8\sqrt{\mathbb{E} \|\mathbf{R}_{\lambda}(X) - \mathbf{R}_{\lambda,\varepsilon}(X)\|^2 + \mathbb{E} \|\mathbf{R}_{\lambda}(Y) - \mathbf{R}_{\lambda,\varepsilon}(Y)\|^2} \\
&\leq \frac{8}{\min(\sqrt{\lambda}, \sqrt{1-\lambda})} \sqrt{\mathbb{E}[\lambda \|\mathbf{R}_{\lambda}(X) - \mathbf{R}_{\lambda,\varepsilon}(X)\|^2 + (1-\lambda) \|\mathbf{R}_{\lambda}(Y) - \mathbf{R}_{\lambda,\varepsilon}(Y)\|^2]} \\
&= \frac{8}{\min(\sqrt{\lambda}, \sqrt{1-\lambda})} \|\mathbf{R}_{\lambda} - \mathbf{R}_{\lambda,\varepsilon}\|_{L^2(P_{\lambda})} \\
&\lesssim \frac{8}{\min(\sqrt{\lambda}, \sqrt{1-\lambda})} \sqrt{\varepsilon^2 I_0(P_{\lambda}, \text{Unif}([0, 1]^d)) + \varepsilon^{\min(\alpha, 3)/2}}
\end{aligned}$$

where for the final inequality we have used Proposition 1 in [76] and where the implicit constant is independent of ε . Here I_0 is the integrated Fisher information along the geodesic from P_{λ} and $\text{Unif}([0, 1]^d)$ which under the assumptions made is guaranteed to be finite, [77, 40]. Taking the limit in the last expression we have

$$\begin{aligned}
0 &\leq \lim_{\varepsilon \rightarrow 0^+} |\mathfrak{sRE}_{\lambda,\varepsilon}(P_X, P_Y)^2 - \mathfrak{RE}_{\lambda}(P_X, P_Y)^2| \\
&\lesssim \lim_{\varepsilon \rightarrow 0^+} \frac{8}{\min(\sqrt{\lambda}, \sqrt{1-\lambda})} \sqrt{\varepsilon^2 I_0(P_{\lambda}, \text{Unif}([0, 1]^d)) + \varepsilon^{\min(\alpha, 3)/2}} = 0
\end{aligned}$$

which shows indeed $\lim_{\varepsilon \rightarrow 0^+} |\mathfrak{sRE}_{\lambda,\varepsilon}(P_X, P_Y)^2 - \mathfrak{RE}_{\lambda}(P_X, P_Y)^2| = 0$. \square

11 Proof of Theorem 3

The proof is relative simple and is mostly a matter of wrangling long expressions.

Proof. Using the notation that $\mathbf{R}_{\lambda,\varepsilon}^{m+n}$ is the random independently estimated map and $X^m = (X_1, \dots, X_m), Y^n = (Y_1, \dots, Y_n)$ are the samples used to evaluate the statistic (which are independent of $\mathbf{R}_{\lambda,\varepsilon}^{m+n}$) we immediately have the following

$$\|\mathfrak{sRE}_{\lambda,\varepsilon}^{m,n}(P_X, P_Y)^2 - \mathfrak{sRE}_{\lambda,\varepsilon}(P_X, P_Y)^2\|_{L^2}^2 = \mathbb{E}_{\mathbf{R}_{\lambda,\varepsilon}^{m+n}} \left[\mathbb{E}_{X^n, Y^m} \left[\left(\mathfrak{sRE}_{\lambda,\varepsilon}^{m,n}(P_X, P_Y)^2 - \mathfrak{sRE}_{\lambda,\varepsilon}(P_X, P_Y)^2 \right)^2 \middle| \mathbf{R}_{\lambda,\varepsilon}^{m+n} \right] \right].$$

We first consider the inner expectation. For brevity we suppress the conditioning on $\mathbf{R}_{\lambda,\varepsilon}^{m+n}$ and also introduce the following six collections of random variables

$$\begin{aligned}
R^X &\triangleq \frac{1}{m^2} \sum_{i,j=1}^m \|\mathbf{R}_{\lambda,\varepsilon}(X_i) - \mathbf{R}_{\lambda,\varepsilon}(X_j)\|, & \hat{R}^X &\triangleq \frac{1}{m^2} \sum_{i,j=1}^m \|\mathbf{R}_{\lambda,\varepsilon}^{m+n}(X_i) - \mathbf{R}_{\lambda,\varepsilon}^{m+n}(X_j)\|, \\
R^Y &\triangleq \frac{1}{n^2} \sum_{i,j=1}^n \|\mathbf{R}_{\lambda,\varepsilon}(Y_i) - \mathbf{R}_{\lambda,\varepsilon}(Y_j)\|, & \hat{R}^Y &\triangleq \frac{1}{n^2} \sum_{i,j=1}^n \|\mathbf{R}_{\lambda,\varepsilon}^{m+n}(Y_i) - \mathbf{R}_{\lambda,\varepsilon}^{m+n}(Y_j)\|, \\
R^{XY} &\triangleq \frac{2}{nm} \sum_{i=1}^m \sum_{j=1}^n \|\mathbf{R}_{\lambda,\varepsilon}(X_i) - \mathbf{R}_{\lambda,\varepsilon}(Y_j)\|, & \hat{R}^{XY} &\triangleq \frac{2}{nm} \sum_{i=1}^m \sum_{j=1}^n \|\mathbf{R}_{\lambda,\varepsilon}^{m+n}(X_i) - \mathbf{R}_{\lambda,\varepsilon}^{m+n}(Y_j)\|.
\end{aligned}$$

These are further compressed into

$$\begin{aligned}\hat{R} &\triangleq \hat{R}^{XY} - \hat{R}^X - \hat{R}^Y, \\ R &\triangleq R^{XY} - R^X - R^Y.\end{aligned}$$

We also introduce the notation

$$\begin{aligned}E^X &\triangleq \mathbb{E}_{X, X'} \|\mathbf{R}_{\lambda, \varepsilon}(X) - \mathbf{R}_{\lambda, \varepsilon}(X')\|, \\ E^Y &\triangleq \mathbb{E}_{Y, Y'} \|\mathbf{R}_{\lambda, \varepsilon}(Y) - \mathbf{R}_{\lambda, \varepsilon}(Y')\|, \\ E^{XY} &\triangleq 2 \mathbb{E}_{X, Y} \|\mathbf{R}_{\lambda, \varepsilon}(X) - \mathbf{R}_{\lambda, \varepsilon}(Y)\|, \\ E &\triangleq E^{XY} - E^X - E^Y.\end{aligned}$$

With this notation we have

$$\begin{aligned}\mathbb{E} \left[\left(\mathbf{sRE}_{\lambda, \varepsilon}^{m, n}(P_X, P_Y)^2 - \mathbf{sRE}_{\lambda, \varepsilon}(P_X, P_Y)^2 \right)^2 \right] &= \mathbb{E}(\hat{R} - E)^2 \\ &= \mathbb{E}([\hat{R} - R] - [R - E])^2 \\ &\leq 2\mathbb{E}(\hat{R} - R)^2 + 2\mathbb{E}(R - E)^2\end{aligned}$$

We now control the two expectations separately:

$$\begin{aligned}\mathbb{E}(\hat{R} - R)^2 &= \mathbb{E} \left([\hat{R}^{XY} - R^{XY}] + [R^X - \hat{R}^X] + [R^Y - \hat{R}^Y] \right)^2 \\ &\leq 3\mathbb{E}(\hat{R}^{XY} - R^{XY})^2 + 3\mathbb{E}(\hat{R}^X - R^X)^2 + 3\mathbb{E}(\hat{R}^Y - R^Y)^2.\end{aligned}$$

Next we control these three expectations separately:

$$\begin{aligned}\mathbb{E}(\hat{R}^{XY} - R^{XY})^2 &= \mathbb{E} \left(\frac{2}{nm} \sum_{i=1}^m \sum_{j=1}^n \|\mathbf{R}_{\lambda, \varepsilon}^{m+n}(X_i) - \mathbf{R}_{\lambda, \varepsilon}^{m+n}(Y_j)\| - \|\mathbf{R}_{\lambda, \varepsilon}(X_i) - \mathbf{R}_{\lambda, \varepsilon}(Y_j)\| \right)^2 \\ &\leq 4\mathbb{E} \frac{1}{nm} \sum_{i=1}^m \sum_{j=1}^n \left(\|\mathbf{R}_{\lambda, \varepsilon}^{m+n}(X_i) - \mathbf{R}_{\lambda, \varepsilon}^{m+n}(Y_j)\| - \|\mathbf{R}_{\lambda, \varepsilon}(X_i) - \mathbf{R}_{\lambda, \varepsilon}(Y_j)\| \right)^2 \\ &\leq 4\mathbb{E} \frac{1}{nm} \sum_{i=1}^m \sum_{j=1}^n \left\| [\mathbf{R}_{\lambda, \varepsilon}^{m+n}(X_i) - \mathbf{R}_{\lambda, \varepsilon}^{m+n}(Y_j)] - [\mathbf{R}_{\lambda, \varepsilon}(X_i) - \mathbf{R}_{\lambda, \varepsilon}(Y_j)] \right\|^2 \\ &\leq 4\mathbb{E} \frac{1}{nm} \sum_{i=1}^m \sum_{j=1}^n \left(\|\mathbf{R}_{\lambda, \varepsilon}^{m+n}(X_i) - \mathbf{R}_{\lambda, \varepsilon}(X_i)\| + \|\mathbf{R}_{\lambda, \varepsilon}^{m+n}(Y_j) - \mathbf{R}_{\lambda, \varepsilon}(Y_j)\| \right)^2 \\ &\leq 8\mathbb{E} \frac{1}{nm} \sum_{i=1}^m \sum_{j=1}^n \left(\|\mathbf{R}_{\lambda, \varepsilon}^{m+n}(X_i) - \mathbf{R}_{\lambda, \varepsilon}(X_i)\|^2 + \|\mathbf{R}_{\lambda, \varepsilon}^{m+n}(Y_j) - \mathbf{R}_{\lambda, \varepsilon}(Y_j)\|^2 \right) \\ &= 8\mathbb{E} \frac{1}{m} \sum_{i=1}^m \|\mathbf{R}_{\lambda, \varepsilon}^{m+n}(X_i) - \mathbf{R}_{\lambda, \varepsilon}(X_i)\|^2 + 8\mathbb{E} \frac{1}{n} \sum_{i=1}^n \|\mathbf{R}_{\lambda, \varepsilon}^{m+n}(Y_i) - \mathbf{R}_{\lambda, \varepsilon}(Y_i)\|^2 \\ &= 8\mathbb{E} \|\mathbf{R}_{\lambda, \varepsilon}^{m+n}(X) - \mathbf{R}_{\lambda, \varepsilon}(X)\|^2 + \|\mathbf{R}_{\lambda, \varepsilon}^{m+n}(Y) - \mathbf{R}_{\lambda, \varepsilon}(Y)\|^2 \\ &\leq \frac{8}{\min(\lambda, 1 - \lambda)} \mathbb{E} \lambda \|\mathbf{R}_{\lambda, \varepsilon}^{m+n}(X) - \mathbf{R}_{\lambda, \varepsilon}(X)\|^2 + (1 - \lambda) \|\mathbf{R}_{\lambda, \varepsilon}^{m+n}(Y) - \mathbf{R}_{\lambda, \varepsilon}(Y)\|^2 \\ &= \frac{8}{\min(\lambda, 1 - \lambda)} \|\mathbf{R}_{\lambda, \varepsilon}^{m+n} - \mathbf{R}_{\lambda, \varepsilon}\|_{L^2(P_\lambda)}^2.\end{aligned}$$

In the third and fourth lines we have used the reverse triangle inequality followed by the triangle inequality to re-group the terms. In the second to last line we have made use of the inequality valid for all $a, b \geq 0, c \in (0, 1)$

$$a + b \leq \frac{c}{\min(c, 1 - c)} a + \frac{1 - c}{\min(c, 1 - c)} b = \frac{1}{\min(c, 1 - c)} [ca + (1 - c)b].$$

The last line follows from the fact that $P_\lambda = \lambda P_X + (1 - \lambda)P_Y$. Next we have

$$\begin{aligned}
\mathbb{E}(\hat{R}^X - R^X)^2 &= \mathbb{E} \left(\frac{1}{n^2} \sum_{i,j=1}^n \left| \mathbf{R}_{\lambda,\varepsilon}^{m+n}(X_i) - \mathbf{R}_{\lambda,\varepsilon}^{m+n}(X_j) \right| - \left| \mathbf{R}_{\lambda,\varepsilon}(X_i) - \mathbf{R}_{\lambda,\varepsilon}(X_j) \right| \right)^2 \\
&\leq \mathbb{E} \frac{1}{n^2} \sum_{i,j=1}^n \left(\left| \mathbf{R}_{\lambda,\varepsilon}^{m+n}(X_i) - \mathbf{R}_{\lambda,\varepsilon}^{m+n}(X_j) \right| - \left| \mathbf{R}_{\lambda,\varepsilon}(X_i) - \mathbf{R}_{\lambda,\varepsilon}(X_j) \right| \right)^2 \\
&\leq \mathbb{E} \frac{1}{n^2} \sum_{i,j=1}^n \left| \left[\mathbf{R}_{\lambda,\varepsilon}^{m+n}(X_i) - \mathbf{R}_{\lambda,\varepsilon}^{m+n}(X_j) \right] - \left[\mathbf{R}_{\lambda,\varepsilon}(X_i) - \mathbf{R}_{\lambda,\varepsilon}(X_j) \right] \right|^2 \\
&\leq \mathbb{E} \frac{1}{n^2} \sum_{i,j=1}^n \left(\left| \mathbf{R}_{\lambda,\varepsilon}^{m+n}(X_i) - \mathbf{R}_{\lambda,\varepsilon}(X_i) \right| + \left| \mathbf{R}_{\lambda,\varepsilon}^{m+n}(X_j) - \mathbf{R}_{\lambda,\varepsilon}(X_j) \right| \right)^2 \\
&\leq 2\mathbb{E} \frac{1}{n^2} \sum_{i,j=1}^n \left(\left| \mathbf{R}_{\lambda,\varepsilon}^{m+n}(X_i) - \mathbf{R}_{\lambda,\varepsilon}(X_i) \right|^2 + \left| \mathbf{R}_{\lambda,\varepsilon}^{m+n}(X_j) - \mathbf{R}_{\lambda,\varepsilon}(X_j) \right|^2 \right) \\
&= 4\mathbb{E} \frac{1}{n} \sum_{i=1}^n \left| \mathbf{R}_{\lambda,\varepsilon}^{m+n}(X_i) - \mathbf{R}_{\lambda,\varepsilon}(X_i) \right|^2 \\
&= 4\mathbb{E} \left| \mathbf{R}_{\lambda,\varepsilon}^{m+n}(X) - \mathbf{R}_{\lambda,\varepsilon}(X) \right|^2.
\end{aligned}$$

Again in the third and fourth lines we have used the reverse-triangle inequality followed by the triangle inequality. An exactly analogous calculation for Y shows

$$\mathbb{E}(\hat{R}^Y - R^Y)^2 \leq 4\mathbb{E} \left| \mathbf{R}_{\lambda,\varepsilon}^{m+n}(Y) - \mathbf{R}_{\lambda,\varepsilon}(Y) \right|^2.$$

Combining these two we have similarly to above that

$$\begin{aligned}
\mathbb{E}(\hat{R}^X - R^X)^2 + \mathbb{E}(\hat{R}^Y - R^Y)^2 &\leq 4\mathbb{E} \left[\left| \mathbf{R}_{\lambda,\varepsilon}^{m+n}(X) - \mathbf{R}_{\lambda,\varepsilon}(X) \right|^2 + \left| \mathbf{R}_{\lambda,\varepsilon}^{m+n}(Y) - \mathbf{R}_{\lambda,\varepsilon}(Y) \right|^2 \right] \\
&\leq \frac{4}{\min(\lambda, 1 - \lambda)} \left\| \mathbf{R}_{\lambda,\varepsilon}^{m+n} - \mathbf{R}_{\lambda,\varepsilon} \right\|_{L^2(P_\lambda)}^2.
\end{aligned}$$

Combining bounds we have

$$\begin{aligned}
\mathbb{E}(\hat{R} - R)^2 &\leq \frac{24}{\min(\lambda, 1 - \lambda)} \left\| \mathbf{R}_{\lambda,\varepsilon}^{m+n} - \mathbf{R}_{\lambda,\varepsilon} \right\|_{L^2(P_\lambda)}^2 + \frac{12}{\min(\lambda, 1 - \lambda)} \left\| \mathbf{R}_{\lambda,\varepsilon}^{m+n} - \mathbf{R}_{\lambda,\varepsilon} \right\|_{L^2(P_\lambda)}^2 \\
&= \frac{36}{\min(\lambda, 1 - \lambda)} \left\| \mathbf{R}_{\lambda,\varepsilon}^{m+n} - \mathbf{R}_{\lambda,\varepsilon} \right\|_{L^2(P_\lambda)}^2.
\end{aligned}$$

Now we turn our attention to $\mathbb{E}(R - E)^2$. First we show that $R - E$ is mean-zero:

$$\begin{aligned}
\mathbb{E}R &= \mathbb{E} \frac{2}{nm} \sum_{i=1}^m \sum_{j=1}^n \left| \mathbf{R}_{\lambda,\varepsilon}(X_i) - \mathbf{R}_{\lambda,\varepsilon}(Y_j) \right| - \frac{1}{m^2} \sum_{i,j=1}^m \left| \mathbf{R}_{\lambda,\varepsilon}(X_i) - \mathbf{R}_{\lambda,\varepsilon}(X_j) \right| - \frac{1}{n^2} \sum_{i,j=1}^n \left| \mathbf{R}_{\lambda,\varepsilon}(Y_i) - \mathbf{R}_{\lambda,\varepsilon}(Y_j) \right| \\
&= 2\mathbb{E} \left| \mathbf{R}_{\lambda,\varepsilon}(X) - \mathbf{R}_{\lambda,\varepsilon}(Y) \right| - \mathbb{E} \left| \mathbf{R}_{\lambda,\varepsilon}(X) - \mathbf{R}_{\lambda,\varepsilon}(X') \right| - \mathbb{E} \left| \mathbf{R}_{\lambda,\varepsilon}(Y) - \mathbf{R}_{\lambda,\varepsilon}(Y') \right| \\
&= E^{XY} - E^X - E^Y = E.
\end{aligned}$$

Subtracting E from the first and last shows $\mathbb{E}[R - E] = 0$. Using this we have

$$\mathbb{E}[(R - E)^2] = \mathbb{E}[(R - E)^2] - \mathbb{E}[R - E]^2 = \text{Var}(R - E).$$

To control the variance we apply the Efron-Stein inequality ([42] Theorem 3.1) to the function

$$f(X_1, \dots, X_m, Y_1, \dots, Y_n) = \frac{2}{nm} \sum_{i=1}^m \sum_{j=1}^n \left| \mathbf{R}_{\lambda,\varepsilon}(X_i) - \mathbf{R}_{\lambda,\varepsilon}(Y_j) \right| - \frac{1}{m^2} \sum_{i,j=1}^m \left| \mathbf{R}_{\lambda,\varepsilon}(X_i) - \mathbf{R}_{\lambda,\varepsilon}(X_j) \right| - \frac{1}{n^2} \sum_{i,j=1}^n \left| \mathbf{R}_{\lambda,\varepsilon}(Y_i) - \mathbf{R}_{\lambda,\varepsilon}(Y_j) \right|.$$

First note that we have the bounds

$$\begin{aligned}
& |f(X_1, \dots, X_{i-1}, X_i, X_{i+1}, \dots, X_m, Y_1, \dots, Y_n) - f(X_1, \dots, X_{i-1}, X'_i, X_{i+1}, \dots, X_m, Y_1, \dots, Y_n)| \\
&= \left| \frac{2}{nm} \sum_{j=1}^n (|\mathbf{R}_{\lambda, \varepsilon}(X_i) - \mathbf{R}_{\lambda, \varepsilon}(Y_j)| - |\mathbf{R}_{\lambda, \varepsilon}(X'_i) - \mathbf{R}_{\lambda, \varepsilon}(Y_j)|) - \frac{1}{m^2} \sum_{j \neq i}^m (|\mathbf{R}_{\lambda, \varepsilon}(X_i) - \mathbf{R}_{\lambda, \varepsilon}(X_j)| - |\mathbf{R}_{\lambda, \varepsilon}(X'_i) - \mathbf{R}_{\lambda, \varepsilon}(X_j)|) \right| \\
&\leq \frac{2}{nm} \sum_{j=1}^n \left| |\mathbf{R}_{\lambda, \varepsilon}(X_i) - \mathbf{R}_{\lambda, \varepsilon}(Y_j)| - |\mathbf{R}_{\lambda, \varepsilon}(X'_i) - \mathbf{R}_{\lambda, \varepsilon}(Y_j)| \right| + \frac{1}{m^2} \sum_{j \neq i}^m \left| |\mathbf{R}_{\lambda, \varepsilon}(X_i) - \mathbf{R}_{\lambda, \varepsilon}(X_j)| - |\mathbf{R}_{\lambda, \varepsilon}(X'_i) - \mathbf{R}_{\lambda, \varepsilon}(X_j)| \right| \\
&\leq \frac{2}{nm} \sum_{j=1}^n \|\mathbf{R}_{\lambda, \varepsilon}(X_i) - \mathbf{R}_{\lambda, \varepsilon}(X'_i)\| + \frac{1}{m^2} \sum_{j \neq i}^m \|\mathbf{R}_{\lambda, \varepsilon}(X_i) - \mathbf{R}_{\lambda, \varepsilon}(X'_i)\| \\
&\leq \frac{3}{m} \|\mathbf{R}_{\lambda, \varepsilon}(X_i) - \mathbf{R}_{\lambda, \varepsilon}(X'_i)\| \\
&\leq \frac{3\sqrt{d}}{m}
\end{aligned}$$

where we have in the last line used the $\mathbf{R}_{\lambda, \varepsilon}$ maps into $[0, 1]^d$ and the diameter is \sqrt{d} . A completely analogous computation shows

$$|f(X_1, \dots, X_m, Y_1, \dots, Y_{i-1}, Y_i, Y_{i+1}, \dots, Y_n) - f(X_1, \dots, X_m, Y_1, \dots, Y_{i-1}, Y'_i, Y_{i+1}, \dots, Y_n)| \leq \frac{3\sqrt{d}}{m}.$$

Using this bound in the Efron-Stein inequality we have

$$\begin{aligned}
\mathbb{E}[(R - E)^2] &= \text{Var}(R - E) \\
&\leq \frac{1}{2} \sum_{i=1}^m \mathbb{E} (f(X_1, \dots, X_{i-1}, X_i, X_{i+1}, \dots, X_m, Y_1, \dots, Y_n) - f(X_1, \dots, X_{i-1}, X'_i, X_{i+1}, \dots, X_m, Y_1, \dots, Y_n))^2 \\
&\quad + \frac{1}{2} \sum_{i=1}^n \mathbb{E} (f(X_1, \dots, X_m, Y_1, \dots, Y_{i-1}, Y_i, Y_{i+1}, \dots, Y_n) - f(X_1, \dots, X_m, Y_1, \dots, Y_{i-1}, Y'_i, Y_{i+1}, \dots, Y_n))^2 \\
&\leq \frac{1}{2} \sum_{i=1}^m \mathbb{E} \left(\frac{3\sqrt{d}}{m} \right)^2 + \frac{1}{2} \sum_{i=1}^n \mathbb{E} \left(\frac{3\sqrt{d}}{n} \right)^2 \\
&= \frac{9d}{2m} + \frac{9d}{2n} \\
&= \frac{9d(m+n)}{2mn}.
\end{aligned}$$

Collecting terms we have, conditionally on the estimate of $\mathbf{R}_{\lambda, \varepsilon}^{m+n}$ that

$$\begin{aligned}
\mathbb{E} \left[\left(\mathbf{sRE}_{\lambda, \varepsilon}^{m, n}(P_X, P_Y)^2 - \mathbf{sRE}_{\lambda, \varepsilon}(P_X, P_Y)^2 \right)^2 \right] &\leq 2\mathbb{E}(\hat{R} - R)^2 + 2\mathbb{E}(R - E)^2 \\
&\leq \frac{72}{\min(\lambda, 1 - \lambda)} \|\mathbf{R}_{\lambda, \varepsilon}^{m+n} - \mathbf{R}_{\lambda, \varepsilon}\|_{L^2(P_\lambda)}^2 + \frac{9d(m+n)}{mn}.
\end{aligned}$$

Unconditioning and applying Theorem 2 yields

$$\|\mathbf{sRE}_{\lambda, \varepsilon}^{m, n}(P_X, P_Y)^2 - \mathbf{sRE}_{\lambda, \varepsilon}(P_X, P_Y)^2\|_{L^2}^2 \leq \frac{72}{\min(\lambda, (1 - \lambda))} g(N, r, d, \varepsilon) + \frac{9d(m+n)}{mn}.$$

□

12 Proof of Theorem 4

The proof is essentially the same as the proof of Theorem 3. The key difference is that we require a kernel analog of the reverse-triangle, followed by triangle inequality trick:

$$\begin{aligned}
\left| \|\mathbf{R}_{\lambda, \varepsilon}^{m+n}(X_i) - \mathbf{R}_{\lambda, \varepsilon}^{m+n}(Y_j)\| - \|\mathbf{R}_{\lambda, \varepsilon}(X_i) - \mathbf{R}_{\lambda, \varepsilon}(Y_j)\| \right| &\leq \left| \|\mathbf{R}_{\lambda, \varepsilon}^{m+n}(X_i) - \mathbf{R}_{\lambda, \varepsilon}^{m+n}(Y_j)\| - \|\mathbf{R}_{\lambda, \varepsilon}(X_i) - \mathbf{R}_{\lambda, \varepsilon}(Y_j)\| \right| \\
&\leq \|\mathbf{R}_{\lambda, \varepsilon}^{m+n}(X_i) - \mathbf{R}_{\lambda, \varepsilon}(X_i)\| + \|\mathbf{R}_{\lambda, \varepsilon}^{m+n}(Y_j) - \mathbf{R}_{\lambda, \varepsilon}(Y_j)\|
\end{aligned}$$

This is achieved through

$$\begin{aligned}
& |k(\mathbf{R}_{\lambda,\varepsilon}^{m+n}(X_i), \mathbf{R}_{\lambda,\varepsilon}^{m+n}(Y_j)) - k(\mathbf{R}_{\lambda,\varepsilon}(X_i), \mathbf{R}_{\lambda,\varepsilon}(Y_j))| \\
&= |[k(\mathbf{R}_{\lambda,\varepsilon}^{m+n}(X_i), \mathbf{R}_{\lambda,\varepsilon}^{m+n}(Y_j)) - k(\mathbf{R}_{\lambda,\varepsilon}(X_i), \mathbf{R}_{\lambda,\varepsilon}^{m+n}(Y_j))] + [k(\mathbf{R}_{\lambda,\varepsilon}(X_i), \mathbf{R}_{\lambda,\varepsilon}^{m+n}(Y_j)) - k(\mathbf{R}_{\lambda,\varepsilon}(X_i), \mathbf{R}_{\lambda,\varepsilon}(Y_j))]| \\
&\leq |k(\mathbf{R}_{\lambda,\varepsilon}^{m+n}(X_i), \mathbf{R}_{\lambda,\varepsilon}^{m+n}(Y_j)) - k(\mathbf{R}_{\lambda,\varepsilon}(X_i), \mathbf{R}_{\lambda,\varepsilon}^{m+n}(Y_j))| + |k(\mathbf{R}_{\lambda,\varepsilon}(X_i), \mathbf{R}_{\lambda,\varepsilon}^{m+n}(Y_j)) - k(\mathbf{R}_{\lambda,\varepsilon}(X_i), \mathbf{R}_{\lambda,\varepsilon}(Y_j))| \\
&\leq l\|\mathbf{R}_{\lambda,\varepsilon}^{m+n}(X_i) - \mathbf{R}_{\lambda,\varepsilon}(X_i)\| + l\|\mathbf{R}_{\lambda,\varepsilon}^{m+n}(Y_j) - \mathbf{R}_{\lambda,\varepsilon}(Y_j)\|.
\end{aligned}$$

With this key inequality established, one can show the result by following the proof of Theorem 3, substituting this inequality in the two places where the reverse-triangle followed triangle inequality is used. In both places these inequalities are done inside of a squaring so ultimately we gain a factor of l^2 .

13 Related Works on Knockoff Generation

The seminal work [55] assumes that the joint feature distribution follows a multivariate Gaussian distribution and satisfies the pairwise exchangeability condition (18) via approximating only the first two moments (mean and covariance). In cases where the distributions are not multivariate Gaussian, the second order method in [55] cannot guarantee any control of the FDR. In contrast, methods like knockoffGAN [56], deep knockoff [58], auto-encoding knockoff [57] focus on learning generative models to sample knockoffs. KnockoffGAN is a complex architecture which consists of four different neural networks and optimizes a difficult minimax problem. A comparatively simpler approach adopted by deep knockoff employs MMD [31] as the discriminating statistic for testing pairwise exchangeability in (18). As we see in Section 14.2 the generator learned using the MMD performs poorly in high dimensions, and fails to approximate the input distribution properly. Auto-encoding knockoff uses a variational autoencoder [50] that learns a low-dimensional latent space for the high-dimensional data. The performance of the auto-encoding knockoff depends on the latent space dimension. A higher dimensional latent space can be used to make the model better but may lead to diminished power if the covariates violate the low-dimensional approximation. Another method, called deep direct likelihood knockoff (DDLK) [59] minimizes the KL (Kullback-Liebler) divergence to test for pairwise exchangeability.

13.1 Schematic of the Knockoff Generator

Figure 3 shows the schematic of the deep generative model used for the knockoff generator (Section 5.2.1). The model has a fully connected neural network f_θ , where θ represents the parameters of the network (weights w and biases b). f_θ has 6 hidden layers each of them having $6 \cdot d$ units. The first layer of the neural network takes a vector of original variables $X \in \mathbb{R}^d$ and a d -dimensional noise vector $V \sim \mathcal{N}(0, I)$. Each unit in the hidden layers is produced by first taking linear combinations of the input followed by applying to each a nonlinear activation function. Parametric rectified linear unit is used as the activation function [78]. The output layer returns a d -dimensional knockoff vector as depicted in Figure 3.

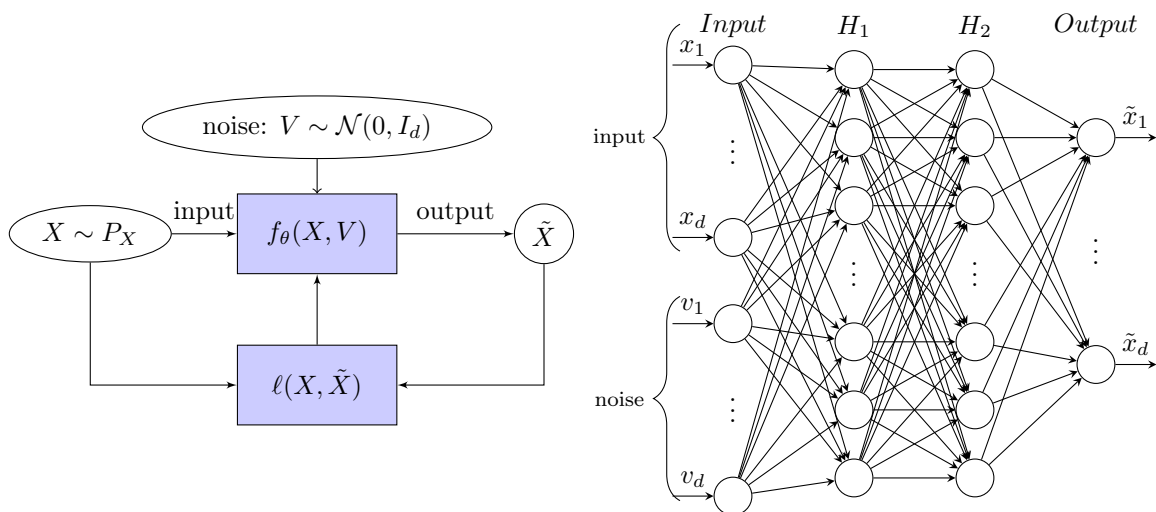


Figure 3: *Left*: schematic of the deep generative model for knockoff generation. *Right*: schematic of f_θ is shown for 2 hidden layers (for all experiments we use 6 hidden layers).

13.2 Algorithm to Train Knockoff Generator

Algorithm 1: Training of the Knockoff Generator

Input : training data: $\mathbf{X} \in \mathbb{R}^{n \times d}$, learning rate: η , entropic regularizer: ε , decorrelation parameter: γ ,
 θ_0 : initialization of network parameters, no of epochs: T , batch size: m , no of batches: n_b

Output : knockoff generator: f_{θ_T}

```

1 for  $t \leftarrow 0$  to  $T$  do
2   for  $j \leftarrow 0$  to  $n_b$  do
3      $X_i$ , for all  $1 \leq i \leq m$  // samples for a minibatch
4      $V_i \sim \mathcal{N}(0, I)$  for all  $1 \leq i \leq m$  // noise sampling.
5      $\tilde{X}_i \leftarrow f_{\theta_t}(X_i, V_i)$ , for all  $1 \leq i \leq m$  // knockoff generation.
6      $B \subset \{1, \dots, d\}$  // picking a random subset.
7      $J_{\theta_t}(\mathbf{X}_m, \tilde{\mathbf{X}}_m) \leftarrow \ell(\mathbf{X}_m, \tilde{\mathbf{X}}_m)$  // loss calculation using (18)
8      $\theta_{t+1} = \theta_t - \eta \nabla_{\theta_t}(J_{\theta_t})$  // parameter update
9   end for
10 end for

```

13.3 Compute Resources

We use NVIDIA TESLA-K80 24 GB GPU for each simulation. On average, training time of the proposed knockoff generator is around 2 hours for each distributional setting and for the MNIST image generator, it is about 45 minutes.

13.4 Baseline Models for Knockoff Generation

For KnockoffGAN, we use the code from <https://bitbucket.org/mvdschaar/mlforhealthlabpub/src/master/>. For DDLK, code is taken from a publicly available repository <https://github.com/rajesh-lab/ddlk>. For other two benchmarks, second-order and MMD knockoffs, we use the code from this repository <https://github.com/msesia/deepknockoffs>.

14 Additional Experiments

14.1 Effect of ε , σ on sRMMD-Based MNIST Image Generator (Section 5.1)

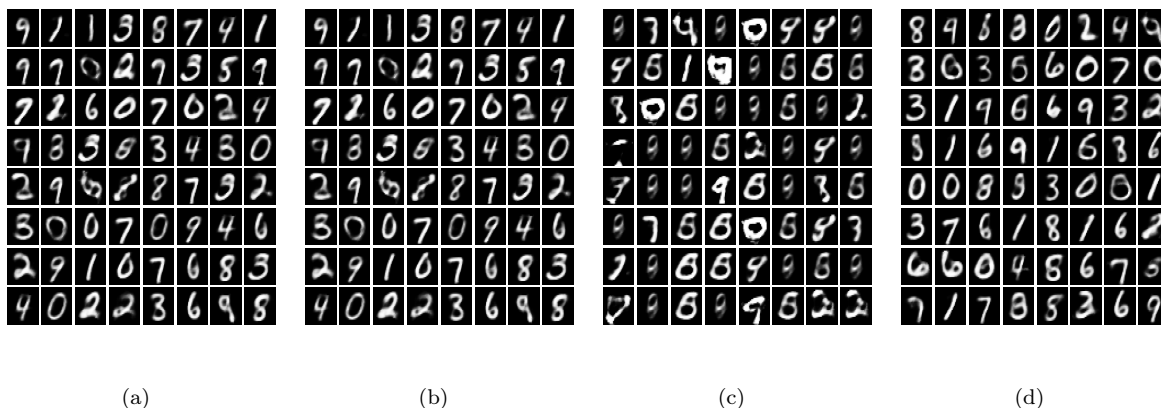


Figure 4: sRMMD-based MNIST image generator (latent space dimension 8) using (a) $\varepsilon = 10, \sigma = (1, 2, 4, 8, 16, 32)$. (b) $\varepsilon = 10, \sigma = (0.01, 0.02, 0.04, 0.06, 0.08)$ (c) $\varepsilon = 20, \sigma = (0.01, 0.02, 0.04, 0.06, 0.08)$, and (d) $\varepsilon = 20, \sigma = (0.001, 0.002, 0.004, 0.006, 0.008)$.

MNIST-image generator minimizing the sRMMD loss produces a lot of ambiguous digits of similar shape when $\varepsilon = 10$ and $\sigma = (1, 2, 4, 8, 16, 32)$ are used. To understand why this may be the case, we plot the generator’s loss over the training epochs (Figure 5). We observe that the loss is nearly zero at the beginning of the training, does not decrease smoothly and becomes very unstable after few epochs. This instability consequently leads to a poor trained generator. In contrast, for $\varepsilon = 10$, using $\sigma = (0.01, 0.02, 0.04, 0.06, 0.08)$ maintains a smooth, and decreasing loss over the epochs and the generator converges rapidly which brings about an improved image generator (Figure 4(b)).

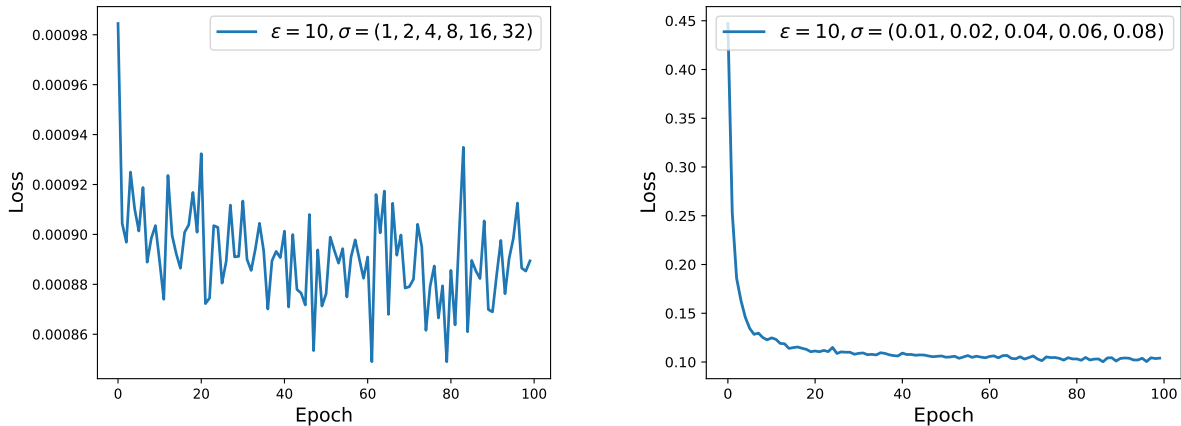


Figure 5: In these plots, the y -axis is the generator’s loss (sRMMD) and the x -axis is the training epoch for $\varepsilon = 10$ with two different σ . Left: with large σ , the loss fluctuates and model does not converge. Right: for small σ loss gradually decreases with the epochs and model converges faster.

We also observe that if we increase ε further e.g., $\varepsilon = 20$, using $\sigma = (0.01, 0.02, 0.04, 0.06, 0.08)$ still leads to a poor generator (Figure 4c). This situation can be avoided by reducing σ to $(0.001, 0.002, 0.004, 0.006, 0.008)$. Based on these empirical evidences, it can be said that using smaller bandwidth in case of larger ε leads to a better generator. Note that the choices of ε and σ we mentioned are specific to our case where we use latent space with dimension 8. It may require to find the optimal combination of ε and σ to get a good generator in case a different latent space dimension is used.

14.2 Effect of ε on sRMMD-Based Knockoff Generator (Section 5.2.1)

To examine the impact of the entropic regularizer ε on the knockoff generator minimizing sRMMD, we consider a Gaussian mixture model with 4 different modes, $P_X = \sum_{k=1}^4 \tau_k \mathcal{N}(\xi_k, \Sigma_k) \in \mathbb{R}^d, d = 100$. The covariance matrices are $\Sigma_k = \rho_k^{|i-j|}$ with the correlation coefficients $(\rho_1, \rho_2, \rho_3, \rho_4) = (0.6, 0.4, 0.2, 0.1)$. Mean tuple $(\xi_1, \xi_2, \xi_3, \xi_4)$ and the proportion tuple $(\tau_1, \tau_2, \tau_3, \tau_4)$ are set to $(0, 20, 40, 60)$, and $(0.27, 0.23, 0.23, 0.27)$, respectively. The generator is trained with different values of ε . The training is done on $n = 2000$ samples according to Algorithm 13.2 and we keep other training parameters same for each ε .

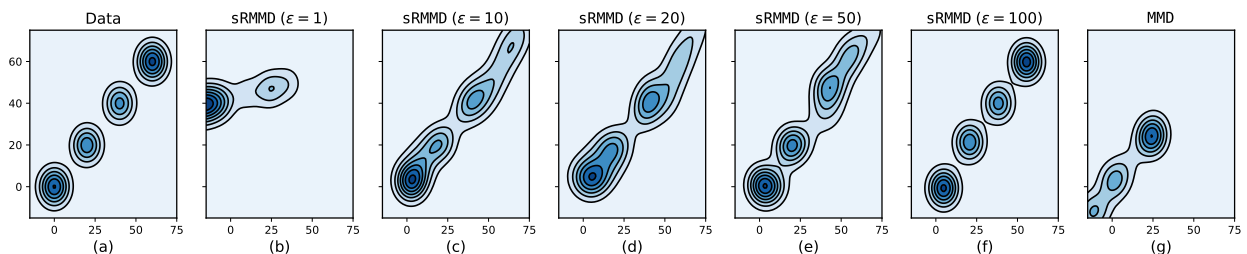


Figure 6: Visualizing two randomly selected dimensions of the original data and the generated knockoffs. The rightmost plot shows the reconstructed distribution when using MMD in (18) instead of sRMMD.

From Figure 6, it is evident that when $\varepsilon \ll d$, the knockoff generator fails to reconstruct the data distribution. As we increase ε , the generator improves and perfectly reconstructs the original distribution when $\varepsilon = 100$. On the other hand, MMD-based generator fails to capture all the modes. This indicates that for an appropriate choice of entropic regularizer ε , sRMMD is a better loss function to minimize compared to MMD.

14.3 Why sRMMD not sRE?

Figure 7 shows that unlike sRMMD, the generator minimizing sRE in (18) cannot capture all four modes perfectly with $\varepsilon = 100$ when $d = 100$. Though similar to sRMMD, the reconstruction ability gets better with ε , sRE still fails to capture every mode even when ε is doubled. Moreover, a direct comparison between sRE and sRMMD when $\varepsilon = 20, 50, 200$ indicates that sRMMD outperforms sRE in reconstructing the original distribution.

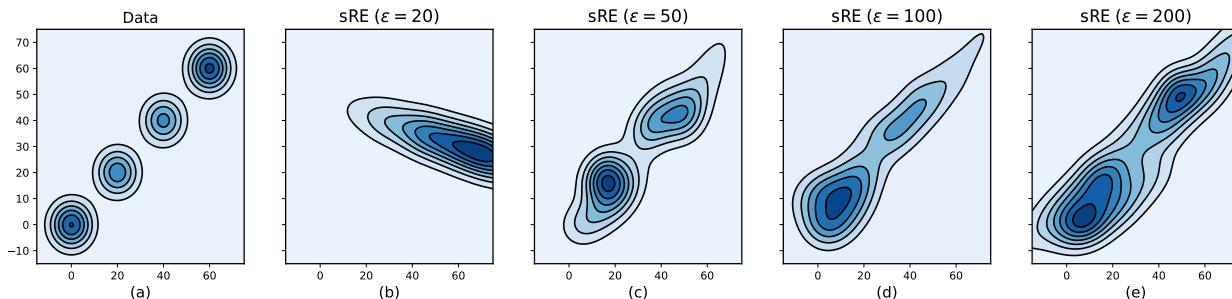


Figure 7: Visualizing two randomly selected dimensions of the original data used in Section 14.2 and the generated knockoffs. sRE-based knockoff generator did not converge when using $\varepsilon = 1$ and 10 (we encountered ‘nan’ after few epochs). That is why we refrain from adding it here.

14.4 Impact of Choice of Decorrelation Parameter γ

The selection of the optimal decorrelation parameter γ is difficult as we cannot perform cross-validation due to lack of access to the ground truth. Therefore we pick the optimal γ for each distributional setting by investigating the sensitivity of the results to different values of γ . Figure 8 shows the FDR versus power tradeoff w.r.t. the amplitude parameter for several values of γ for each distributional setting considered in Section 5.2.2.

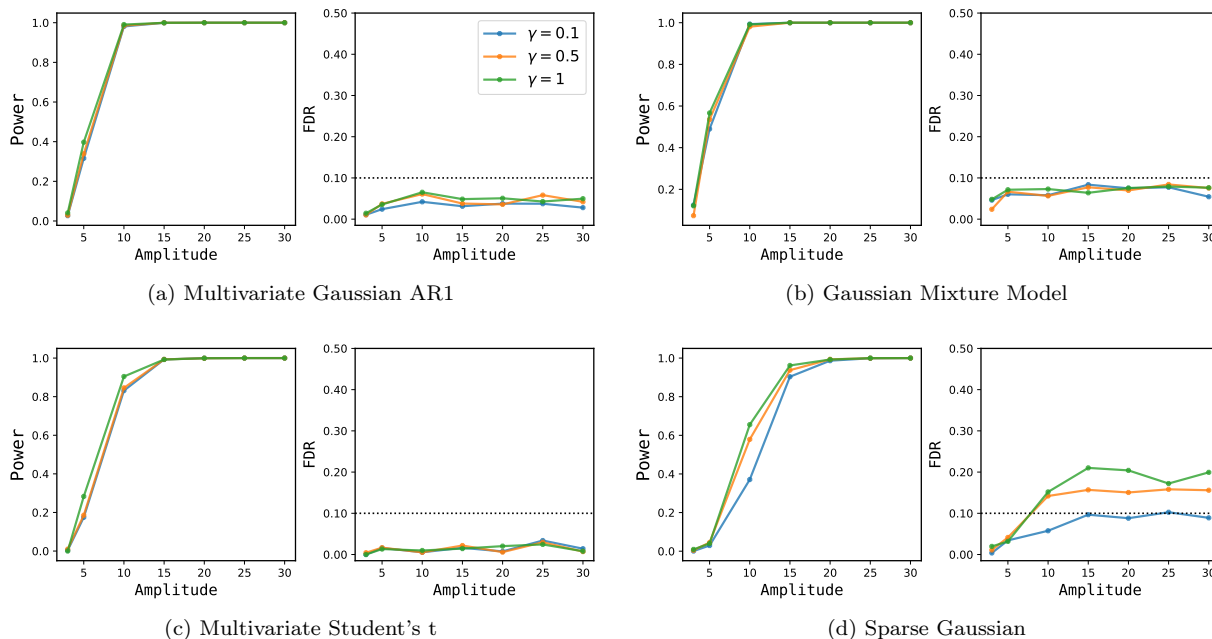


Figure 8: Average FDR and power computed over 200 independent experiments are shown on the y -axis for each synthetic benchmark. The FDR level is set to 0.1. The x -axis represents the amplitude parameter v .

For multivariate Gaussian, GMM and multivariate Student's t distributions, sRMMD-based knockoff generator is not sensitive to the value of γ . In these cases, each γ , sRMMD controls the FDR at $q = 0.1$ and achieves nearly identical power over the entire amplitude region. In case of sparse Gaussian setting, $\gamma = 0.1$ controls the FDR at $q = 0.1$. As γ increases e.g., 0.5, 1, the power also increases but fails to keep the FDR below 0.1.

14.5 Quality of the sRMMD Knockoffs w.r.t. ε

In this section, we measure the GoF of knockoffs for each distributional setting considered in Section 5.2.2 w.r.t. different entropic regularization parameters ε . For a fixed covariate distribution P_X and corresponding conditional distribution $P_{\tilde{X}|X}$ of the knockoffs, we test the following hypothesis:

$$H_0^{\text{parital}} : P_{(X, \tilde{X})} = P_{(X, \tilde{X})_{\text{parital}(B)}},$$

where B is a random subset of $\{1, \dots, d\}$, such that each $j \in B$ with probability $1/2$ independent of other elements. We draw n independent observations from $P_{(X, \tilde{X})}$ and $P_{(X, \tilde{X})_{\text{parital}(B)}}$ and generate two matrices $\mathbf{Z}, \mathbf{Z}' \in \mathbf{R}^{n \times 2d}$, $n = 200, d = 100$, respectively. Then, we compute an estimate of MMD to measure the GoF via:

$$\text{MMD}(\mathbf{Z}, \mathbf{Z}') \triangleq \frac{1}{n(n-1)} \sum_{i,j=1}^n k(Z_i, Z_j) - \frac{2}{n^2} \sum_{i,j=1}^{n,n} k(Z_i, Z'_j) + \frac{1}{n(n-1)} \sum_{i,j=1}^n k(Z'_i, Z'_j),$$

where $k(\cdot, \cdot)$ is a Gaussian mixture kernel with bandwidth parameter $\sigma = (1, 2, 4, 8, 16, 32, 64, 128)$. A small value of MMD indicates that the knockoffs achieve greater pairwise exchangeability 16 compared to the knockoffs that yield higher values of MMD.

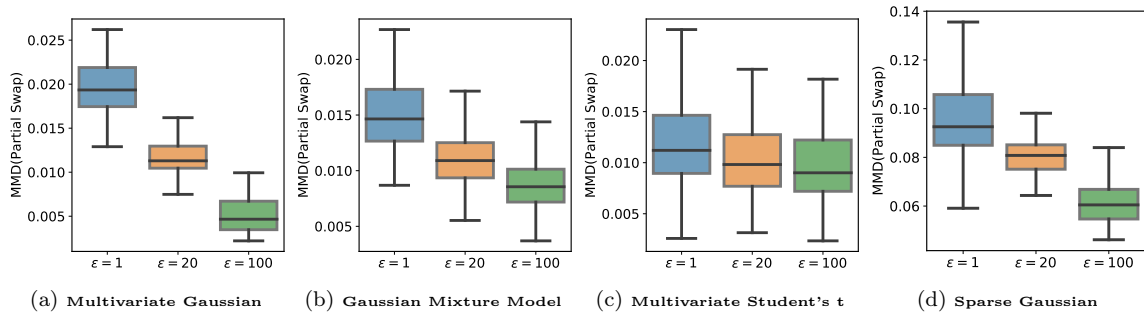


Figure 9: Boxplot showing the quality of the knockoff generator w.r.t. ε . Lower MMD indicates better quality knockoffs compared to higher value of MMD.

Figure 9 shows the quality of the knockoffs produced by a generator trained using different ε . For each distributional setting, we observe that knockoffs generated using larger entropic regularizer, (e.g., $\varepsilon = 100$) have better quality compared to using the smaller values (e.g., $\varepsilon = 1, 20$). As a result, we observe that in most cases using larger ε leads to better FDR control (Figure 10). In addition, using larger ε reduces the computational complexity to a great extent and helps the model to converge faster.

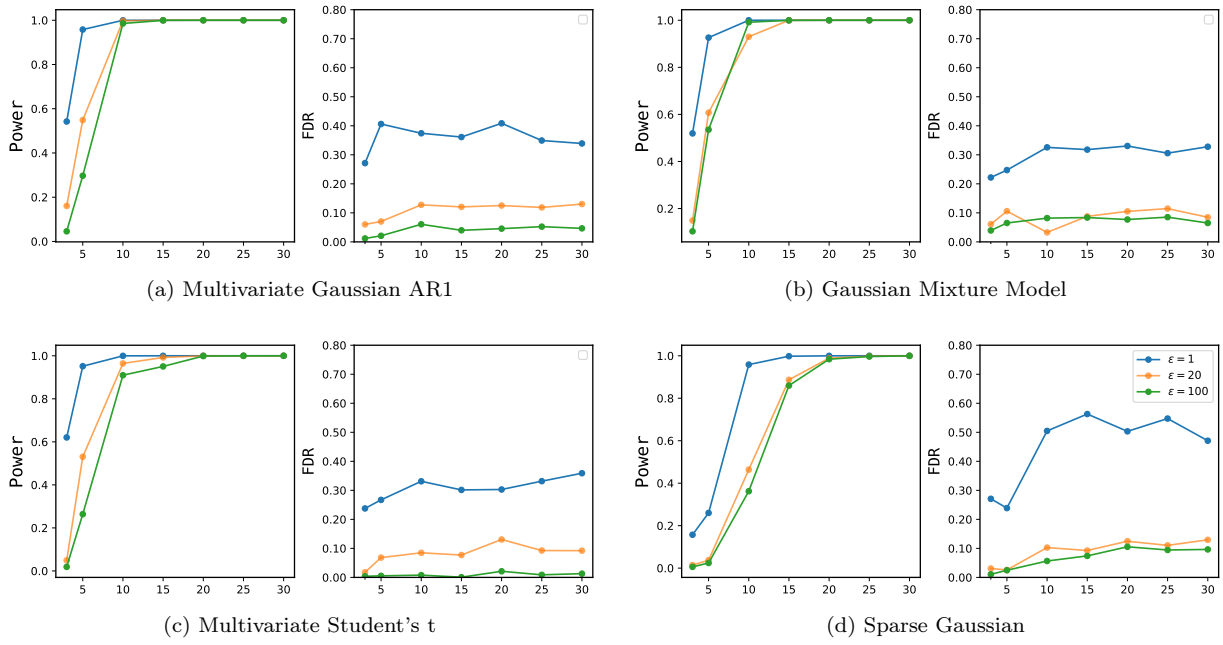


Figure 10: Average FDR and power computed over 200 independent experiments are shown on the y -axis for each synthetic benchmark. The FDR level is set to 0.1. The x -axis represents the amplitude parameter v .